DEVELOPMENT OF SILICON CARBIDE BASED IMPLANTS WITH IMPROVED BIOCOMPATIBILITY AND MECHANICAL PROPERTIES

Katarina Rade

Doctoral Dissertation
Jožef Stefan International Postgraduate School
Ljubljana, Slovenia, March 2012

Evaluation Board:

Asst. prof. dr. Goran Dražić, Chair member, Jožef Stefan Institute, Jamova cesta 39, 1000 Ljubljana

Prof. dr. Metka Filipič, Member, National Institute of Biology, Večna pot 111, 1000 Ljubljana

Prof. dr. Michael Gasik, Member, Department or Materials Science and Engineering, Aalto University Foundation, 00076 Aalto, Espoo, Finland

MEDNARODNA PODIPLOMSKA ŠOLA JOŽEFA STEFANA
JOŽEF STEFAN INTERNATIONAL POSTGRADUATE SCHOOL

Katarina Rade

DEVELOPMENT OF SILICON CARBIDE BASED IMPLANTS WITH IMPROVED BIOCOMPATIBILITY AND MECHANICAL PROPERTIES

Doctoral Dissertation

RAZVOJ VSADKOV NA OSNOVI SILICIJEVEGA KARBIDA Z IZBOLJŠANO BIOKOMPATIBILNOSTJO IN MEHANSKIMI LASTNOSTMI

Doktorska disertacija

Supervisor: asst. prof. dr. Saša Novak Krmpotič

Co-Supervisor: prof. dr. Spomenka Kobe

Ljubljana, Slovenia, March 2012

Index

Abstract

With emerging need for orthopaedic implants and prolonged exposure of organism to implants also problems connected to elution of metal ions that in some cases cause adverse reactions in the human body, emerge. The main aim of our work was therefore to investigate the potential of silicon carbide (SiC) to be used instead of currently employed metallic implants.

Our work consisted of ceramics processing to produce green parts of high density, densification of produced parts and analyses of properties, regarding mechanical and magnetic properties as well as bioactivity, dissolution of ions and response of cells.

Throughout the whole work electrophoretically deposited samples were compared to dry pressed samples. To produce a bulk part with high green density, electrophoretic deposition was proven as more successful technique, for this reason suspension had to be optimized. We aimed at high zeta potential and moderate conductivity and samples of SiC without sintering additives with more than 62 % of theoretical density were prepared. Tetramethyl ammonium hydroxide was chosen as an efficient additive for anodic deposition while cetyltrimethyl ammonium bromide did not result in deposits with sufficient green density.

When sintering additives (i.e. carbon black and boron carbide or magnesium oxide) were added, suspensions had to be further optimized due to dissimilar colloidal behaviour of additives. In the case of boron carbide and carbon black, surface of the latter had to be made hydrophilic but conductivity of resulting suspension with additives was too high for a successful EPD. Therefore this set of samples was only dry pressed.

In the case of MgO ethanol had to be used for suspension preparation due to solubility of MgO in water. Cathodic deposition with addition of polyethyleneimine was employed and deposits with high green density were produced.

Samples were sintered in vacuum at temperatures above 2000 °C or in open air at 1350 °C and their properties were measured. Mechanical properties for samples with addition of boron carbide and carbon sintered in vacuum at 2200 °C exhibited flexural strength 220 MPa, elastic modulus 250 GPa and fracture toughness 3.9 $MPa \cdot m^{1/2}$ while these properties for air-sintered sample containing MgO were 180 MPa, 80 GPa and 2.9 $MPa \cdot m^{1/2}$ for flexural strength, elastic modulus and fracture toughness, respectively. It is important to note that these specimens have different porosity levels. Since trabecular bone is a composite material it will always have superior properties to bulk ceramics, namely tensile strength of trabecular bone is 90-140 MPa, elastic modulus 10-40 GPa and fracture toughness between 1 and 15 $MPa \cdot m^{1/2}$. The properties of our material are still not ideal, especially in terms of fracture toughness, but these properties can be further tailored and improved.

None of the SiC samples showed any notable response to the magnetic field which makes it an appropriate implant material regarding use of magnetic resonance imaging. Samples were immersed in physiological solution to measure the eluted elements. After 7 days silicon, magnesium and vanadium were detected.

Cell tests that were performed showed the most beneficial response towards samples containing MgO; cells attached on the surface and after first day 50 % of cells were

attached compared to the control (glass plate coated with polylysine). Overall, SiC can be considered a potential, though not ideal, material for orthopaedic implants

Povzetek

Povečana potreba po ortopedskih vsadkih in daljša izpostavljenost materialom sta na plano prinesla tudi težave, povezane s sproščanjem kovinskih ionov, ki v nekaterih primerih lahko povzročijo odklonilno reakcijo organizma. Glavni cilj našega dela je bil raziskati prednosti silicijevega karbida pred trenutno uporabljanimi kovinskimi vsadki in oceniti, ali bi bil silicijev karbid primeren kandidat za nadomestitev določenih kovinskih vsadkov.

V našem delu smo se najprej posvetili oblikovanju keramike s ciljem izdelati surovec s čim višjo zeleno gostoto, ker je le-ta poglavitnega pomena za uspešno zgoščevanje. Zgoščevanju so sledile analize mehanskih in magnetnih lastnosti ter biokompatibilnosti, izločanja ionov in celičnega odziva.

Depozite, izdelane z elektroforetsko depozicijo, smo primerjali s suho stisnjenimi vzorci. Za izdelavo surovca z visoko zeleno gostoto je elektroforetska depozicija mnogo primernejša od stiskanja, vendar pa zato potrebujemo optimalno suspenzijo. Cilj je bil čim višji zeta potencial pri zmerni prevodnosti suspenzije, iz katere smo pripravili surovec z več kot 62 vol.% suhe snovi. Tetrametil amonijev hidroksid smo uspešno uporabili za spreminjanje zeta potenciala in anodno depozicijo, medtem ko se kationska površinsko aktivna snov, cetil trimetil amonijev bromid, ni izkazala kot primeren dodatek, saj nismo mogli proizvesti depozitov z zadostno zeleno gostoto.

Ko smo suspenziji dodali dodatke za sintranje (borov karbid in ogljik oz. magnezijev oksid), so se njene koloidne lastnosti spremenile zaradi drugačnega obnašanja dodanih prahov v suspenziji. Lastnosti suspenzije je bilo zatorej potrebno dodatno prilagoditi. Dodajanje ogljika v suspenzijo je otežkočeno zaradi njegove hidrofobne narave, ta problem smo rešili z oksidacijo površine v dušikovi kislini. Še vedno pa je bila težava, ki je nismo uspeli zaobiti, previsoka prevodnost suspenzije, ki je onemogočila uspešno depozicijo in visoko gostoto surovca. To kombinacijo prahov smo zato samo suho stiskali.

V primeru dodatka MgO smo se odločili za uporabo etanola, saj je MgO v vodi topen, slednje pa predstavlja velike težave, ki zadevajo stabilnost suspenzije. Namesto depozicije iz vodnih suspenzij smo izvedli katodno depozicijo z dodatkom polietilen imina. Na ta način smo dobili vzorce z visoko zeleno gostoto in enakomerno porazdeljenim MgO.

Vzorce smo po sušenju sintrali bodisi v vakuumu pri temperaturah nad 2000 °C ali na zraku na 1350 °C ter jim izmerili mehanske lastnosti. Vzorcem, sintranim z dodatkom bora in ogljika na 2200 °C, smo izmerili upogibno trdnost 220 MPa, elastični modul 250 GPa in zlomno žilavost 3.9 $MPa \cdot m^{1/2}$. Vzorci, sintrani na zraku z dodatkom MgO so imeli upogibno trdnost 180 MPa, elastični modul 80 GPa in zlomno žilavost 2.9 $MPa \cdot m^{1/2}$. Potrebno je poudariti, da se ti vzorci razlikujejo po stopnji poroznosti. V primerjavi s scelno kostjo, ki ima kompresijsko trdnost 90-140 MPa, elastični modul med 10 in 40 GPa in zlomno žilavost v mejah med 1 in 15 $MPa \cdot m^{1/2}$, vrednosti naših vzorcev še vedno niso popolnoma primerne, vendar pa jih lahko še spreminjamo, bodisi z vgrajevanjem vlaken (izboljšujejo zlomno žilavost) ali s povečano poroznostjo (znižuje elastični modul).

Magnetno polje ni imelo znatnega vpliva na nobenega od SiC vzorcev, kar bi ob potencialni uporabi SiC v ortopedske namene še vedno omogočalo uporabo slikanja z magnetno resonanco v diagnostične namene. Da bi izmerili izluževanje ionov, smo vzorce pustili v fiziološki raztopini (0.9 % raztopina NaCl) in po enem tednu dokazali prisotnost silicijevih, magnezijevih in vanadijevih ionov.

Preverili smo tudi odziv celic na vzorce; izkazalo se je, da na celice najbolj ugodno vpliva vzorec, ki vsebuje magnezij. Po prvem dnevu se je na površino, v primerjavi s kontrolo (stekelce s prevleko iz polilizina), pritrdilo 50 % celic. Na podlagi vsega povedanega silicijev karbid lahko smatramo kot potencialen, vendar pa ne idealen material za ortopedske vsadke.

Abbreviations

% TD	=	percent of theoretical density
BAG	=	bioactive glass
co-EPD	=	electrophoretic co-deposition
CTAB	=	cetyl trimethyl ammonium bromide
E	=	elastic modulus [GPa]
EDS	=	energy dispersive spectroscopy
EPD	=	electrophoretic deposition
EtOH	=	ethanol
FESEM	=	field-emission scanning electron microscopy
HV	=	Vickers hardness
ICP-MS	=	inductively coupled plasma mass spectroscopy
IP	=	isostatic pressing
K_{Ic}	=	fracture toughness [MPa·$m^{1/2}$]
MRI	=	magnetic resonance imaging
O.pH	=	operational pH
PBS	=	phosphate buffer saline
PDLLA	=	poly-D,L-lactic acid
PEEK	=	polyether ether ketone
PEI	=	polyethyleneimine
PVD-SiC	=	SiC prepared with physical vapour deposition
S	=	conductivity [mS/cm]
SAED	=	selected-area electron diffraction
SBF	=	simulated body fluid
SEM	=	scanning electron microscopy
TEM	=	transmission electron microscopy
TMAH	=	tetramethyl ammonium hydroxide
U	=	applied voltage [V]
UHMWPE	=	ultra-high molecular weight polyethylene
UP	=	uniaxial pressing
VPS-Ti	=	vacuum plasma sprayed titanium
VSM	=	vibrating sample magnetometer
XRD	=	X-ray diffraction
Y-TZP	=	yttria-stabilized tetragonal zirconia polycrystal
ZP	=	zeta potential [mV]
θ	=	contact angle [°]
ρ	=	density [g/cm^3]
σ_{flex}	=	flexural strength [MPa]

1 Introduction

Average age of the population as well as life expectancy in the modern world is increasing due to improved health system and more advanced healing techniques, e.g. bioengineering. With the advent of it, the future prospective seems to be in growing tissues in the laboratory. Unfortunately, this approach is yet not enough developed for certain tissues and in the case of bone reconstruction. Especially when there is a need of larger parts, or when quick response is required, it is much too slow. Various bone diseases and in particular bone fractures that can also result from osteoporosis, modern disease of mainly elderly people, relatively frequently call for bone reconstruction. Due to the arguments stated above, artificial bone implants are still the best option.

1.1 Properties of bone and why we need orthopaedic implants

Bone is a complex living tissue which has an elegant structure at a range of different hierarchical scales. As a specialized connective tissue that is a part of skeletal system, bone has three main functions: (1) mechanical: support and site of muscle attachment for locomotion; (2) protective: for bone marrow and vital organs; and (3) metabolic: as a reserve of ions, specially calcium and phosphate, for the maintenance of serum homeostasis, which is essential to life. However, since bone is a living tissue it requires constant supply of oxygen and nutrients, and is limited in the size of fracture or defect to be able to restore healthy tissue. Furthermore, bone can suffer from pathological conditions, (e.g. cancer) and is subject to degeneration as a result of age and disease (i.e. osteoporosis) as well as lack of load (i.e. long-term immobility, zero-gravity space). In these cases, to return a patient comfort and health, bone function can only be restored by surgical reconstruction [1]. Bone engineering in terms of various implants/bone defect fillers is therefore a good alternative to conventional treatments for fracture, non-union, spinal fusion, joint replacement, and pathological loss of bone. In general, human bone is from materialist's point of view, really astonishing material since it combines light weight (~2 g/cm^3) and extraordinary good mechanical properties despite its high porosity. These properties arise from combination of mineralized part that is mainly composed of hydroxyapatite and related calcium phosphates and organic part that consists of collagen and other proteins.

Development of materials for orthopaedic applications has emerged as an inter-disciplinary field, which require the development of new biomaterials and fabrication methods to engineer appropriate scaffolds for regeneration of specific organs and tissue functions. In particular, the design of an ideal scaffold, focused on regeneration of bone tissue, should replicate the architecture and hierarchical 3D structure of the bone, with predetermined density, pore shape and size, and interconnected pathways. Besides, to avoid undesired effects, such as shielding that is the result of elastic moduli mismatch, mechanical properties of such materials should also be strongly considered.

Most of the therapeutic approaches to repair moderately large bone defects include graft transplant (auto-, allo-, and xeno- grafts; different biomaterial implants). Bone auto-grafts, both non-vascularized and vascularized, are considered at the moment the optimal choice for osteogenic bone replacement in osseous defects however, it is

connected with several disadvantages. Even though autologous bone grafts reliably fill substance deficits and induce bone tissue formation at the defect site following transplantation, this approach has an unavoidable size limitation. Chips, larger pieces, even blocks of several centimetres in size could be harvested but the larger the defect, the higher impact on the secondary site of operation. Although success rate is high indeed, complications, such as infections, bleeding, hematoma, non-unions, etc. are very frequent, especially in large shift reconstructions. Furthermore, large reconstructions with autologous bone require significant harvests of healthy tissue with important donor site morbidity. Therefore, this approach is limited by definition.

Many of the problems presented by the autografts, in particular the immediate availability of tissue for transplant, and the size of the defect, could be solved by allo- (transplant material from another subject of the same species, e.g. human; most usually tissues from dead bodies are extracted) and possibly xeno-grafts (from organism of another species, e.g. animal), which are commonly used when autologous transplantation is not applicable. Although the initial properties of allo- and xeno-grafts resemble those of autologous bone in terms of biomechanical stability and elasticity, host immune response, and potential risk of infectious diseases transmission raise several concerns limiting their applications. Immune response and potential diseases can be overcome by de-proteinizing the tissue but with that the mechanical properties of the material are deteriorated [2].

If none of the abovementioned approaches is sufficient, novel materials, cellular transplantation, and bioactive molecule delivery are being explored alone and in various combinations to address the problem of bone regeneration and repair. The aim of these strategies is to exploit the body's natural ability to repair injured bone and replace it with new bone tissue, i.e. to remodel the newly formed bone in response to the local stresses that it is exposed to [1].

The bone bonding behaviour of a bioactive material depends not only on the chemical composition, crystallinity, and solubility of the material, but also on the type (cancellous or cortical bone), and the quality of bone to which it bonds [3]. Bone is mechanosensitive, that is, it responds and adapts to its mechanical environment. Controlled (non-extensive) bone loading has been found to be related to increased bone mineral content, increased bone density, or to controlled bone loss. A significant increase of bone-to-implant contact was demonstrated under various loading conditions when compared with non-loaded conditions. Biomechanical forces can stimulate the proliferation of osteoblasts as well as their activation to produce more and denser peri-implant bone. As a result, bone metabolism can be significantly increased with a resulting increase in bone-implant contact. Therefore, it is hypothesized that weight-bearing should play an important role in the bone-bonding behaviour of bioactive bone cements as well as other bone graft materials and is therefore connected with the efficiency of healing process.

In addition, cells are sensible to the surface properties, bulk geometry, and topography of the biomaterial. Characteristics such as surface charge and wettability (hydrophobicity or hydrophilicity of the surface) can affect specific protein adsorption and consequently cell interactions, and the process of osteogenesis (i.e. the capacity to generate bone tissue *de novo*) linked to gene expression and protein adsorption [4].

Implants are defined as medical devices which have been developed to replace and act as a missing biological structure. Since they are in close contact with tissue (especially when bone ingrowth is required), biocompatible materials need to be used. It was defined that "*biocompatibility is the ability of a material to perform with an appropriate host response in a specific application*" [5]. Nowadays, medical biomaterials/implants have a huge number of different applications and uses in different parts of the human body ranging from orthopaedic applications: joint replacements (hip, knee), bone cements, defect fillers, plates for fracture fixation to artificial tendons and ligaments;

cardiovascular applications, blood substitutes, ophthalmic applications and cochlear replacements. There are also other applications including renal implants, artificial hearts, skin repair templates, tissue screws and tacks and drug-delivery systems. This results in numerous different materials and morphologies used [6].

Many possibilities exist regarding classification of biomaterials: according to the material, duration, and response of the body. Regarding the material used, biomaterials are classified as follows: 1) metals, 2) polymers, 3) ceramics, 4) composites and 5) biological materials [7]. Regarding the duration, biomaterials can be divided in two classes: 1) permanent and 2) temporary, i.e. bioreabsorbable materials. The former are mainly metals and fully dense bioinert ceramics or polymers that are used in load bearing places (i.e. joint prostheses and screws, plates, etc.). Temporary implants are either taken out after certain time (e.g. bone plates and screws can be removed after bone is healed) or are, in relation to their composition, rapidly or slowly degraded and replaced by regenerating tissues either fully or partially. However, in this case the mechanical properties during the degradation cannot be controlled, which is a significant drawback of such biomaterials. They can be also sorted according to their interactions with their surrounding tissue: 1) biotolerant or bioinert, 2) biocompatible and 3) bioactive materials. In biotolerant materials with almost inert, smooth or porous surfaces, the tissue response is a foreign body reaction, where a fibrous scar-like tissue forms around the implant, isolating it from the surrounding tissue. Their main advantage is that they do not result in toxic response. On the other hand, bioactive materials with chemically reactive surfaces are able to encourage bony tissue around the implant material and integrate strongly to the bone with the implant surface.

As stated above, the main reason behind the increasing need for medical biomaterials, with the stress on bone implants in the western population is the increased number of elderly people and age-related diseases. Typically reduced bone density and bone loss are linked with weaker motoric skills in the old which act together to predispose these people to fall-related fractures. The other reason for joint replacements is associated with diseases such as osteoporosis, osteoarthritis and trauma [6]. Because of that, even the replacement of bone is a challenging task and has to be treated from the multidisciplinary point of view. Therefore, according to the requirements, many different material types, such as metals, ceramics and polymers are used as implants. However, materials can fail due to several reasons but nevertheless, the major economic costs related to every revision and also the pain to the individual patient should not be overlooked. The statistics and the fact that the average orthopaedic implant lasts only about a decade or two, reveal that perfect bone implant has not yet been developed. Many different reasons for bone implant revisions include fractures, dislocations and changes in the biomechanics of the implant due to wear or corrosion of implant material. However, a significant part of the revisions can be traced to poor biocompatibility signs of which are osteolysis, necrosis and formation of a thick fibrotic capsule between the implant and bone as well as infection. Another aspect that should be also taken into consideration is either immediate or delayed hypersensitivity or even allergy to the released metal ions that are dissolved from the implant and that will be discussed in the following sections [8, 9].

Bone lesions/defects occur in a wide variety of clinical situations, and for the patient's successful rehabilitation process, their reconstruction to provide mechanical and functional as well as aesthetical integrity is a necessary step. Moreover, a bone graft or a bone substitute is often required in maxillo-facial and orthopaedic surgery to assist healing in the repair of osseous congenital deformities, or in the repair of defects due either to trauma or to surgical excision of bone pathological lesions exceeding a certain size.

1.2 Bone and biomaterials

Bone as a specialized connective tissue and a living system is also susceptible to injuries and diseases that are commonly associated with ageing. Therefore there has always been a need, since the earliest time, for the repair of damaged hard tissue. The earliest attempts to replace hard tissue with biomaterials aimed to restore basic functions by repairing the defects caused by injury and disease; however the aim was to elicit minimal biological response from the physiological environment. These materials are now largely classed as "bioinert" and the absence of a toxic response would have then been considered a successful outcome. "Bioinert" is a term that should be used with care, since it is clear that any material introduced into the physiological environment will induce a response. For the purposes of biomedical implants, the term can be defined as a minimal level of response from the host tissue in which the implant becomes covered in a thin fibrous layer which is non-adherent [2].

During the past 30-40 years there has been a major advance in the development of medical materials and this has been in the innovation of ceramic materials for skeletal repair and reconstruction. The materials within this class of medical implant are often referred to as "bioceramics" and the expansion in their range of medical applications has been characterised by a significant increase in the number of patents as well as numerous publications in the field. Bioceramics are now used in a number of different applications throughout the body. According to the type of bioceramics used and their interaction with the host tissue they can be categorized as either "bioinert" or "bioactive" and the bioactive ceramics may be resorbable or non-resorbable. The materials currently used include: polycrystalline materials, glasses, glass ceramics and ceramic-filled bioactive composites, and all these may be manufactured either in porous or in dense form in bulk, as granules or in the form of coatings.

Although material science technology has resulted in clear improvements in the field of regenerative medicine, no ideal bone substitute has been developed yet and hence large bone defects still represent a major challenge for orthopaedic and reconstructive surgeons. A number of bone substitute biomaterials are easily available. The intended clinical use defines the desired properties of engineered bone substitutes. Anatomical defects in load bearing bones, for instance, require devices with high mechanic stability whereas for craniofacial applications, initially injectable or mouldable constructs are favourable. Scaffold chemical composition is of crucial importance for the osteoconductive properties and the resorbability of the material. In addition, scaffolds should have an internal structure permissive for vascular invasion. Porous bioceramics are very promising candidates in bone substitution, because of their bone-like chemical composition and osteoconductivity while mechanical properties are questionable due to degradation. They are also particularly advantageous for bone tissue engineering application as they induce neither an immune nor an inflammatory response in recipient organisms [10].

It was reported [11] that the history of most widely known osteoconductive material, Bioglass® began in 1967 with Professor Larry Hench. The need for the development of materials that would help in the repair of tissues by forming a direct bond with them emerged, rather than the interfacial scar tissue that occurred around metallic and polymeric implants of that time. *In vitro* tests showed that the 45S5 Bioglass® (consisting of 45 wt.% SiO_2 and having the CaO to P_2O_5 ratio of 5) composition undergoes a surface reaction which occurs very rapidly. This is a complex, multi-stage process which results in the formation of a biologically active hydroxy-carbonate apatite layer. This phase is chemically and structurally similar to the mineral phase in bone and thus it provides a direct bonding by bridging host tissue with implants. It was proven that melt-derived bioactive glass (from CaO-P_2O_5-Na_2O-SiO_2 system) remains bioactive to the SiO_2 content

from 20 to 55 mol%. However, further research on the field of sol-gel process and production of bioactive glass extended the possibilities and now the pure SiO_2 produced by sol-gel is also considered bioactive.

At around the same time that the original work on Bioglass® was being undertaken, Kokubo with co-workers was developing a new glass-ceramic material in Japan and they first reported the production and behaviour or apatite-wollastonite glass-ceramic in 1982. It became one of the most extensively studied glass-ceramics for use as a bone substitute material. Apatite-wollastonite glass-ceramics is an assembly of small apatite particles effectively reinforced by wollastonite. The bending strength, fracture toughness and elastic modulus of this material are the highest among bioactive glass and glass ceramics, enabling it to be used in some major compression load bearing applications, such as vertebral prostheses and iliac crest replacements. It is said to combine high bioactivity with suitable mechanical properties (the reported values for dense rather than porous material are in the range of 230 MPa for bending strength and ~90 GPa for elastic modulus [12], but still literature mainly focuses on bioactivity rather than on mechanical properties). However, these mechanical properties progressively deteriorate due to solubility in the biological environment and worse in the case of porosity of the material.

The increase in the biomedical application of bioactive ceramics is occurring simultaneously with the growth of interest in tissue engineering. This is a process whereby cells are delivered to a particular clinical treatment site via a scaffold. The requirements for the scaffolds are very high porosity with full interconnectivity. The fenestrations between the pores need to be sufficiently large to allow the movement of cells into the scaffold and should also permit vascularisation. Whether a bioceramic scaffold is seeded with cells prior to implantation or whether it is intended that cells will invade and populate the structure after implantation will influence the precise terms of reference to the material. In orthopaedic surgery there is a major need for bone grafts, since as stated in the previous section bone grafting currently mainly relies on the use of natural materials, often bone from another operation. To ensure adequate supply and reproducibility, there is a need for the development of chemically synthesized materials with reproducible structures and chemical composition [10] as well as with sufficient mechanical properties.

1.3 Types of biomaterials

1.3.1 Metals

Metallic materials are habitually used as biomaterials to replace structural components of the human body. In present, most widely used materials for such replacements are titanium and its alloys which are generally proven to have good biocompatibility. These alloys are commonly used for dental implants, joints and even for artificial bones. The corrosion resistance, chemical inertness and even the biocompatibility of such alloys are ascribed to the presence of a native oxide layer formed on the surface. Compared to polymeric and ceramic materials, they possess more superior tensile strength, fatigue strength, and fracture toughness. Hence, metallic biomaterials are currently used in medical devices such as artificial joints, bone plates, screws, intramedullary nails, spinal spacers and fixations, external fixations, pace maker cases, artificial heart valves, wires, stents, and dental implants [7].

Metallic materials that are typically used for orthopaedic applications (e.g. stainless steel, Co- and Ti-based alloys and Ta as well as alloying elements, such as Al, Nb, V, Mo, Zr, Ni and Cr) have many desirable properties like high strength and fracture toughness, hardness and acceptable biocompatibility which make them a practical choice for bone

implant applications. Still the disadvantages, such as their high elastic modulus compared to bone and release of ions are notable concerns. Besides, some of the elements used (such as Ni, Co and Cr) are still the most common metal sensitizers in human body and are known to be released from alloys in the body environment. When these metal ions are released from the implant, they behave like haptens (metal ions that bind to proteins) and may trigger a type-IV hypersensitivity (this is a cell-mediated delayed response that occurs hours to days after exposure to immunogen) and type-V (mixed) hypersensitivity reactions which can be a significant factor in a process of osteolysis and promoting the prosthetic device loosening [8]. Especially in latter decades there are many evidences of people who are hypersensitive or even allergic (immediate reaction) to certain metals (most known is nickel, but also titanium is said to cause effect of delayed hypersensitivity in about 4 % of people [8]). Since we do not yet have any reliable substitute, there is an increased need for material that would not release abovementioned metal ions and would not cause allergic response.

Besides, some metals that are used in biomedical alloys are even suspected to be neurotoxic (aluminium and vanadium) and may cause some related diseases. For instance, although the results are still controversial and inconclusive, aluminium is suspected to be associated with some neurological diseases [13-16].

For implant applications (i.e. dental implants, joint replacements and bone fixation as well as in cardiac and cardiovascular applications), commercially pure Ti (cp-Ti) and Ti-6Al-4V are the most commonly used. Their lower elastic modulus (100-112 GPa) compared to stainless steel (195 GPa) and Co-Cr-Mo alloys (230 GPa) in addition to their beneficial osteoconductive properties makes them a better choice for bone applications and cementless joint replacements. Their mechanical properties are listed in Table 1.

Table 1: Properties of metal materials and ultra-high molecular weight polyethylene (UHMWPE) used for orthopaedic applications [17]

Material	E [GPa]	Ultimate strength [MPa]	K_{Ic} [MPa·m$^{1/2}$]
Stainless steel 316L	195	615	In the range of a few 10 to 100, 200
Co-Cr-Mo	230	655	
cp-Ti	105	785	
Ti6Al4V	110	960	
Bone	10-40	90-140	1-15* [18]
UHMWPE	0.5-1.5	15-20	4 [19]

*depends on the direction (longitudinal vs. transverse)

Beside beneficial mechanical properties titanium and Ti-alloys also have acceptable biocompatibility, low toxicity and low corrosion rates which are partly due to the spontaneously formed covering oxide layer. However, the release of Al ions from Ti alloys might cause long-term health problems. In addition, the difference compared to bone elastic modulus (10-40 GPa) may lead to stress shielding and consequential decomposition of the surrounding bone. Still, as a hard tissue replacement, the relatively low elastic modulus of titanium and its alloys (compared to other metallic materials and also dense ceramics) is generally viewed as a biomechanical advantage because the smaller difference in elastic moduli results in smaller stress shielding. Ti alloys are also relatively softer than stainless steel and Co based alloys. Therefore, they cannot be used on articulating surfaces without a coating. Besides, among problems connected with toxicity of corrosion products, mechanical failure can occur due to corrosion fatigue and

fretting corrosion fatigue, implant can be rejected because of lack of biocompatibility, and inadequate affinity for cells and tissues. In particular, the toxicity problem brought about other problems such as allergy reaction, tumour formation, teratogenicity, and inflammation [20]. In this sense, a modification or functionalization of the metallic surface is required to avoid external corrosion, avoid toxicity, and mechanical problems [21, 22]. Therefore, a lot of effort has been put into making metals suitable as biomaterials. One option is hydroxyapatite coating, which shows very good corrosion resistance and biocompatibility. In this case, degree of crystallinity affects mechanical properties while amorphous phase, due to higher dissolution rate, enables faster linkage of implant to the bone tissue.

It has to be also stressed that beside all the advantageous properties of titanium and its alloys, and generally accepted compatibility with magnetic resonance imaging procedures some specialists avoid MRI technique to ensure complete safety of patients. Besides, this technique is still not applicable on the very place of the implantation since metals cause distortion of an image and besides, radio frequencies can cause heating of the implanted material [23, 24].

1.3.2 Ceramics

Despite the indications of their non-desired and potentially harmful long-term effects that were mentioned above, metals remain apparently indispensable in reconstructive medicine. This is mostly due to the fact that available alternative materials, such as ceramics, currently cannot compete with metals at least in terms of toughness and reliability. Despite, ceramic materials possess many useful properties like high stiffness, inert behaviour under physiological conditions and excellent wear resistance. Therefore, ceramic-on-ceramic, mainly alumina (Al_2O_3) on alumina, bearing surfaces have been commonly used in total hip arthroplasty and in reconstruction of knee joints. However, their brittleness and low tensile strength may cause the fractures of femoral head component and breakage of ceramic cup. In addition, insufficient osseointegration may be a problem, though this might be inhibited by nanostructuring. In addition to still present modest hesitation in use due to the poor fracture resistance (mainly characteristics of some early grades), concerns about potentially harmful effect of aluminium ions in the body are also present [25].

Compared to alumina ceramics, zirconia (ZrO_2) [26] is well known as having better fracture toughness and flexural strength. It has been demonstrated to possess potential as dental implants and hip replacement applications. Because of its tetragonal phase, pure zirconia exists in an unstable state, and thus it is typically stabilized with yttrium. However, yttrium-stabilized tetragonal polycrystalline zirconia undergo low-temperature aging degradation caused by phase transformation (hydrothermal degradation) to monoclinic phase leading in long term to a severe degradation in mechanical properties [27, 28].

Lately, ZrO_2/Al_2O_3 composites [29] have been examined to avoid the disadvantages of ZrO_2 ageing, for instance in the bearing surfaces of total joint replacements. In general, use of alumina, and zirconia in biomedical applications have been FDA-approved, the only concern is about the use of nanoparticles in the materials. However, still ZrO_2 and Al_2O_3 are in the class of bioinert ceramics.

Among bioactive ceramics the most widely explored is hydroxyapatite since this is also the mineral part of the natural bone. Its degradation rate can be tailored with degree of porosity of the material; however, its mechanical properties are too low to allow successful implantation in load bearing parts. Reported mechanical properties for dense hydroxyapatite ceramics are up to 250 MPa, 120 GPa and 1.2 $MPa \cdot m^{1/2}$ for flexural strength, elastic modulus and fracture toughness, respectively. It is also reported that

fracture toughness decreases almost linearly with increasing porosity of the material, reaching only 0.6 $MPa \cdot m^{1/2}$ at 75 % density [30].

Surprisingly, non-oxide ceramics have not been seriously considered as suitable materials for implants. To our best knowledge there were only a few reports mentioning silicon nitride (Si_3N_4) and carbide (SiC) as candidate materials for implants [29, 31-35], despite favourable cell response was indicated in a few *in vitro* studies [31, 36]. Silicon is ubiquitous in the environment and is also naturally involved in bone formation [37], which allows speculation that silicon-based materials are in general much better accepted as artificial bone materials than heavy metals. For example, the advantageous effect of silica-rich bioactive glasses, i.e. stimulation of bone growth, has been confirmed in numerous studies as well as in clinical practice [38-40]. Unfortunately, their mechanical properties are far too poor to allow the use in load-bearing applications, not even as a resorbable temporary support. On the other hand, silicon carbide (or oxy-carbide) could be a good alternative as it is non-resorbable or at least its resorption is due to high chemical stability very slow, which suggests that possibly it could be used as permanent (or long-term) implant releasing only essential and non-toxic elements.

1.3.3 Polymers

Polymeric materials for biomedical and orthopaedic applications have emerged for use in artificial hip and knee joints for metal-on-polymer articulations [41] (e.g. ultra-high molecular weight polyethylene). A great problem is the formation of wear particles that then cause osteolysis and consequential failure of artificial joint. Another problem regarding polymeric materials is oxidation that tends to take place in body environment. Therefore polymeric materials were to a great extent replaced with metal-on-metal or ceramic-on-metal articulations.

Polymers are also used in numerous other applications, of which only a few will be mentioned here. Polymer that has been given a lot of attention is polyether ether ketone (PEEK) that has better mechanical properties comparing to other polymer materials (8.3 GPa and 139 MPa against ~2 GPa and ~30-40 MPa for elastic modulus and tensile strength, respectively) and besides it is reported to have a good wear resistance. PEEK and its composites are currently used in medical screws, in spine cage, for plates, rods, in total hip replacement, etc. [42] and since it is not biodegradable it is used as a permanent material.

As another example, also biodegradable polymers are frequently used, much attention given to poly-D,L-lactic acid (PDLLA) that is used in sutures as well as in drug delivery systems [43]. Degradation product is lactic acid that is then further metabolized in the body.

1.3.4 Bioactive glasses

The bioactive glasses have been reported to induce bone growth three times faster than hydroxyapatite, when implanted in bones [44]. Bioglass' network is made of silica (SiO_2), as the former component, and alkaline earth metals (e.g. magnesium or calcium), or alkali metals (e.g. sodium and potassium) as the network modifiers. When in contact with physiological solution as part of bone defect fillers, the bioactive glasses release ions that precipitate into a bone-like apatite on the host-bone interface, thus inducing bioactivity reactions. Due to their mechanical properties (tensile strength 40-60 MPa, elastic modulus ~35 GPa) [45], bioactive glasses are not suitable for load bearing applications and that is also their main disadvantage. However, bioactive glasses revealed to be successful when applied as nonload-bearing material for bone repair in dental and orthopaedic surgery.

1.4 Properties of permanent and temporary implants

As stated before, permanent implants can be made of metals, non-biodegradable ceramics and non-biodegradable polymers. The main requirements of permanent implants are high toughness (high reliability), high strength and good ingrowth. Mechanical properties are intrinsic properties of the material as well as the result of its micro- and macrostructure while ingrowth can be tailored via surface modification (i.e. oxidation, coatings, etc.). In surface-active materials that are bonded to bone through an intervening apatite layer, dissolution-precipitation mechanism is commonly proposed for the formation of biological apatite. In the case of resorbable surface layer (e.g. bioactive glass), calcified bone reaches the chemically and biologically degraded surface, eventually making direct material-bone contact resulting in mainly mechanical bonding by interlocking [46]. Therefore it is of special importance for the implanted material not to contain any ions that would have detrimental effect on the organism. Permanent implants are usually employed as joint replacements while temporary implants are used as scaffolds to overcome larger bone defects.

Several requirements that a 3D temporary scaffold should fulfil are mentioned in the literature: (1) a scaffold has to have high porosity and proper pore size (i.e. pores greater than 50 μm in diameter); (2) a high surface area; (3) biocompatibility (i.e. no cytotoxicity); (4) proper mechanical integrity of the scaffold is needed to retain the predesigned tissue structure; (5) biodegradability is usually required, and the degradation rate should match the rate of neotissue formation; (6) the scaffold should interact with proteins and cells, promoting cell adhesion, growth, migration, and differentiation; (7) osteoconductivity (induction of osteoblastic cells adhesion, growth, and differentiation) and osteoinductivity; (8) if possible, the scaffold material should be radiographically distinguishable from the new bone, easy to produce, sterilize, and handle in the surgery room [1].

Macroporosity (pore size >50 μm) has a critical impact on bone formation while microporosity (pore size ~10 μm) and pore wall roughness also play an important role because they contribute to the increase of the surface area resulting in better protein adsorption, to ion exchange, and to bone-like apatite formation by dissolution and re-precipitation. Surface roughness improves the integrin-dependent attachment of bone cells. Currently, it is commonly accepted that 3D scaffolds have to contain nanoporosity to allow diffusion of molecules for nutrition and signalling, micropores to ensure cell migration, and capillary formation as well as macropores for arteries and veins [47].

Indeed an important advancement in the field of tissue engineering has been represented by the introduction of synthetic porous scaffolds. In these cases in fact the internal architecture can be intelligently designed and the density, pore shape, pore size and pore interconnection pathway of the material can be predetermined. An incomplete pore interconnection or a limiting calibre of the interconnections could represent an important constraint to the overall biological system by limiting blood vessels invasion. Therefore, bioceramics with high porosity and appropriate interconnection pathway should allow the tissue to infiltrate and to fill the scaffold.

1.5 The role of chemical elements in the human body

In the chemist’s view, corrosion is the visible destruction of a metal, but in the terms of biological implants, any corrosion, even if it is invisible to the naked eye, may lead to deteriorating reaction leading to the release of undesirable metal ions products, which may not be biocompatible. However, despite the great progress in providing corrosion resistant metallic biomaterials, in a physiological environment corrosion remains a slow and continuous process, which leads to the release of significant amounts of metal ions

and other corrosion products [8]. Consequently, the formation of periprosthetic osteolytic lesions causes deterioration of the interface stability between the implant and the bone, aseptic loosening develops in ~15-20 % of all patients within 20 years of a primary hip arthroplasty. Recently, great effort has been directed toward understanding the pathophysiological cascade of events initiated by biocorrosion products, resulting in periprosthetic bone loss and ultimately aseptic loosening. Normal bone maintenance relies on the balance between bone formation and bone resorption. The net bone loss at the metal-tissue interface occurs because of an increased bone resorption or reduced bone formation. This can be the result of increased concentration of various ions, however, it has been shown by Cadosch that also **titanium** ions directly induce the differentiation of osteoclast precursors toward mature osteoclasts in ~20 % of individuals. This argument is of special importance since titanium was generally considered to be bioinert and even resistant to any oxidation and dissolution. In summary, studies demonstrate that metal wear and ions induce increased differentiation and activation of osteoclast precursors leading to a large number of mature osteoclasts able to effectively resorb the bone surrounding metal implants, but also potentially enhance biocorrosion of the implant, resulting in more ion release and the development of a vicious cycle [48].

As a consequence of corrosion, metal ions from implants have been found in various parts of the body: in the spleen, kidney, liver, brain etc. This was observed not only in the case of moving implants exposed to wear, e.g. hip-joint, but also in the case of non-moving implants such as screws, plates etc. [49-54]. Metals that form multivalent ions like titanium, aluminium and other have relatively high affinity to proteins, which after adopting the foreign metal ions, follow in vivo the biological route of iron (III) ions [55]. It has been suggested that in addition to a hypersensitivity reaction they have potential to induce autoimmune reactions and systemic diseases [54, 56-58]. Immune sensitivity, especially type IV, may be reflected distantly from the implant, and may even demonstrate a systemic reaction that remains unnoticed or may be incorrectly interpreted [9].

Different mechanisms of corrosion of implanted metal in the human body have been found to be responsible for release of significant levels of metal ions into the peri-implant tissues as well as into the systemic blood circulation from where metals can accumulate and reach also more distant parts of the body. Those ions bind to proteins in the blood plasma and can be transferred or even cause denaturation of those proteins. Titanium and other elements released from titanium implants have been observed in tissues and organs near implants [53].

For example, **aluminium** that is used as an alloying element in biomedical alloys, does not have an essential role in any biochemical system in any extant organism [59]. Although the quantity of aluminium in the implants is generally small and solubility of the metals is considered to be negligible, there is still some elution of this neurotoxic element after the implantation in the body. Aluminium was reported to accumulate in the nuclei of neuronal cells [14, 60]. It was also reported that accumulation of aluminium was detected in newly-formed lamellar bone after implantation of Ti plates containing 6 % aluminium [49].

Vanadium that is found in metallic alloys is on one hand vital element since it builds some enzymes and on the other hand, it can, when in excess, also have some (neuro)toxic effects on the organism [61]. The researches suggest that overall toxicity of vanadium compounds is low and that the most toxic effects of vanadium compounds result from local irritation rather than systemic toxicity. The daily intake of the US population is estimated to 10-60 μg [62]. In another review article it has been suggested that the toxicity of vanadium depends on its concentration and that the mechanisms behind are still unknown [63].

Magnesium is reported to be a body-friendly element. It is involved in cellular proliferation and this may have implications for cellular differentiation in innate immunity. Magnesium is generally protective against pro-inflammatory conditions. It is also the natural biochemical antagonist to the pro-inflammatory aluminium [64]. The oxidized, Mg-incorporated implant demonstrated significantly stronger integration in bone compared to the oxidized implant that consisted mainly of TiO_2 [65]. Another study concluded that the osteoclast surface was significantly reduced during the first four weeks around the $Mg(OH)_2$ cylinder, while an increase in osteoid surface was observed at the same time [66]. Thus, the enhanced bone formation and temporarily decreased bone resorption resulted in a higher bone mass around the slowly dissolving $Mg(OH)_2$ cylinder.

Magnesium metal was also suggested as a degradable orthopaedic material since with time it is replaced by natural bone and since its elastic modulus (45 GPa) resembles more to that of a natural bone than titanium [67]. Hypothesis is that enhanced osteoblast activity *in vivo* is due to increased concentration of magnesium ions or due to local alkalosis of the surrounding tissue. Still, highly excessive concentrations of Mg (above 25.5 μg/mL) can cause serious problems, such as muscular paralysis, hypotension and respiratory distress, as well as cardiac arrest (when Mg concentration exceeds 140 μg/mL) so also magnesium should be carefully monitored [68].

There were only a few investigations that were dealing with magnesium as potentially enhancing element for bone growth although magnesium is among the most abundant cations in human body, more than 50 % is located in bones.

Boron is an element that was also reported to have stimulating effect on bone formation while in material science processing it was proven to enhance densification of SiC. It was reported that presence of boron in cell medium did not statistically affect cell viability and proliferation while remarkable regulation in favour of osteoblastic function for collagen type I and other proteins connected with bone mineralization was detected in boron-treated groups [69]. Boron is also involved in calcium and bone metabolism while excess of boron has toxic effect on reproductive function. It has to be stressed that the amount of boron to induce toxic effects is relatively high (i.e. >70 mg/kg) [70, 71] and so boron does not present a great health risk.

Silicon was already mentioned in previous sections as a potential bone-stimulating element. It is, after oxygen, the most abundant element on earth. It was proven in 1972 that silicon was an essential element for the chicken and the rat [37]. An important role for silicon in bone mineralisation and connective tissue development was demonstrated. Also for calves, silicon seemed to be involved in the formation of extracellular matrix components and in calcium metabolism. Since then, silicon is claimed to have beneficial effects on several human disorders; for example osteoporosis, aging of skin, hair and nails and arteriosclerosis. It was shown that concentration of silicon is significantly higher in healthy children (1-18 years) than in healthy adults (19-60 years) and especially high concentrations of silicon in serum was detected in infants (< 1year). Compared to age-matched nonpregnants, the serum silicon content was very low in pregnant women and that indicates the increased need of silicon for developing foetus [72]. Silicon has no known role in biochemical reactions to describe its requirements by biota, but although it is not widely regarded as an essential element in mammals, it has been reported to have some beneficial actions, sometimes at rather higher amounts. Due to abundance of silicon in nature not many chances are that one would suffer from its deficiency. Among symptoms that point to silicon deficiency are reduced amount of water in cartilage and connecting tissues, loose connective tissue, wrinkled skin, varicose veins, cellulitis, soft and breakable fingernails, problems with gums and teeth. The primary effect of silicon in bone and cartilage appears to be on formation of the organic matrix that is later mineralized. Since bone and cartilage abnormalities are associated with a reduction in

matrix components, sufficient amounts of silicon are necessary to sustain healthy tissues. Additional evidence of silicon's metabolic role is provided by the finding that silicon is a major ion of osteogenic cells, especially of those that are in the highly metabolically active state. Silicon also makes important relationships with other elements, e.g. with calcium in the early stage of bone mineralization and with aluminium, by forming insoluble alumosilicates and thus preventing aluminium from crossing the blood-brain barrier [73]. It was also stated that in contrast to aluminium, silicon showed no toxic effect even when in increased amounts (serum concentration of Si in dialysis patients rose to 500-5000 µg/L due to problems with urinal excretion while physiological concentrations of Si in healthy population is 100 µg/L) [74].

1.6 Silicon carbide as a potential biomaterial

According to the reports in literature, silicon is beneficial element for human organism. Silicon in form of silicon dioxide (SiO_2) is the main component of bioactive glass and is released to human body by dissolution process [58]. Therefore, SiC, as a material with sufficient mechanical properties that always contains some SiO_2 was investigated as potential biomaterial.

SiC is material that is mainly used in engineering applications and extreme environments since it possesses unique combination of properties, such as high hardness and chemical resistance. Due to the covalent character of the bond it offers advantageous properties such as considerable strength at high temperatures and good thermal conductivity. Its mechanical properties are strongly dependent on its chemical composition and density. Examples for respective technical applications of SiC are cutting tools, bearings, parts in metallurgy and automotive, forming tools and components for space technology. The same covalent nature that provides these properties also tends to retard solid-state sintering without additives since the bulk diffusion in absence of ionic bonds is slow. Sintering without additives therefore remains a challenging task [75]. SiC is usually sintered either by aid of boron and carbon or in presence of a transient liquid phase, typically Al_2O_3-Y_2O_3-SiO_2. Vacuum sintering at temperatures above 1900 °C and high pressures results in relatively high densities and reasonable mechanical properties. Another possible route for densification that does not contain harmful elements is infiltration of bulk SiC with polymeric pre-ceramic precursor (e.g. polycarbosilane) and subsequent pyrolysis followed by crystallization [76]. Only recently SiC has been considered also as potential biomaterial [29, 31].

To author's best knowledge the first time SiC was mentioned as a potential biomaterial (attachment of cells on SiC surface) was in 1991 by Harmand et al. [36] and it was concluded that *"silicon carbide looks cytocompatible both on basal and specific cytocompatibility levels. However, fibroblast and osteoblast attachment is not highly satisfactory, and during the second phase of osteoblast growth, osteoblast proliferation is very significantly reduced by 30 %."* Later on SiC was again mentioned in the literature in 1995 [77] (toxicity towards the cells was checked), and after that cell response and attachment on fibres was checked in 1996 [78]. It was concluded that cells do spread on the surface of SiC fibres but preferably cells were suspended between the fibres and not attached along the long axis. It was shown in another study that although free SiC particles inhibited colony outgrowth to some extent (approximately one third at particle size 5 µm), SiC-coated pins did not cause any inhibition and acted similarly to uncoated titanium pins, suggesting that SiC is not cytotoxic material [79]. It was also concluded that the non-oxide ceramic materials Si_3N_4 and SiC, either produced via pressureless sintering or hot pressing, are cytocompatible for human mesenchymal stem cells, and allow for osteogenic differentiation [31]. Moreover, Si_3N_4 and SiC exhibit higher strength

and higher reliability than the clinically well-accepted oxide ceramics alumina and zirconia. Therefore, these non-oxide ceramics can now be considered for implant components of minimal invasive clinical applications like resurfacing hip prostheses and for tissue engineering concepts.

SiC has a potential to be used for orthopaedic implants (e.g. spinal implant) either as bulk, in porous form or as coating. Bulk SiC has not yet been widely explored for use in biomedical applications. For fabrication of porous SiC the most frequently applied technique is wood pyrolization followed by liquid silicon infiltration into carbon preform (i.e. biomorphic SiC). Silicon then reacts with carbon to form SiC, whereas the remaining silicon is then removed with hydrofluoric acid. However, closer look of the search results reveals that only in few cases the main motivation was to produce SiC for orthopaedic applications [80]. Also in these cases, more biocompatible coating (e.g. bioactive glass, calcium phosphates) was frequently used [81, 82]. Reports show that mechanical properties of such produced porous implants are quite high (compressive strength above 100 MPa) and therefore favourable for use in human medicine [80]. In 2010 two important articles on cytocompatibility of SiC were published; one entitled *"Cytocompatibility of high strength non-oxide ceramics"* and the second *"Cytocompatibility of bio-inspired silicon carbide ceramics"*, first dealing with SiC in general and second focusing on biomorphic SiC. Both are reporting beneficial response of the cells. Study, comparing BioSiC and titanium alloy by means of cell response has demonstrated that BioSiC presents a biological response similar to titanium controls, but it incorporates the unique property of interconnected porosity, which is colonized by bone tissue, together with lightweight and high strength for optimum biomechanical performance [83]. Authors conclude that *"Bio-derived SiC stands as a new material for biomedical applications."*

SiC was also proposed as a potential coating material of titanium-based total hip replacement implants. The idea was to prevent wear debris formation from the soft titanium surface [84]. SiC is a hard and tightly bonding ceramic surface material, and because of these physical properties it is not easily degradable. SiC deposited by radio-frequency sputtering on Ti resulted in significant corrosion resistance improvement reflected in decrease of corrosion current density by 300 times. Previous *in vivo* and *in vitro* studies have indicated that SiC is biocompatible depending on particle size for phagocytosis [85, 86].

Because of all the above mentioned arguments ceramics, especially SiC-based ceramics seems an ideal candidate for replacement of currently used implantable materials.

2 Aims and Hypothesis

World population is growing and life expectancy is increasing. In order to keep high quality of life, there is an emerging need for orthopaedic implants. With increasing use of orthopaedic materials new problems are identified, including toxicity of metal ions that are released from metallic implants and are connected to allergies and to delayed hypersensitivity.

It is believed that these problems can be prevented by employing non-metallic materials that still meet the demands for implantable biomaterials: mechanical properties and compatibility with cells. It is hypothesized that those criteria can be fulfilled by using suitably prepared silicon carbide (SiC) either in dense or in porous form.

In comparison to another widely used silicon-containing material, bioactive glass SiC is a material that is durable and does not dissolve extensively; that also preserves its mechanical properties and enables long-term use in the body. In comparison to metals that serve as permanent implants, pure SiC does not contain any harmful metal ions that would cause adverse reactions in the body; in general only silicon ions are released from the material. For several decades it is known that silicon has beneficial effect on osteoblasts and therefore it stimulates bone ingrowth.

The aim of this thesis was to prepare SiC without any potentially harmful elements and to verify its use for permanent bone implants (e.g. spinal implants) as an alternative to metallic ones. The goal was to prepare SiC-based ceramics with chemical composition that would provide optimal biological response and at the same time with suitable mechanical properties. Since SiC designed for engineering applications contains elements that could cause undesired or even toxic response in the organism, the aim of our work was also to check whether sintering of SiC without such additives is possible. The hypothesis is that high green density is of crucial importance and can be achieved in different ways, of which the most promising is colloidal processing.

Besides sintering without any additive “conventional” sintering with addition of boron and carbon and also sintering in open air in presence of MgO were checked. In order to avoid any potentially adverse short or long-term effect, aluminium was avoided and instead, bone growth stimulating elements were included (Mg, B), preliminary *in vitro* studies of the materials with HepG2 and HeLa cells were also performed.

Although elastic modulus of dense SiC is high compared to bone it can be substantially lowered by porosity. Therefore, shielding effect that causes degradation of an underlying bone can be avoided. Besides, increased porosity positively affects bone-forming and enables cell ingrowth.

The work comprises three main stages:

a) Preparation of green parts of either pure SiC, or with addition of sintering additives, with sufficient green density and comparison of dry pressing with colloidal processing
b) Sintering of green parts in vacuum or in open air in order to achieve sufficient mechanical properties while still maintaining some porosity
c) Testing of samples regarding mechanical properties, wetting behaviour, leaching of ions, magnetic properties and finally cell response.

3 Materials and Methods

Green samples were formed by two different routes; dry pressing (uniaxial and isostatic) and colloidal shaping, i.e. electrophoretic deposition.

3.1 Dry pressing

Commercially available ß-SiC powder (SiC BF-12, H. C. Starck, Germany, mean particle size 0.5 µm. Starting powder has a composition of 80.4 % ß-SiC (3C), 8.6 % a-SiC (6H) and 11 % of amorphous phase, SiO_2) was either uniaxially (100 MPa) or isostatically (740 MPa) pressed, while combination of powders (SiC with addition of B_4C (boron carbide, grade HS, H. C. Starck, Germany) and carbon black (grade M-1300, Cabot Europa, France) or with MgO (magnesium oxide, 99.5 %, Ventron, Alfa Produkte, Germany, 325 mesh)) was first homogenised in ethanol and then suspensions were left to dry at elevated temperature (60 °C). For solid-state sintering, carbon was added in the form of carbon black, and boron was added as boron carbide. For sintering in air magnesium was introduced in the form of MgO. All pellets were uniaxially and then isostatically pressed and sintered.

3.2 Suspension preparation

Suspensions were prepared in such way that the surfactant was first added/dissolved in the liquid medium (TMAH (tetramethylammonium hydroxide, Merck, Germany) or PEI (polyethyleneimine, branched, M.W. 10000, 99 %, Alfa Aesar, Germany) in water or ethanol, respectively) to ensure good dispersion of the powder that was subsequently added. Suspensions were mixed using ultrasonic finger for 3 minutes at 50 % power and 50 % frequency. pH and O.pH were measured using pH meter with glass electrode (pH meter Knick Portamess 913 pH). O.pH (operational pH) denotes the value measured in ethanol suspension with glass pH electrode and in this work serves mainly for comparison of various ethanol-based suspensions. Conductivity of the suspensions was measured with conductometer (Knick Portamess 913).

In order to stabilize the suspension, CTAB (cetyl trimethyl ammonium bromide, Sigma) and PEI (polyethyleneimine) were used as cationic surfactants, while NaOH (Kemika, Croatia) and TMAH (tetramethylammonium hydroxide) were used to increase the negative values of the zeta potential. The main requirement that has to be fulfilled when choosing the proper deflocculant is its solubility in medium from which the suspension is prepared. For example, CTAB is practically insoluble in ethanol while PEI is soluble in ethanol and insoluble in cold water. PEI is soluble only in hot water at low pH values but since this is not relevant for our work, PEI was only used in ethanol suspensions. TMAH can be only added in the form of aqueous solution and was therefore not used in ethanol suspensions while NaOH can be used as O.pH modifier also for ethanol suspensions since it is soluble. Structures of surfactants are shown in Figure 1.

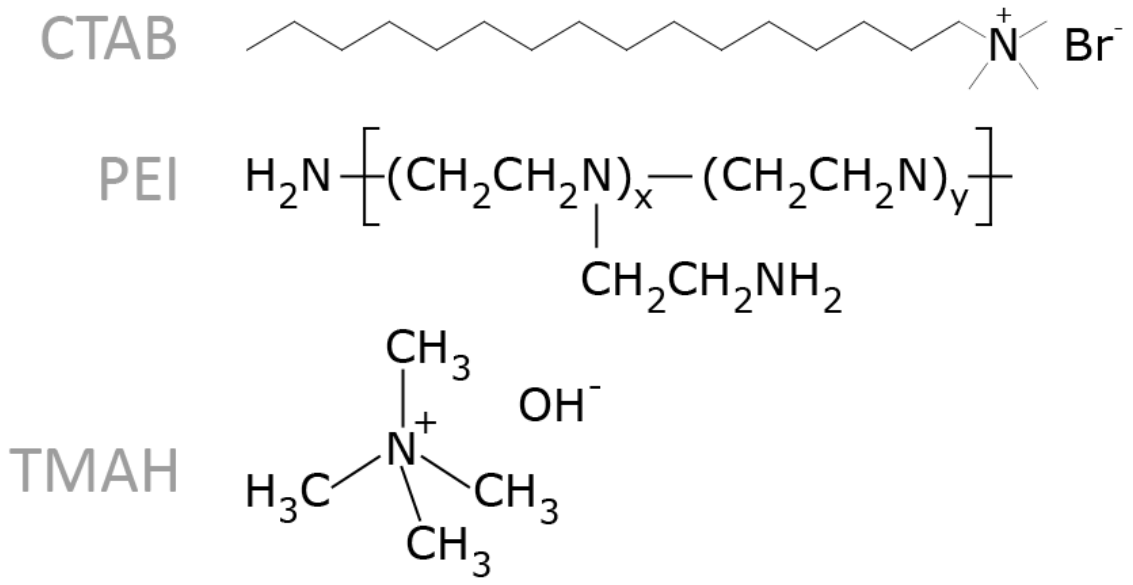

Figure 1: Structures of surfactants used in this work

The suspensions were prepared with distilled water and a sufficient amount of the additive; they were then dispersed and homogenised using an ultrasonic finger (UP400S, 400 W, 24 kHz with an acoustic power density of 10^9 W/m^2, Hielscher Ultrasonics, Germany) for 3 min. The surface charge of the particles (zeta potential, ZP) in as-prepared or additionally stabilized suspensions at 25 °C was determined using zeta meter (ZetaProbe, Colloidal Dynamics, USA). The correlation with the pH, the amount of additive and the conductivity was monitored and quantified. The concentration of the suspensions varied from 2.5 to 60 wt. %, while the amount of CTAB and TMAH varied from 0.05 % to 0.4 % with respect to the mass of the powder. The amount of PEI varied from 0.5 % to 2.15 %. Suspensions with different solids contents were prepared from a 60 wt.% suspension by dilution. For the determination of the zeta potential's dependence on pH we used 3 wt. % suspensions. Since it was not possible to disperse carbon black in water due to its hydrophobicity, surface of the powder was oxidized using concentrated nitric acid (HNO_3, Sigma).

3.3 Electrophoretic deposition

The electrophoretic deposition (EPD) experiments were performed from aqueous or ethanol SiC suspensions with various additives. Depending on surface charge either anodic or cathodic depositions were performed. Depositions were performed on graphite electrodes (2x2 cm^2 or 4x4 cm^2) that were placed on 2 cm distance. Applied electric field strength varied from 7.5 to 30 V/cm while in the case of SiC/B_4C/C suspension co-deposition was performed at constant current 40 mA. Deposits were left to dry at ambient temperature and humidity to reach a constant mass.

For ethanol suspension electric field strength was risen up to 150 V/cm to ensure faster deposition. Due to longer deposition times ethanol suspensions were stirred during deposition. Samples were deposited either directly to the electrode or onto a cellulose membrane that was placed in front of the electrode in order to prevent direct contact between electrode and deposit, thus preventing pore formation due to bubble evolution. For the electrophoretic co-deposition (co-EPD) 50 wt. % of SiC and 3 wt. % of MgO were admixed into EtOH, and 1.5 wt. % PEI according to the mass of SiC was added as a

dispersant. The deposits prepared from ethanol suspensions were dried in ethanol rich atmosphere to prevent extensive cracking due to faster drying rates. For measurement of mechanical properties (ball-on-three-ball) disc-shaped specimens were produced and that was achieved by direct deposition into polymeric preform that was glued on the electrode.

3.4 Deposits evaluation

The relative density (% of theoretical density, % TD, also denoted as vol.% of solids) of the EPD parts was calculated from the ratio between the mass of the wet and dry deposits using the formula:

$$\%TD = 100/(1+\rho_{SiC}(m_{wet}/m_{dry}-1))$$

Where, m_{wet} and m_{dry} correspond to the mass of the wet and the dried deposit, respectively. The densities of the green and sintered samples were additionally determined with a densitometer (Densitec, Exelia AG, Switzerland) on the basis of Archimedes method. Porosity of few deposits as well as pore size distribution was determined by Hg intrusion technique.

3.5 Sintering/densification

Sintering was performed either in open air or in vacuum, depending on the composition of the samples.

Samples without additives and samples containing boron (in the form of boron carbide) and carbon (in the form of carbon black) were sintered in Astro furnace (Thermal Technology Inc.) in vacuum (<100 mtorr = $1.3\cdot10^{-4}$ bar) at 2000-2150 °C; that was determined from the literature [87]. The sintering programme was set to a heating and cooling rate of 600 °C/h and holding time 2 hours.

Samples without additives and samples containing magnesium oxide were sintered in open air at 1350 °C in Nabertherm furnace (model RHTC 80-450/15). Temperature was determined using heating microscope on the MgO-containing SiC sample. The sintering programme was set to a heating and cooling rate of 200 °C/h and a 1 h hold at 1350 °C.

3.6 Surface modification

In order to obtain more bioactive surface, the bioactive glass coating was applied to the samples. Two-component polymeric bioactive glass was synthesized by mixing tetraethoxysilane (TEOS, Sigma) with calcium nitrate tetrahydrate ($Ca(NO_3)_2\cdot4H_2O$, Sigma) that was dissolved in ethanol. 1 M HNO_3 (Sigma) was added to slow the gelation process and water was added to enable the hydrolysis of TEOS. Sintered SiC samples were then immersed into polymeric sol, left to dry and heat treated in open air, following the programme: heating rate 200 °C/h, holding time 30 min @ 600 °C, heating to 850 °C (heating rate 200 °C/h) and holding time 30 min. Cooling rate was also set to 200 °C/h.

3.7 Microstructure evaluation and wetting angles

Microstructure of either green or sintered samples' fracture surface or polished surface was observed under SEM Jeol 5800 and SEM Jeol 7600F (JEOL Ltd., Tokyo, Japan). Elemental composition of the samples was determined using Energy dispersive X-ray spectroscopy (EDS) system and INCA Operator software for quantitative determination and ZAF correction of the results. Some samples were examined under TEM Jeol

JEM-2010F. Elemental composition was determined using EDS and crystal structure was determined by selected area electron diffraction (SAED).

The samples were analysed using X-ray diffractometry (XRD) (Endeavor D4, Bruker AXS) monitoring 2θ from 10° to 70° with a step of 0.02° for 3 s and the phases present in the samples were determined according to DIFFRACplus Evaluation Package Release 2003-EVA V9. The crystalline phases were identified according to the JCPDS powder-diffraction files.

Wetting angles were measured with distilled water or serum with Theta Lite optical tensiometer (Attension, Biolin Scientific, Finland).

3.8 Testing of mechanical properties

The flexural strength was determined on 5 to 10 samples of each type using a ball-on-three-ball test on an Instron 1362 or Galdabini Quasar 50 with a head speed of 1 mm/min using disc-shaped samples with diameters from 15 to 18 mm and thicknesses of ~ 4 mm. Samples were produced either by dry pressing or by EPD. After drying and sintering the discs were grinded to achieve parallel planes and their flexural strength was measured. The elastic modulus was measured with an impulse-excitation-measurements device RFDA MF basic (IMCE, Belgium) and additionally estimated with a Vickers nanohardness tester, Fischerscope H100C (Helmut Fischer, Germany), with a load of 1000 mN. Hardness of the material was measured with Vickers indentation pyramid. The fracture toughness was estimated on the basis of the Vickers indents and calculated using the equation proposed by Niihara [88]:

$$K_{Ic} = 0.035 \cdot \frac{a}{l^{1/2}} \cdot E^{0.4} \cdot \left(\frac{HV}{\phi}\right)^{0.6}$$

Where K_{Ic} is fracture toughness in MPa·m$^{1/2}$, a is the half of the diagonal left by the indenter in μm, l is the length of the crack in μm, E is the elastic modulus in GPa, HV is Vickers hardness in GPa and ϕ is ~ 3.

3.9 Magnetic measurements

Magnetic measurements (response of the samples against external magnetic field) were carried out using a vibrating sample magnetometer VSM LakeShore 7003 device at room temperature, field ranging from –15 kOe to +15 kOe. Samples were cut into platelets of 7x7 mm^2; results were normalized to 1 g of each sample.

3.10 Inorganic bioactivity

Inorganic bioactivity was examined by immersion of samples in simulated body fluid (SBF) for 3 weeks at 36.5 °C, following protocol established by Kokubo [89]. SBF is a solution that has concentration of ions similar to that in human blood plasma (Table 2). The difference is that SBF does not contain any proteins that are naturally present in human plasma, concentration of HCO_3^- ions is approximately 6.5-times lower in SBF (4.2 mM vs. 27 mM), concentration of chloride ions is about 50 % higher and there are no sulphate ions in originally proposed SBF. Besides, as a buffering agent for SBF Tris buffer is used that is not present in living organisms. Therefore, SBF serves as an approximation of the body response to the implant material; appearance of hydroxyapatite crystals on the surface suggests the bioactivity of the tested material. Bioactivity was tested on as-prepared samples as well as on samples coated with bioactive glass.

Table 2: Ion concentration of original SBF and human blood plasma [89]

	Ion concentration (mM)							
	Na^+	K^+	Mg^{2+}	Ca^{2+}	Cl^-	HCO_3^-	HPO_4^{2-}	SO_4^{2-}
Human blood plasma	142.0	5.0	1.5	2.5	103.0	27.0	1.0	0.5
SBF	142.0	5.0	1.5	2.5	148.8	4.2	1.0	0

3.11 Dissolution of elements

The dissolution of elements from the sintered samples was determined in a way that samples were first extensively cleaned by ultrasonication in MiliQ water. Afterwards, they were soaked in physiological solution (0.9 % NaCl in MiliQ water) for half an hour in ultrasonic bath to remove potential impurities from the surface and then the samples were immersed in 10 mL of fresh solution for various periods (3, 5, 7 or 10 days) at 36.5 °C in static conditions in aluminium-free polyethylene containers. 10 mL of solution was also placed in containers without samples to serve as blank. Samples were then removed and concentration of ions (with emphasis on magnesium and silicon ions) was measured using inductively coupled plasma connected to mass spectrometer (Agilent 7500ce ICP-MS, Agilent Technologies, Tokyo, Japan). Three parallels were made for each sample, blank solution served as determination of background concentration of ions that was then subtracted from measured values.

3.12 Cell response

In order to determine cell response to tested materials, we used two different cell lines, HeLa (human cervical cancer cell line, endothelial cells) and HepG2 (human hepatoma cells). Cells were seeded onto the surface of tested materials in two parallels; one was used for assessing cell viability and other for observation under scanning electron microscopy (SEM). Samples (round discs) were placed into 12-well microtitre plates (Corning Costar Corporation, Corning, New York, USA). 50 µL of the suspension of HeLa (HepG2) cells at density of 10^6 cells/mL was spread over the samples and incubated for 2 hours at 37 °C to allow the cells to attach. Then the 2 mL of complete cell growth medium was added and incubated for 24 h at 37 °C and 5 % CO_2. As a control glass covered with polylysine was used.

The cell viability was determined by the trypan blue exclusion assay. It is based on the principle that viable cells possess intact cell membranes that exclude certain dyes, such as trypan blue, whereas dead cells do not. This method is widely used as an objective method of determining viable cell count. At the end of the 24 h incubation cells in the first parallel (assessment of cell viability) were washed with phosphate buffer saline (PBS), harvested by trypsinisation, washed and re-suspended in 500 µL of complete cell growth medium. Then the 10 µL of cell suspension was mixed with 40 µL of 0.4 % trypan blue. A drop of trypan blue/cell mixture was placed to a haemocytometer and the unstained (viable) and stained (nonviable) cells were counted. The % of viable cells was determined by dividing the number of unstained cells by the total number of cells (stained+unstained). Three independent experiments were performed.

Another parallel was prepared for SEM. Cells were washed with PBS and fixed with 5 % glutaraldehyde solution in PBS. After one hour the samples were washed with PBS and dehydrated using series of alcohols with increasing concentration (from 20 to 100 vol.%). Samples were left to dry overnight, sputtered with carbon and observed under SEM.

4 Results

4.1 Properties of suspensions and electrophoretic deposition

Success of electrophoretic deposition relies on optimization of colloidal properties of the starting suspension. Colloidal properties and stability of suspensions depend on surface charge of the particles (i.e. zeta potential, ZP) but also on conductivity (S) and pH. Zeta potential curve as well as isoelectric point is characteristic for each powder, according to its surface layer (e.g. SiC particles that are covered with thin SiO_2 layer behave more like SiO_2). Therefore, zeta potential curve and conductivity of the suspension were determined first. The results of such titration for aqueous suspension containing 25 wt.% SiC are shown in Figure 2.

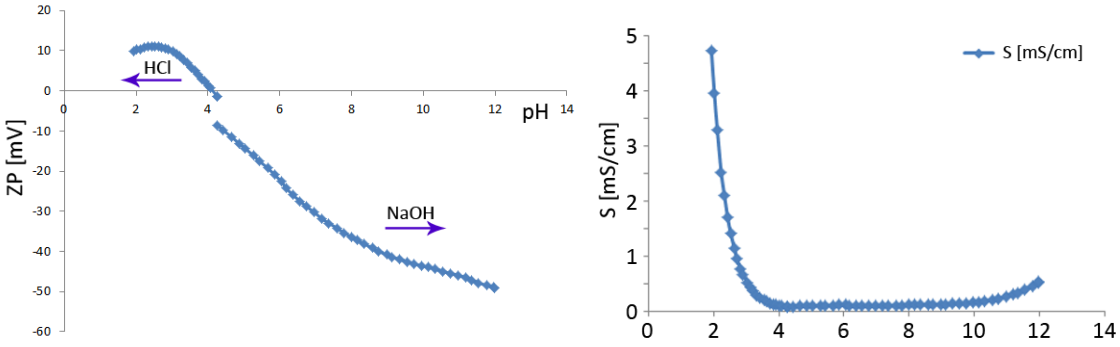

Figure 2: Dependence of zeta potential and conductivity of 25 wt. % aqueous SiC suspension; HCl and NaOH were used for pH modification

Natural pH of as-prepared suspension is 4.2 and zeta potential at that pH, when suspension is not treated with ultrasonic finger, is slightly negative. Addition of HCl lowers the pH value, while ZP is consequently increased, following the course of sigmoidally shaped curve. Isoelectric point (i.e. pH value where amount of positive charges equals the amount of negative charges on the surface so the net charge is zero) was determined to be at pH 4.1. With further additions of HCl ZP increases while pH decreases to 2.5; there the curve reaches plateau and finally inverts and ZP is again lowered. That can be also described as conductivity effect: when conductivity is too high, free electrolyte causes increase of ionic strength and thus disturbing the electrostatic force among particles. Particles can approach each other to the distance where also attractive forces are not negligible and therefore the suspension becomes less stable [90].

To determine the second part of the curve, pH and ZP were modified with addition of NaOH. Base increases pH value of the suspension and also the (negative) surface charge is increased. Meanwhile conductivity remains fairly low (below 0.3 mS/cm at pH 11). Stability of the suspension is increased with increasing surface charge and such suspension is potentially appropriate for electrophoretic deposition. The origin of surface charge on SiC particles is ascribed to ionization of surface oxide/oxycarbide layer that is naturally present on the particles [91]. Therefore the major functional group on the surface is silanol group and the surface charging of SiC powder in water is attributed to

the dissociation of these silanol groups according to the following reactions:

$$[SiOH_2]^+ \xleftarrow{H^+} [SiOH] \xrightarrow{OH^-} [SiO]^- + H_2O$$

According to the literature NaOH can be also replaced by tetramethyl ammonium hydroxide (TMAH), a strong organic base that also promotes the dissociation of the silanol groups inducing more negative charge to SiC surface [92]. The comparison between addition of NaOH and TMAH is shown in Figure 3.

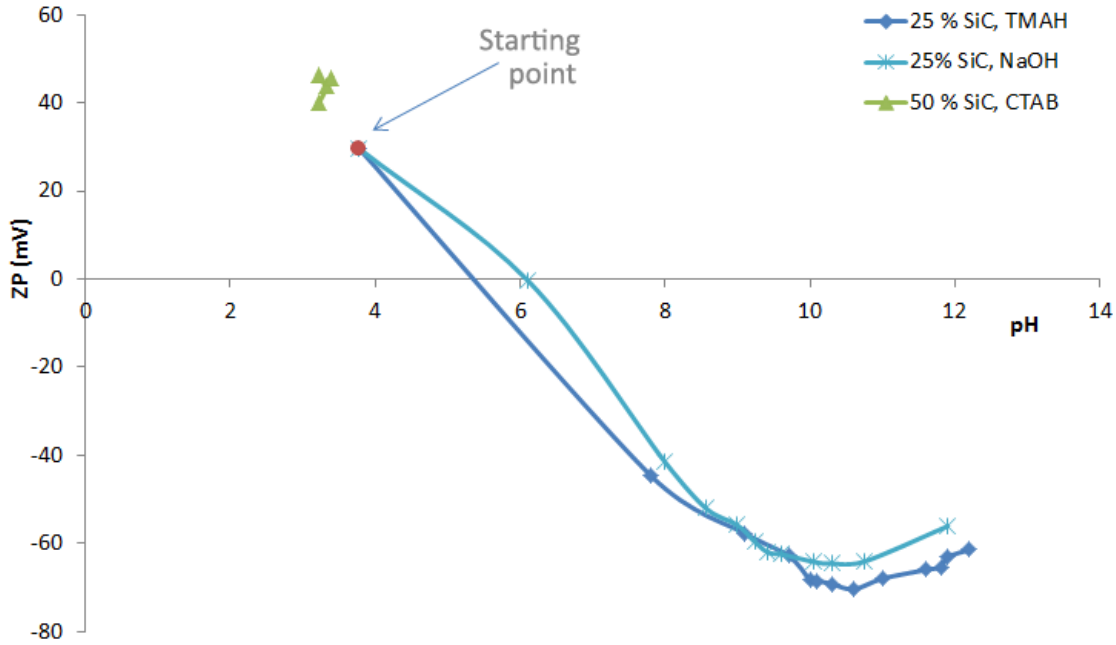

Figure 3: Dependence of zeta potential of 25 wt.% aqueous SiC suspension on addition of NaOH or TMAH and effect of CTAB addition in amounts 0.27 to 0.67 wt.%

Some literature suggests that TMAH also acts as a surfactant and not only as pH modifier [90] but from our measurements this is clearly not evident. Surfactants are in general compounds that bind to the surface of the particles and besides modifying the surface charge they also cause the shift in isoelectric point of the powder. From Figure 3 we can see that course of both ZP curves is practically the same and so on the base of these results we cannot confirm that TMAH also acts as a surfactant but only as a base. The reason for mismatch between ZP curves on Figure 2 and Figure 3 is that in the second case bases (either TMAH or NaOH) were added dropwise and between each addition suspension was ultrasonically mixed while in the first case the stirring was only mechanical. Same turn in zeta potential as it was observed in Figure 2 after excess addition of HCl is observed in Figure 3 after the optimum point (point of highest surface charge) in addition of base is reached (pH ~ 10.5), the reason being the same as already described above.

From the course of ZP curve for SiC we can see that it is relatively easy to obtain highly negative surface charge while for the positive charge this is not the case. If a necessity for highly positive surface charge of SiC particles in aqueous suspension arises, cationic surfactant has to be used. While there is an abundance of anionic surfactants, we are more limited when choosing a cationic surfactant. Beside positive charge, requirement that has to be fulfilled is solubility of the compound in water.

For our purpose we have chosen cetyltrimethylammonium bromide (CTAB); structure is shown in Figure 1. CTAB is a cationic deflocculant with long hydrophobic chain and

positively charged ammonium functional group. It binds to the negative sites of the particles, therefore net surface charge is more positive and because of the long chain CTAB also acts as a steric stabilizer. Increase in zeta potential is not as high as in the case of polyelectrolytes but it is still possible to obtain relatively stable suspension. Effect of CTAB addition on zeta potential is shown in Figure 3 and it can be seen that addition of CTAB to as-prepared 50 wt.% SiC suspension results in increase of ZP from +30 to +45 mV. pH remains practically constant while conductivity slightly increases (see Figure 4), mostly due to presence of free Br^- ions. However, use of CTAB is somehow limited since CTAB (due to its long nonpolar chain) also acts as a foaming agent and ultrasonication of the suspension results in bubble formation.

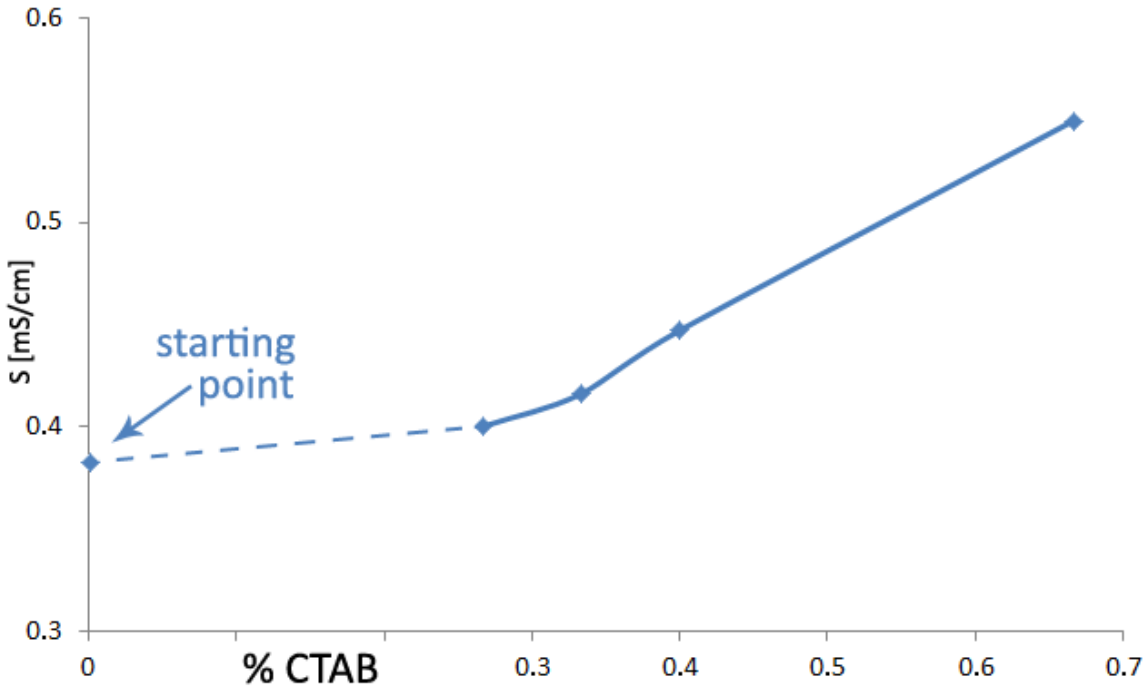

Figure 4: Effect of CTAB addition on increase of conductivity of 50 wt.% aqueous SiC suspension

As it was stated before that conductivity also plays very important role considering efficiency of EPD, in Figure 4 effect of CTAB on conductivity is presented. Conductivity increases nearly linearly with CTAB addition and reaches 0.55 mS/cm at 0.67 % of CTAB. Since our main purpose was to produce a green deposit of good quality and high green density, effect of CTAB on electrophoretic deposition was also checked. Mass of wet and dry deposit as well as volume % of solids in dry deposit are shown in Figure 5.

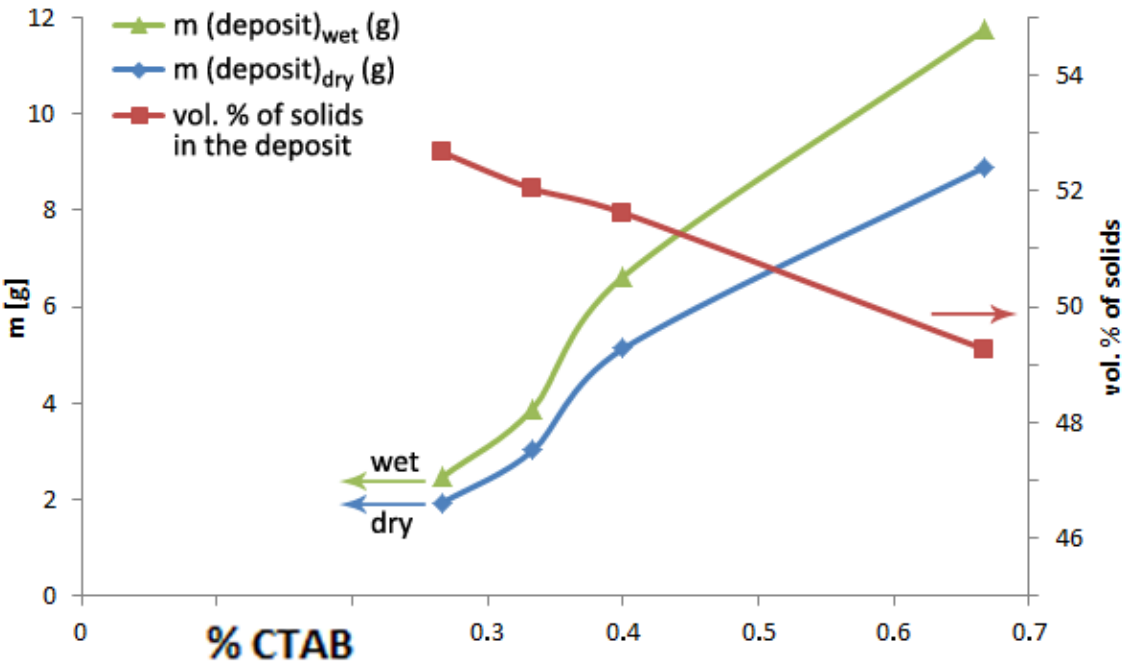

Figure 5: Dependence of deposited wet and dry mass from 50 wt.% aqueous SiC suspension and volume % of solids in dry deposits in relation to addition of CTAB

All depositions were carried out onto graphite electrodes for 5 minutes at 30 V/cm. Positively charged particles deposit onto cathode where in water reduction of hydrogen is a simultaneous process. Therefore in all deposits, disregarding green density, hydrogen bubbles got entrapped, resulting in macroporosity of the samples. The volume % of solids in the final deposit does not exceed 53 % in any case. Also published values for green density of deposits produced by EPD from suspensions containing CTAB are comparably low [93] (i.e. below 40 vol.%) and therefore another possibility had to be explored in order to reach higher green density and homogeneous deposit.

In order to thoroughly evaluate the suspension firstly the effect of solids content on the parameters of the unmodified suspension was observed. The decrease of pH with increasing solids content is shown in Figure 6 while the dependences of zeta potential as well as conductivity are shown in Figure 7 and Figure 8, respectively, in all cases both for aqueous and ethanol suspensions.

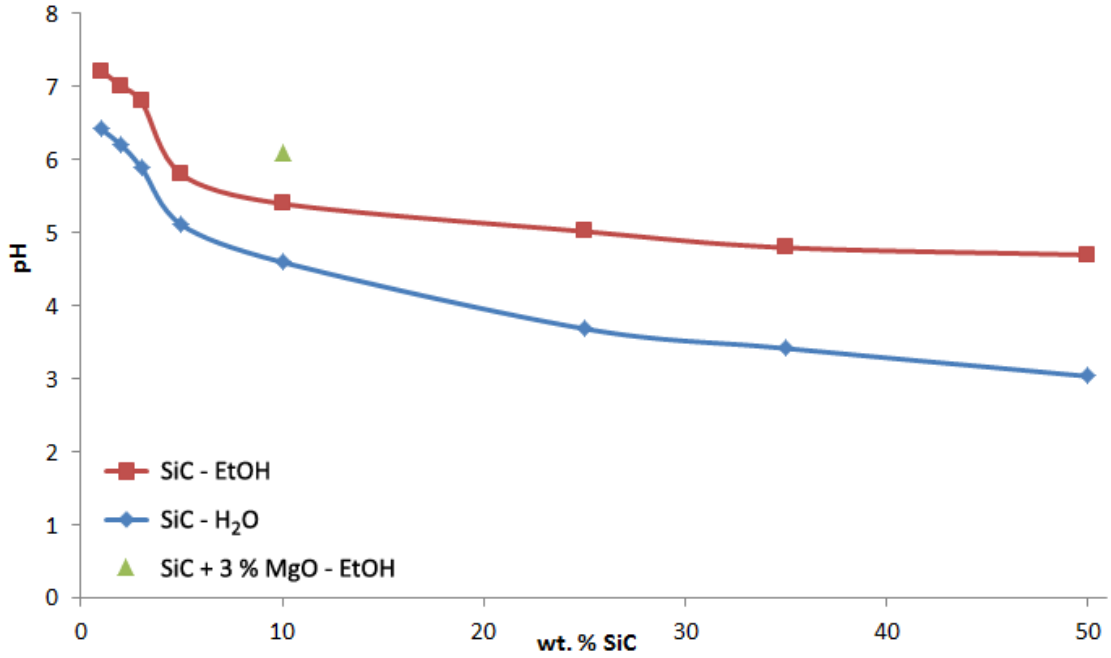

Figure 6: Dependence of pH/O.pH of SiC on solids content in water and ethanol

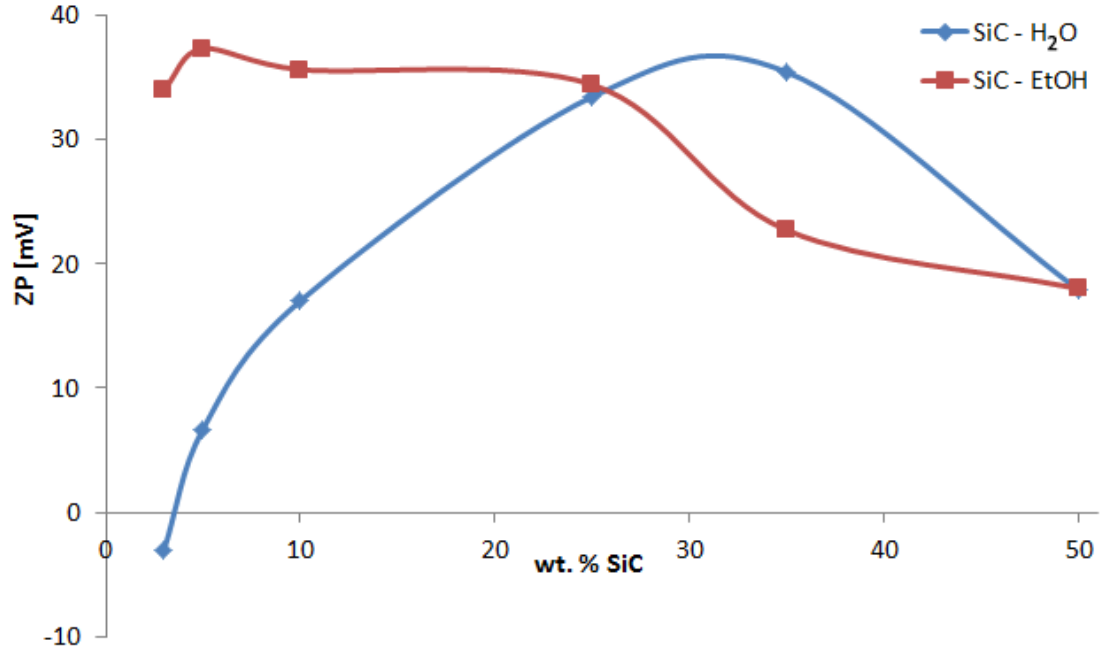

Figure 7: Dependence of zeta potential of SiC on solids content in water and ethanol

In Figure 7 changing of zeta potential with increasing solids content in aqueous and ethanol suspensions is shown. It is clearly seen that ZP in aqueous suspensions rises with increasing solids content. Reason for that lies in decrease of pH values of the suspension; this dependence is shown in Figure 6. It was mentioned before that the surface of SiC particles is covered by thin oxidized layer consisting of SiO_2 that, when put into water, reacts acidic. Higher the amount of SiC in the suspension, more SiO_2 dissolves and pH is

consequently lower. Since it was already shown in titration curve in Figure 2 that zeta potential increases with decreasing pH, also the increase of ZP with increased solids content can be ascribed to the same cause. When amount of SiC in the aqueous suspension exceeds 35 wt.% ZP is again lowered. Though viscosity was not measured here, it was seen with a naked eye that due to high amount of powder suspension became highly viscous. Since particles are only electrostatically stabilized, repulsion forces are not strong enough to sustain stable suspension. Same trend can be observed in ethanol suspensions, only that threshold value for stable suspension is lower (viscosity increases already below 35 wt.% of solids) since dielectric constant of ethanol compared to water is lower (24 vs. 80, respectively).

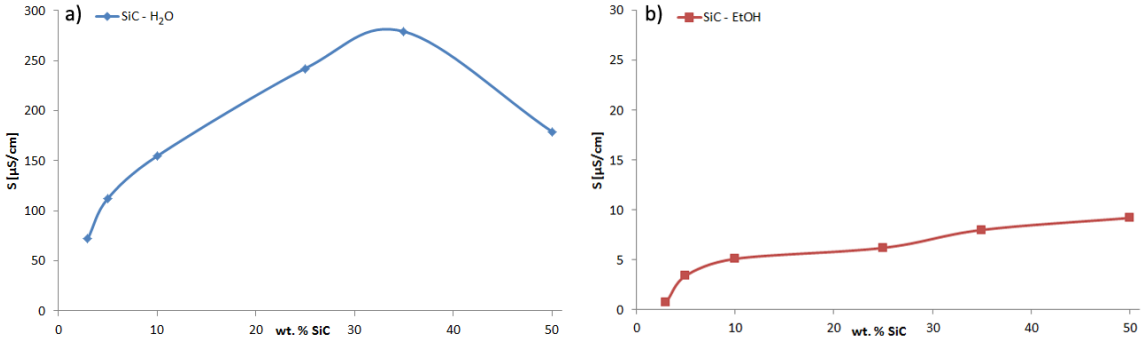

Figure 8: Dependence of conductivity of the SiC suspension in a) water and b) ethanol on solids content

Same trend as for zeta potential was observed in case of conductivity dependence on solids content in aqueous suspensions (see Figure 8a); at first conductivity rises with increasing amount of powder but when the viscosity increases, also the conductivity, same as zeta potential, is decreased. Besides, comparison between curves on Figure 8a and b reveals that conductivity is for an order of magnitude higher in water than in ethanol suspensions.

Additive-free aqueous suspension with the highest zeta potential (i.e. 35 wt.% of SiC, ZP ~ +35 mV) was also subjected to electrophoretic deposition but no firm deposit could be produced. This can be ascribed either to insufficient values of zeta potential or to low conductivity that could be too low for successful EPD [94]. Therefore ZP of suspensions was modified with addition of TMAH and amount of solids was even more increased. In Figure 9 properties of suspensions for deposition (pH, conductivity, ZP) are related to properties of formed deposits.

4.1.1 Effect of TMAH addition

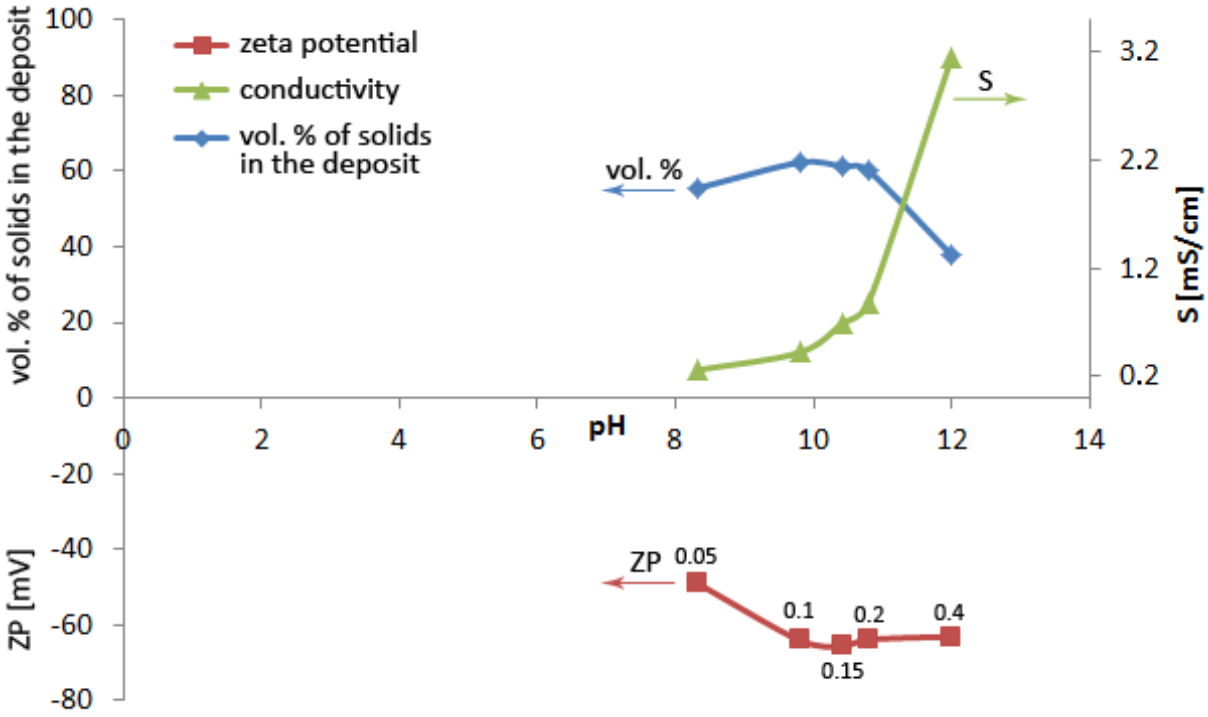

Figure 9: Effect of TMAH addition on the parameters of the suspension and deposit. Next to the points of ZP curve addition of TMAH (wt. % according to the mass of SiC) is denoted.

We have observed the effect of addition of TMAH on colloidal properties of the 60 wt.% aqueous SiC suspension and in parallel also on the quality of the deposits prepared from these suspensions. All the depositions were performed at same conditions (i.e. 5 minutes at 30 V/cm to graphite electrodes with 2 cm distance). Starting point (i.e. ZP and conductivity of 60 wt.% SiC suspension without additives) is not indicated in Figure 9 since due to too high viscosity it is not possible to prepare that concentrated suspension without additives. However, taking into account the results for 50 wt.% suspension (such suspension has ZP +18 mV at pH 3) we can suppose that the zeta potential of 60 wt.% suspension would be slightly positive.

First addition of TMAH (0.05 %) causes crossing of the isoelectric point and results in negative ZP (-49 mV) at simultaneous increase of pH to 8.3. When EPD from this suspension was performed the resulting deposit contained 55.5 vol.% of solids. Further addition of TMAH even increases the charge on the surface (up to -65 mV), pH rises to ~10 and conductivity though increased still remains moderately low (~0.5mS/cm). Also deposits exhibit higher green density (highest value was 62.3 vol.% at 0.1 % TMAH). 0.4 % of TMAH presents excess amount and although ZP was not significantly reduced, conductivity rised to 3 mS/cm at pH 12.

The consistence of the deposit produced from such suspension was really loose; less than 38 vol.% was reached. Besides, extensive water electrolysis can, due to intense bubble formation, even prevent the deposit from adhering to the surface of the electrode. These results also confirm the statement of Moreno [94, 95] that the successful deposition and packing of particles are closely related to the conductivity of the suspension. In suspensions with high conductivity ions are the main charge carriers and motion as well as deposition of the particles is somehow hindered. Besides, due to high conductivity the intensity of the electric field decreases, decreasing the electrophoretic

mobility of particles and rate of deposition [96]. Furthermore, the electrical double layer on the particles is thinned and this drastically reduces the stability of the suspension. From the graph on Figure 9 one can also see that the most optimal area for anodic EPD from aqueous SiC of suspension is around pH 10. Optimized suspension (i.e. 0.1 % of TMAH or setting pH to 10) was used in further experiments.

In the literature, no exact numbers for the ideal conductivity of SiC suspensions suitable for EPD have been found since most of experiments explaining mechanisms of EPD were made with alumina suspensions. For the latter, some authors [94] are reporting on "conductivity window" for aqueous alumina suspensions, i.e. the region of conductivity that enables successful EPD. Those values are also proportional to solids content in the suspension. For example, reported values for 5 and 10 wt.% alumina suspensions were 140-160 and 250-320 µS/cm at 20 °C, respectively [96]. In our experiments we have ascertained that the maximum conductivity that still enables successful deposition should not be more than 0.8 mS/cm for 60 wt.% suspension.

4.1.2 Effect of suspension concentration

Another suspension-related parameter that can be modified is concentration of solids. The influence of the solids content in optimal suspensions for EPD on the zeta potential and the conductivity was verified.

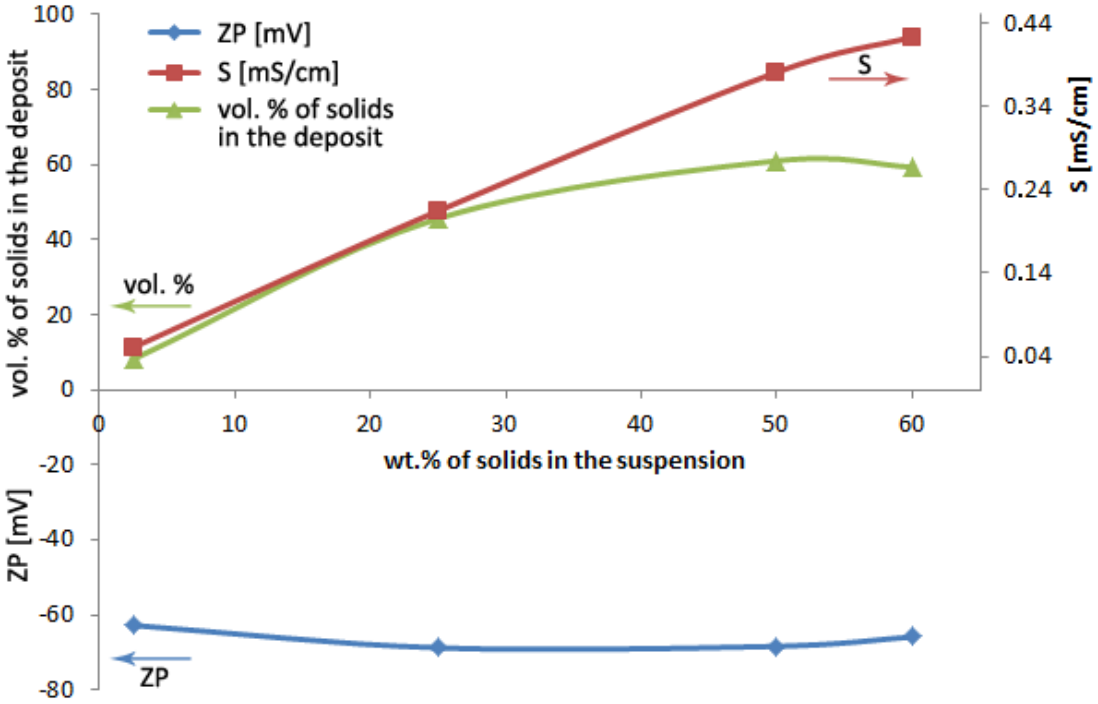

Figure 10: Dependence of zeta potential and conductivity of aqueous SiC suspension with 0.1 % TMAH addition and the vol.% of solids in the resulting deposit on the solids loading of the suspension

In order to keep the ratio between the powder and the TMAH constant, the suspensions were prepared by diluting the most concentrated (i.e. 60 w.%) suspension. The pH change after the dilution was negligible. From Figure 10 it is evident that the effect of the solids content on the zeta potential is minor, while the conductivity increases almost linearly with an increasing solids loading. The effect of solids content on the deposition is frequently overlooked in the literature since it is considered not to affect the quality of the

EPD, but only the deposition rate [96]. However, our results, presented in Figure 10 show that the final amount of powder in the wet deposit is greatly affected by the starting concentration in the suspension. The difference between 50 and 60 wt.% suspension is minor in terms of density of the final deposit (61 vs. 60 vol.%) while the rate of deposition is much higher in the case of more concentrated suspension (11.6 g vs. 7 g regarding the mass of wet deposit after 10 minutes of deposition). Lowering solids content (to 25 wt.%) results in lower conductivity, but also lower deposition rate (only 4.25 g after 10 minutes) and less solids (45.5 vol.%) in the final deposit. When amount of SiC in the suspension is further lowered to 2.5 wt.%, this is also reflected in the deposition; obtained deposit was of very poor quality, its density was below 10 vol.%. Also the conductivity of such suspension was low (50 µS/cm). We can assume that the suspension is not anymore in aforementioned “conductivity window” and so deposition was not efficient.

4.1.3 Effect of electric field strength on deposition

We have observed the effect of electric field strength on EPD from aqueous suspensions containing optimal amount of TMAH to reach high zeta potential while maintaining reasonably low conductivity. Suspensions from which depositions were performed contained 60 wt.% SiC and TMAH was added to adjust pH to 10. The obtained results are shown in Figure 11. It can be seen that applied electric field strength in the observed range (from 7.5 to 30 V/cm) does not essentially affect the fraction of powder (i.e. vol.%) in the resulting deposit, the main effect of the electric field strength is rate of deposition; considering the mass of the formed deposit this correlation is nearly linear.

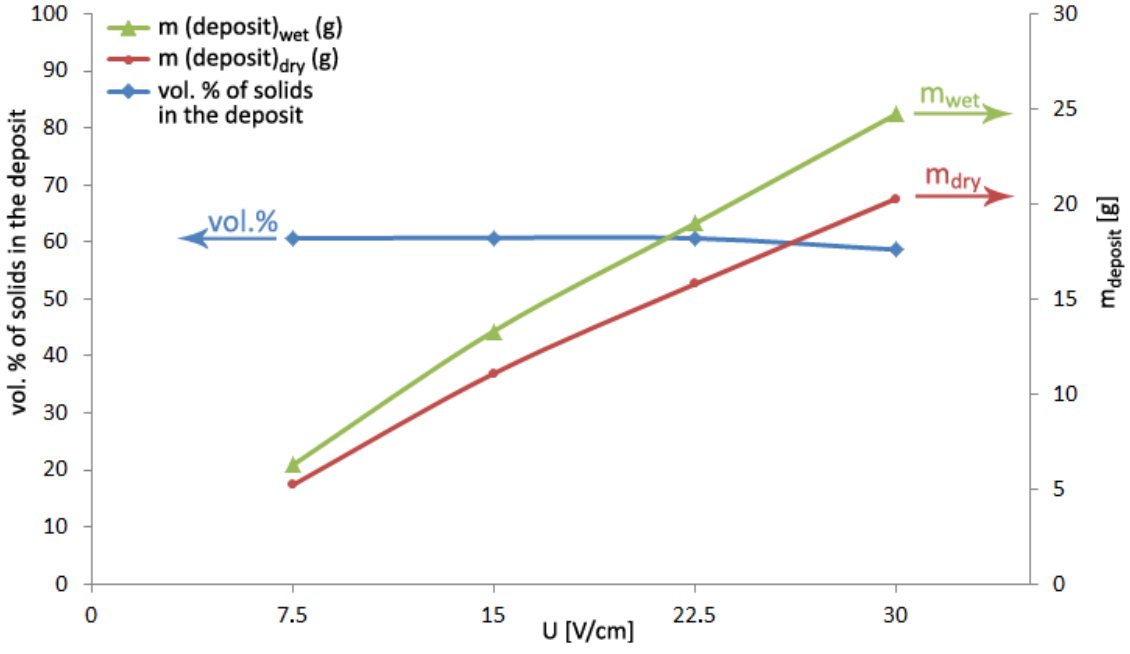

Figure 11: Influence of the deposition electric field strength on deposited mass and vol.% of solids in the deposit

4.1.4 Electrophoretic co-deposition

Now as we have evaluated the influence of main parameters affecting the quality of the final deposit from one-component suspension, we will discuss co-deposition which is, also according to much less hits in the literature, more challenging task. In our work we

have aimed at electrophoretic co-deposition (co-EPD) of SiC with sintering additives not containing potentially harmful elements; therefore two systems were checked. Co-deposition of SiC, carbon black and boron carbide (B_4C) and co-deposition of SiC and magnesium oxide (MgO). In the former case it was determined from the literature [97, 98] that optimal addition of B_4C and carbon black is 0.5 wt.% and 3 wt.%, respectively, while in the latter case, 3 wt.% of MgO was shown to be sufficient amount for successful sintering even though literature suggests 5 wt.% [99].

4.1.5 Silicon carbide with boron carbide and carbon black

SiC with addition of carbon black and boron carbide was produced in two different ways; with uniaxial pressing of powder mixture that was followed by isostatic pressing as described in experimental section and with electrophoretic co-deposition from the suspension of powders mixture. Dry pressing of mixed powders resulted in inhomogeneous distribution of additives throughout the sample and colloidal approach was applied instead. Boron carbide (B_4C) can be added either into water or ethanol and its zeta potential can be easily modified with TMAH or PEI (results for PEI and ethanol are not shown since it was not relevant for this work). Carbon black, on the other hand, is highly hydrophobic material and is not easily dispersed. Its surface was modified by heating carbon black in concentrated HNO_3 for several hours and then the powder was washed to remove excess ions. Treatment in HNO_3 caused partial surface oxidation and consequential hydrophilicity [100]. After drying also carbon black can be dispersed and its surface charge modified. Firstly, colloidal properties of pure powders were checked and after optimization, powders were mixed in the same suspension. Colloidal properties of SiC suspensions were already shown in Figure 7, whereas ZP of carbon black and boron carbide are shown in Figure 12.

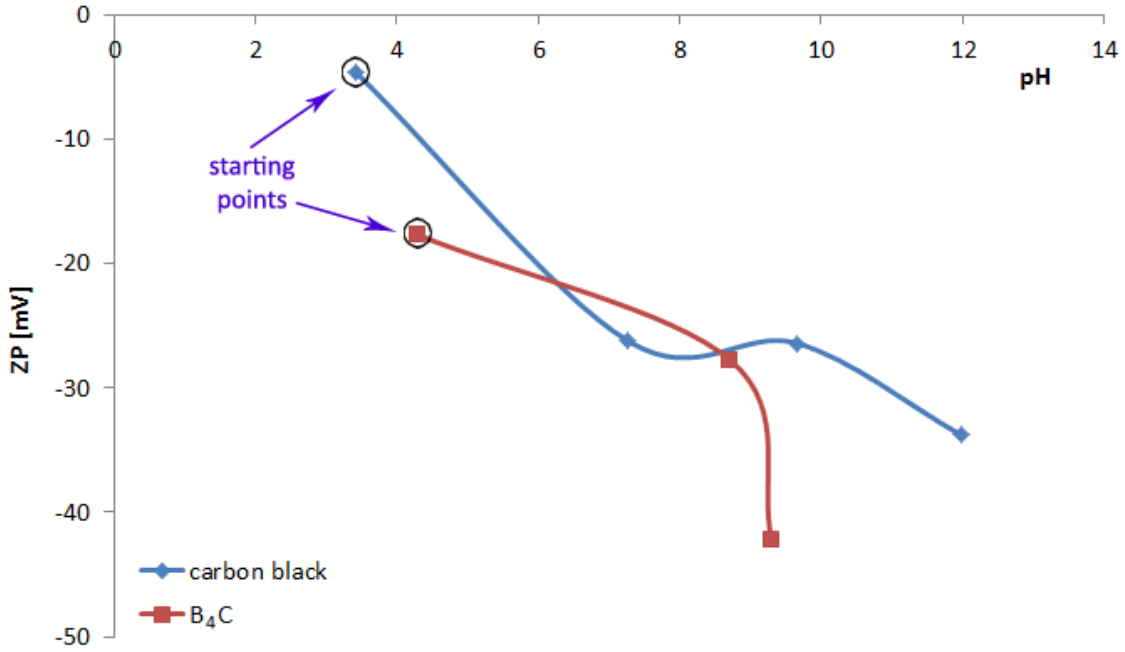

Figure 12: Zeta potential of 3 wt.% carbon black and 3 wt.% B_4C in aqueous suspension with addition of TMAH

Both powders, B_4C and carbon black are in negative region of ZP curve. At their natural pH both have slightly negative zeta potential; negative surface charge can be further increased with addition of TMAH. However, to reach sufficiently high charge on the

particles, conductivity of such prepared suspensions is already high (0.6 mS/cm and 1.6 mS/cm for B_4C and carbon black, respectively).

In the end all powders were mixed together in predetermined ratio (0.5 wt.% of B_4C and 3 wt.% of C according to the mass of SiC) in 50 wt.% SiC suspension and mixture was deposited onto graphite electrodes. EPD from aqueous suspensions containing SiC, carbon black and B_4C was performed at constant current 40 mA for 10 minutes. Due to moderate ZP of the suspension (-45 mV) and high conductivity (1.1 mS/cm) the volume fraction of powder in the resulting deposit is low (only 49 vol.%). Low volume fraction of powder in the wet deposit hinders sintering process, and besides, during drying more cracks are formed in less dense deposit. Due to observed problems only dry pressed and sintered samples were further analysed.

4.1.6 Silicon carbide with magnesium oxide

Since magnesium does not cause any adverse biological response MgO was examined as another possible sintering additive that was also discussed in the literature [99, 101, 102]. Conductivity of MgO suspension in water and in ethanol is shown in Figure 13a and b. Since we have ascertained that 3 wt.% of MgO is a sufficient amount of sintering additive, this was also the highest concentration measured.

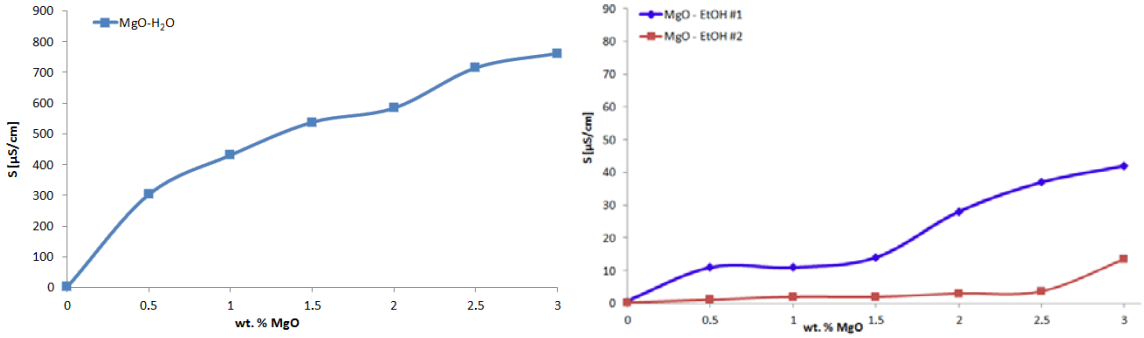

Figure 13: Conductivity of MgO a) aqueous and b) ethanol suspension in concentrations 0-3 wt.%

Since MgO is readily soluble in water the conductivity of 3 wt.% suspension is fairly high (more than 750 µS/cm, even 0.5 wt.% of MgO cause conductivity increase to 300 µS/cm) and it was stated before that too high conductivity has detrimental effects on EPD. Another problem arises when we add MgO to the stable SiC suspension; Mg^{2+}ions adsorb to surface of SiC thus neutralizing negative charge on particles at that pH and causing immediate flocculation of the suspension.

The obstacle presented above can be successfully overcome by replacing water with ethanol, since in the latter MgO is practically insoluble. Conductivity of ethanol suspension with increasing amount of MgO (Figure 13b) increases slowly (the ordinate axis is for an order of magnitude smaller for ethanol than for water) and reaches 42 µS/cm at 3 wt.% of MgO. Another measurement of conductivity of MgO suspension in ethanol reveals almost linear increase, in this case conductivity of 3 wt.% suspension is only 13.5 µS/cm. The lack of reproducibility can be ascribed to high affinity of anhydrous ethanol to water and in this case conductivity is increased due to dissolution of MgO in traces of water.

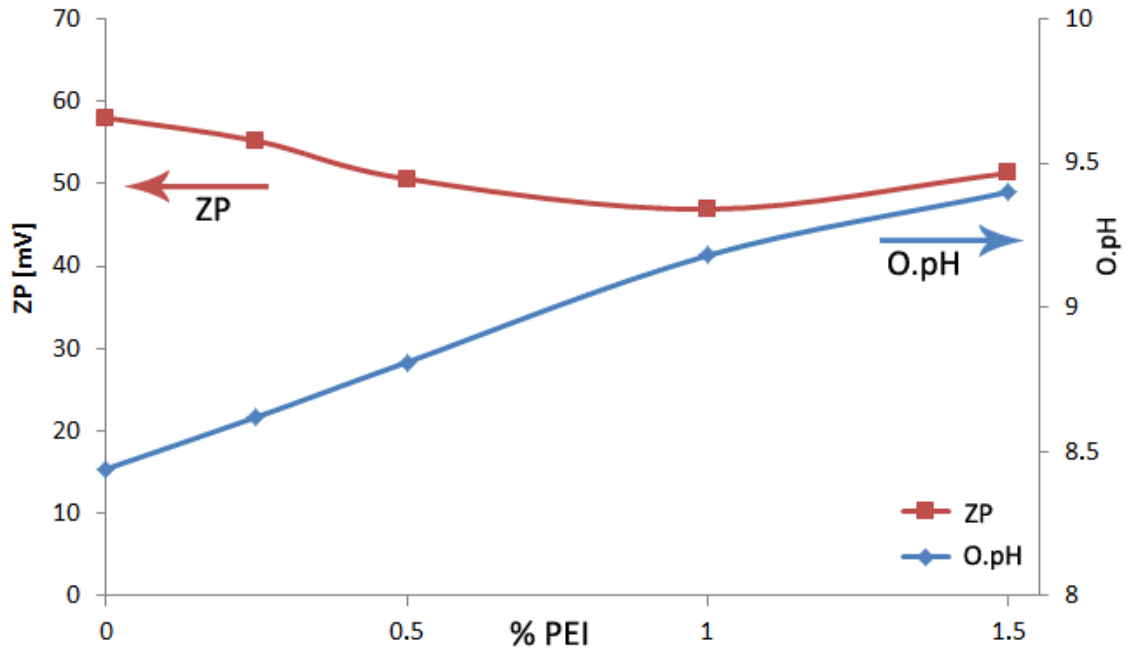

Figure 14: Dependence of ZP and O.pH of 3 wt.% MgO on addition of PEI in ethanol

Surface charge of MgO in ethanol can be modified with addition of PEI. Zeta potential and O.pH of 3 wt.% MgO suspension in ethanol with increasing amount of PEI is shown in Figure 14. The overall stability of suspension is increased due to steric interactions between PEI molecules. Conductivity of the suspension is not risen significantly (from 10 to 16 µS/cm, results not shown here) so the slight decrease in ZP with addition of PEI can be only ascribed to higher O.pH values (that results in less amino groups being positively charged).

Conductivity of 50 wt.% SiC suspension in ethanol was also measured; the results are shown in Figure 8b and conductivity was determined to be only 9 µS/cm, which is two orders of magnitude less than conductivity of aqueous suspension. Reason for that lies in higher solubility of SiO_2 (that is on the surface of SiC particles) in water than in ethanol. According to the literature [103], solubility of amorphous silica in water is 0.0125 % (i.e. 125 ppm) and in ethanol it is practically insoluble. What is important here is that conductivity of both ethanol suspensions lies well in the range suitable for EPD.

However, stability of SiC as well as MgO itself in ethanol is not sufficient, suspension is prone to flocculation. In order to achieve higher stability of suspensions, several attempts have been made. In Figure 15 dependence of SiC suspension in ethanol on O.pH is presented. O.pH was increased with addition of NaOH solution in ethanol so that no water was introduced to the suspension.

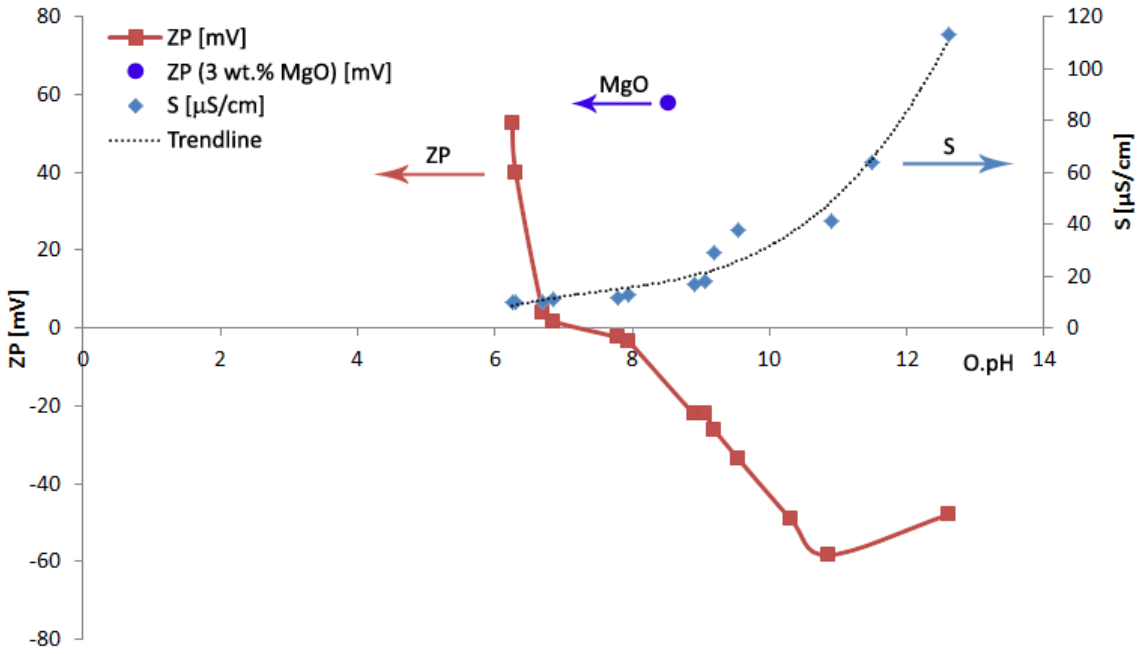

Figure 15: Dependence of ZP and conductivity of 3 wt.% suspension of SiC in ethanol on O.pH that was modified with addition of NaOH/EtOH and ZP of 3 wt.% suspension in ethanol

One can see that as-prepared SiC suspension in ethanol has highly positive zeta potential (+53 mV) and low conductivity (5 µS/cm), while O.pH is slightly acidic (6.25). Addition of NaOH increases O.pH and at first lowers ZP so the ZP curve approaches isoelectric point. Further addition of base increases ZP in negative region. The curve has its maximum at O.pH 10.8 where ZP is -58 mV. Then ZP is shifted towards less negative values. The conductivity of SiC suspension is increasing, the course is approximated with second degree polynomial curve. By O.pH 9 conductivity is fairly low (20 µS/cm) while by O.pH 12.6 conductivity is increased to 115 µS/cm.

ZP of as prepared 3 wt.% MgO suspension in ethanol is also presented in Figure 15. Its ZP is highly positive (+58 mV) at O.pH 8.4. Since MgO has high zeta potential at relatively high O.pH it is difficult to obtain highly negative surface charge solely by changing the O.pH. Therefore ZP was increased with addition of PEI which acts as a cationic surfactant. The effect of PEI on surface properties of separate powders as well as on mixed suspension is shown in Figure 16.

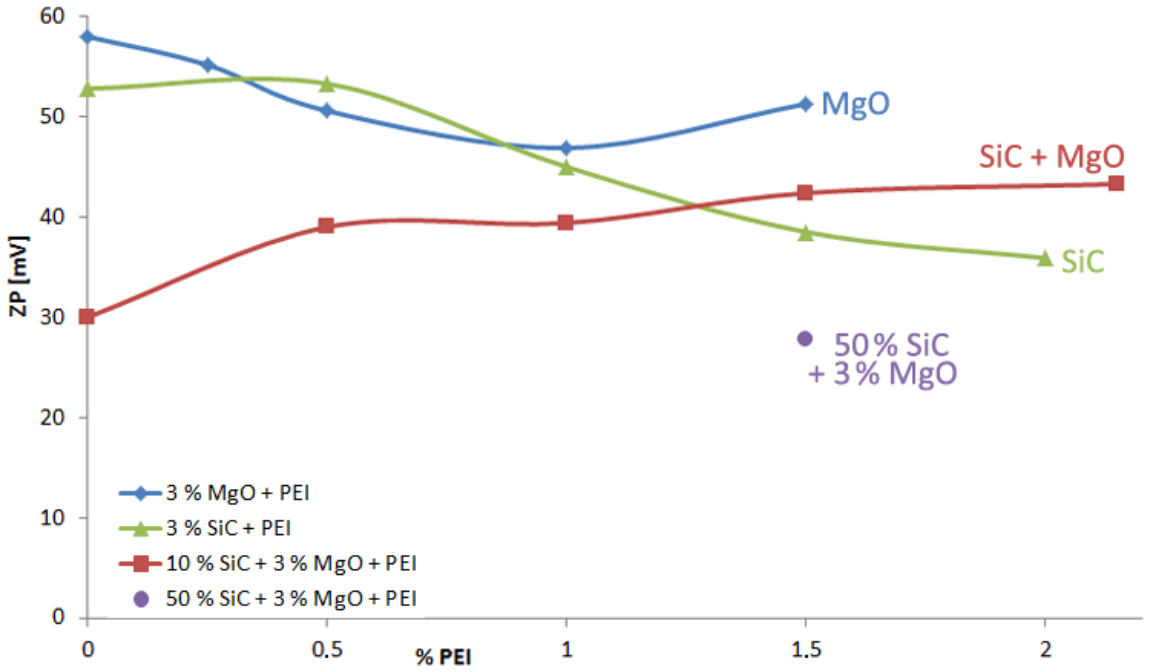

Figure 16: ZP of ethanol suspensions of 3 wt.% SiC, 3 wt.% MgO, 10 wt.% SiC containing 3 % MgO in dependence of PEI addition and ZP of 50 wt.% SiC suspension containing 3 % MgO

Any addition of PEI increases the O.pH of the suspension (values not shown). Structure of PEI is presented in Figure 1; each N atom acts as possible ionization centre. The charge of PEI molecules depends on O.pH; at more acidic O.pH they are more positively charged while at higher O.pH values more amino groups remain neutral. However, PEI binds to the negatively charged parts of the surface, thus increasing the net positive charge and also stabilizing the suspension through steric repulsions between particles. This behaviour explains why addition of PEI to SiC and MgO suspensions results in lowering ZP while still stabilizing the suspension. Effect of PEI addition was also observed on the SiC/MgO mixture (Figure 16); zeta potential slowly increases with amount of added PEI up to constant value at 1.5 % PEI.

Since ZP reaches constant values at 1.5 % PEI in SiC/MgO mixture, and any further addition of PEI only increases the conductivity of the suspension, this amount was chosen for further experiments. When PEI was added to 50 wt.% SiC suspension containing 3 % MgO, the ZP reached nearly 30 (+29) mV. Lower surface charge can be again ascribed to higher O.pH values that are the result of higher absolute amount of MgO thus neutralizing potentially acidic O.pH of SiC. However, also due to steric interactions suspension is highly stable and suitable for EPD. Reason for lower absolute values of ZP in ethanol suspensions also lie in lower dielectric constant compared to water, but since long chains of PEI molecules also contribute to steric stabilization, suspension is stable despite relatively low surface charge. Another problem when dealing with ethanol-based suspensions is the rate of EPD which is very low even at moderate voltages (i.e. 60 V or 30 V/cm, regarding the electric field strength). Deposits that were produced were of good quality but the formation was slow. The voltage was increased to 300 V and the deposition was fast while still no bubbles were formed since there was no water present. Therefore first deposition that was performed from ethanol suspension containing SiC and MgO at 300 V (i.e. electric field strength was 150 V/cm) resulted in deposit with density 1.83 g/cm^3 which corresponds 57 vol.% (i.e. 57 % of theoretical density). Photograph of bulk deposit is shown in Figure 17. Also the homogeneity of the deposition was examined; results are shown in Figure 18.

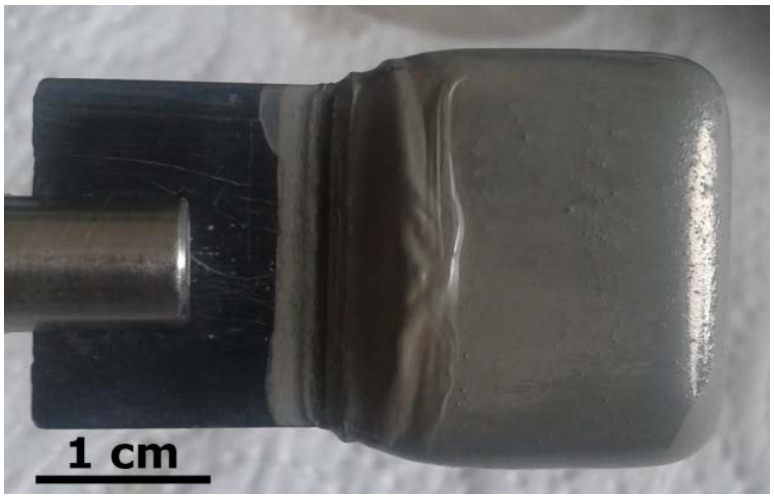

Figure 17: Image of SiC co-deposited with MgO from ethanol suspension at 300 V in 15 minutes

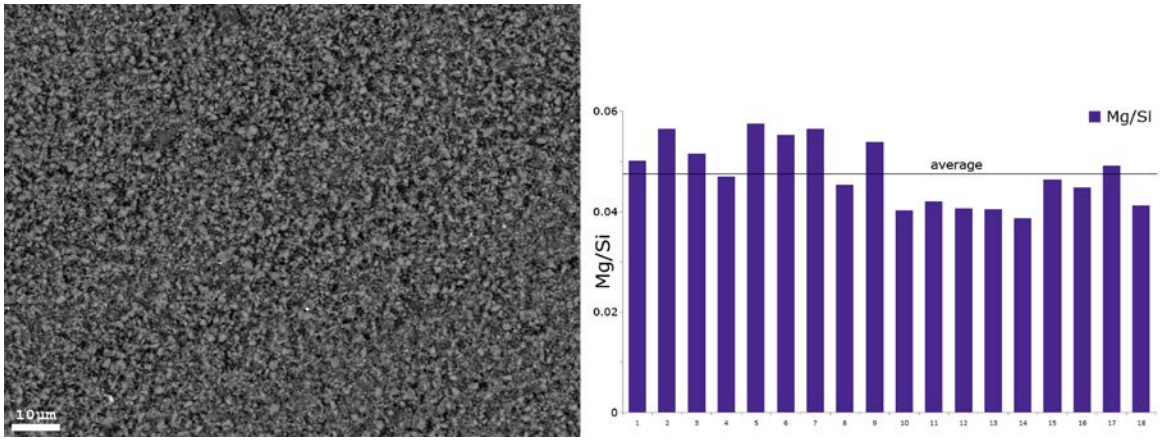

Figure 18: Homogeneity of co-deposition of SiC and MgO was evaluated by backscattered electron image of green deposit (a) and the results of EDS analyses (b)

To prove the homogeneity of MgO distribution we have prepared a flat green sample deposited from ethanol suspension containing 50 wt.% SiC, 10 wt. % MgO (according to the mass of SiC) and 1.5 wt. % PEI. We have performed EDS analyses on various areas at different magnifications (20x20 to 200x200 μm^2); some characteristic results are shown in Figure 18a and b (backscattered electron image and results of quantitative analyses as a Mg/Si wt.% ratio) and are significant for the whole sample. Estimated homogeneity of Mg distribution (i.e. uniformity of distribution of MgO particles), defined as relative standard deviation of Mg concentration is below 15 % so the co-deposition can be considered as a technique to produce fairly homogeneous samples even from multi-component suspensions. The amount of MgO in deposit is lower than in starting suspension; specified size of MgO particles is larger than that of SiC so it can be presumed that only fraction of smaller MgO particles have sufficient electrophoretic mobility.

4.1.7 Comparison of techniques

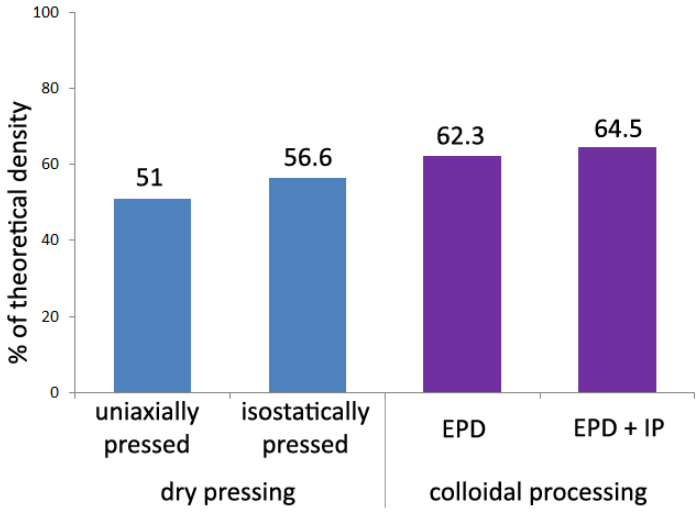

Figure 19: Comparison between dry pressing and colloidal techniques in terms of green density; EPD = electrophoretic deposition, IP = isostatic pressing

Finally, comparison between dry pressing and colloidal shaping was made on SiC samples without additives prepared by dry pressing or colloidal shaping and the results (densities of green samples in % of theoretical density) are given in Figure 19. Green density of SiC pellet that was uniaxially pressed at 100 MPa reached 51 % of theoretical density while subsequent isostatic pressing at 740 MPa caused increase in density up to 56.6 % of TD. However, much higher green density was obtained by EPD from optimized aqueous suspension; in this case, the green density was 62.3 % of TD. Sample can be further isostatically pressed and in this case density of the sample was increased to 64.5 % of TD.

Although EPD is from many points of view advantageous technique still some potential problems have to be overcome. Effects of electrolysis that is the consequence of high strength of electric field applied to aqueous suspension can be overcome by placing cellulose membrane in front of the electrode thus preventing the direct contact between the electrode and the deposit. Therefore, bubbles are not trapped in the deposit and dense deposit without macropores can be produced. Another way to avoid the detrimental effects of electrolysis is to replace the stainless steel electrode with one that is readily oxidized. Either copper (in this case copper ions are incorporated into the material) or graphite electrodes can be employed. Due to oxygen formation electrodes are oxidized and CO_2 is formed. CO_2 is then dissolved in water and local pH decreases [104]. Also graphite electrodes are slightly porous and consequently some of the oxygen can be absorbed in the material.

On the other hand, when cathodic deposition is performed, hydrogen evolution from aqueous suspensions cannot be prevented. Porous palladium electrode that is proven to absorb hydrogen could be used but due to porosity it would not be possible to remove the deposit. Therefore either cellulose membrane should be used or non-aqueous system should be investigated.

4.2 Sintering/densification and microstructural evaluation

Sintering was performed following two different routes; sintering in vacuum at high temperatures for SiC without additives or with addition of B_4C and carbon black and sintering in open air at considerably lower temperatures for pure SiC or SiC with addition of MgO. Sintering conditions for sintering in vacuum were taken from the literature [97, 98] whereas sintering temperature in open air was determined using dilatometer. Results of dilatometer experiment are shown in Figure 20 applying that the highest shrinkage takes place at 1350 °C. More detailed descriptions of sintering regimes are given in experimental section.

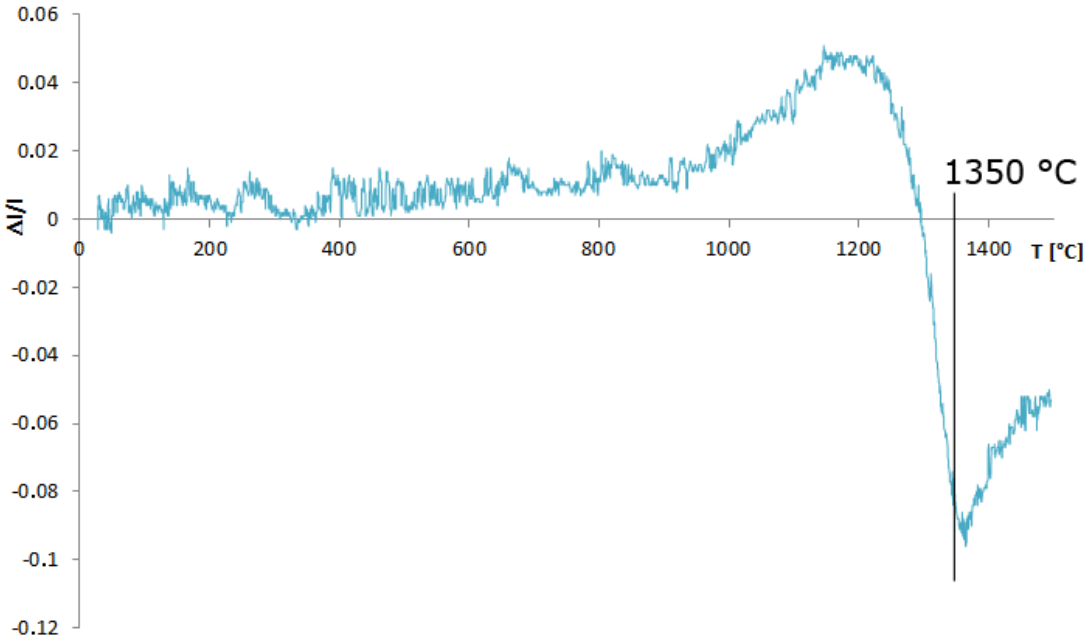

Figure 20: Shrinkage as a function of temperature of the sample SiC containing 3 wt.% MgO when sintered in open air. The swelling at high temperature might be the result of SiC oxidation

4.2.1 Sintering in vacuum

To prove the effect of solids content in the green deposit on sintering efficiency, various deposits were sintered in vacuum at high temperatures. Microstructures of sintered samples without additives are shown in Figure 21.

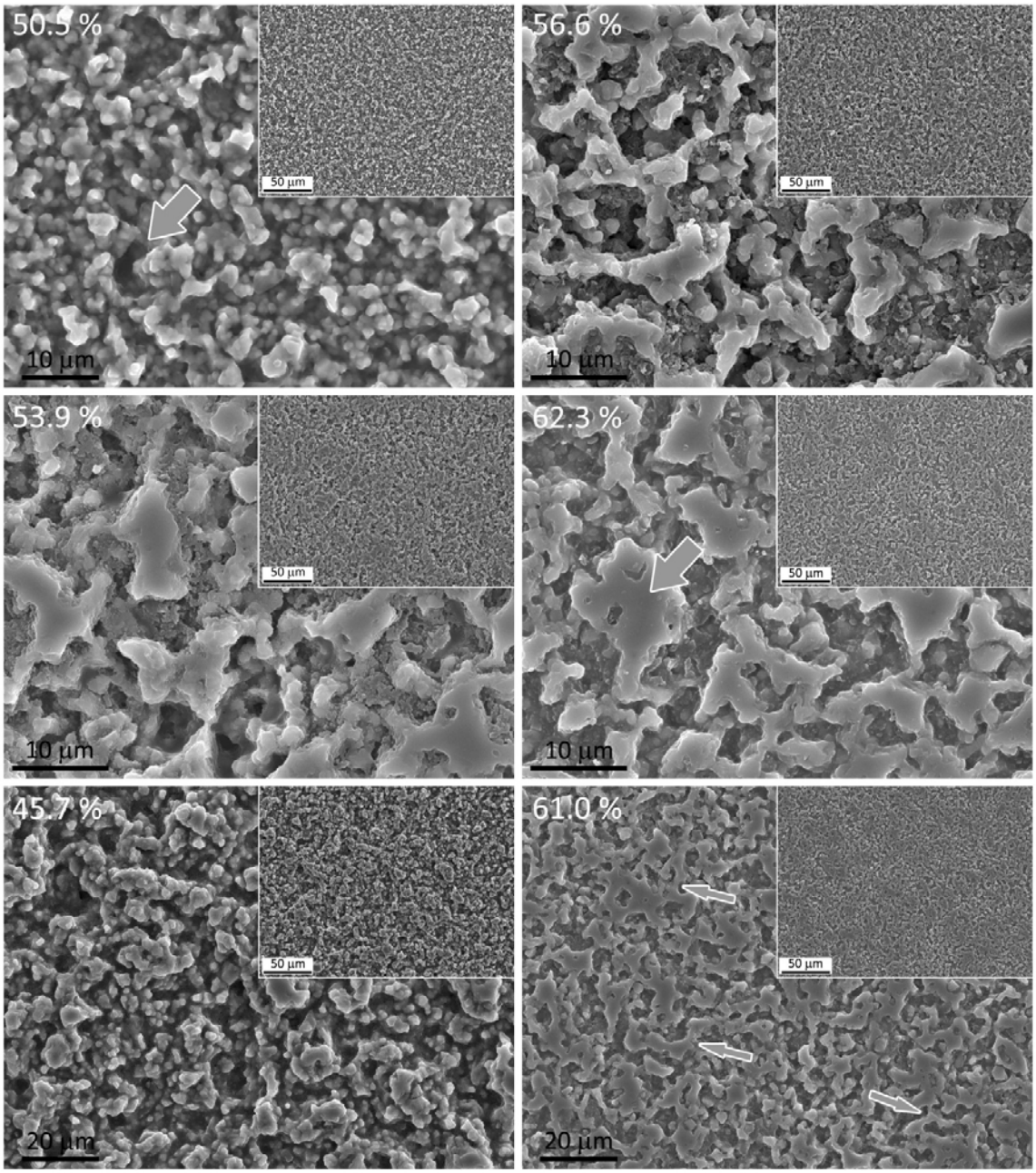

Figure 21: Microstructures of the polished surfaces of sintered samples without additives: a, b) uniaxially and isostatically pressed ß-SiC, c, d) samples deposited from suspensions with 0.05 and 0.1 % TMAH, e, f) samples deposited from 25 and 50 wt.% suspensions. Inserts show lower magnifications, numbers in top left corners denote relative green density (i.e. % of TD). All samples were sintered 2 h at 2100 °C. Arrows on a) show large pore as a result of insufficient deaglommeration of the powder whereas arrows on f) show formation of necks between grains

It has been shown before that, also in other systems, the density of sintered ceramics significantly depends on the density of green parts [105]. This is even more expressed in the case of solid state sintering where diffusion is hindered or even prevented, like in the

case of SiC without sintering additives. Sinterability of pure SiC samples produced under various conditions (that affected green density) was observed after firing at 2100 °C in vacuum. In Figure 21a and b microstructures of two dry-pressed samples are shown. One was only uniaxially while the second was subsequently isostatically pressed. In the first microstructure particles are still isolated from each other, since starting green density was only 50.5 % of theoretical one. When particles are not completely deagglomerated even some large pores can be observed, as labelled with an arrow on Figure 21a. When sample was isostatically pressed, reaching the density 56.6 % of theoretical, some neck formation can be observed, but the grains are still too far apart to be able to form a solid though porous network of SiC grains.

The same happens in the case of 0.05 % (sub-optimal) TMAH addition and deposition from 25 wt.% suspension (Figure 21c and e, respectively) where green densities reach 53.9 % and 45.7 % of TD, respectively. Samples with optimal TMAH addition (i.e. 0.1 %) and prepared from more concentrated suspensions reach over 60 % of TD which also enables some neck formation as well as grain growth. Grains reach sizes up to 10 µm or more (arrow in Figure17d) while neck formation is also observed and is marked with arrows in Figure 17f. The highest obtained density was reached by deposition from optimized suspension, followed by isostatic pressing of the dried deposit. Final green density was 64.5 vol.% and microstructure of obtained sample is shown in Figure 22. Here the neck formation is even more pronounced, being the result of easier solid state diffusion because the grains were closer together. Density measurements reveal that there was no observable change between green and sintered density in most samples while observation of microstructure reveals that a threshold green density exists (above ~58 % of TD) below which no neck formation or grain growth occurs. In contrast to lack of density increase in majority of samples, in the case of isostatically pressed EPD sample density increased from 64.5 % to 65.4 % during sintering.

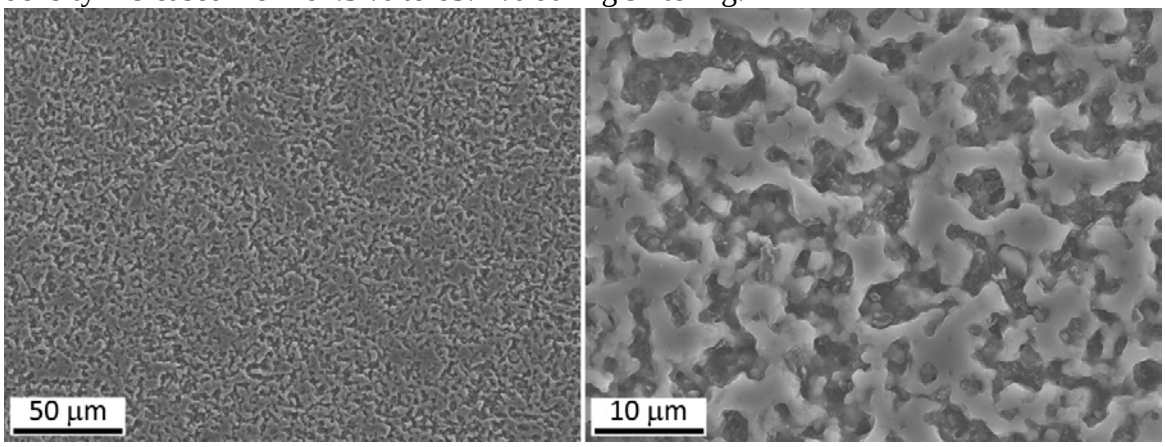

Figure 22: Microstructure of polished surface of electrophoretically deposited sample followed by isostatic pressing and sintered at 2100 °C for 2 hours

Even though no extensive densification is observed during heat treatment, first signs of sintering process are grain growth as well as growth of pores. In Figure 23 pore size distribution in three different samples is presented. Overall (open) porosity is shown as area under peaks while curves present pore opening distributions.

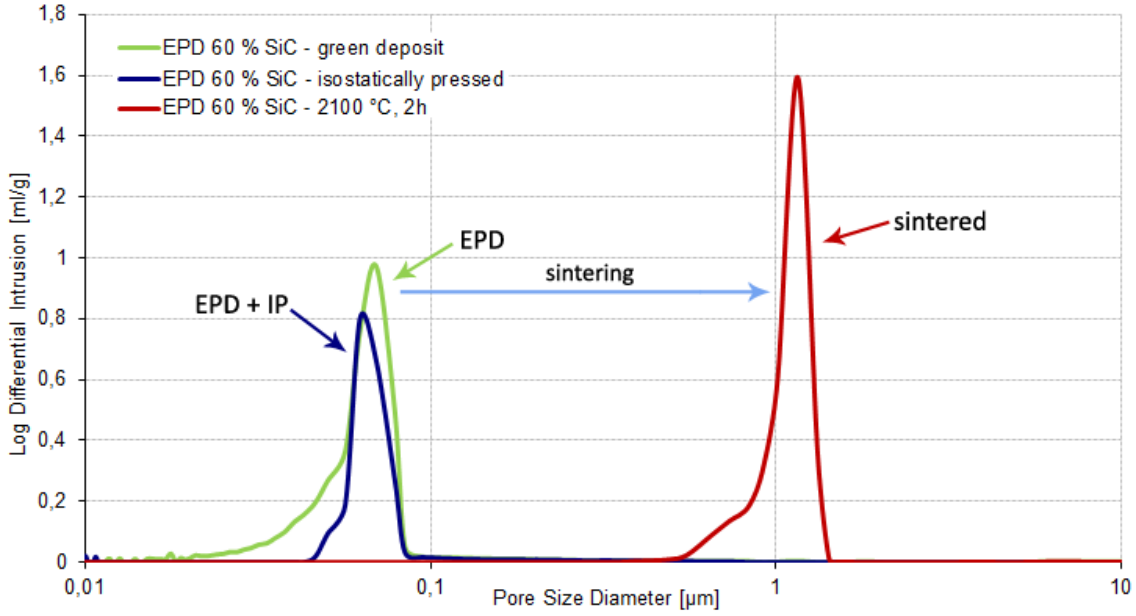

Figure 23: Pore size and distribution of open porosity in green EPD SiC sample (as-deposited and isostatically pressed) and in sintered EPD-IP sample determined by Hg intrusion

Results of the measurements with Hg porosimetry show that volume of open pores does not change significantly during sintering (density increases from 1.94 g/cm^3 in green sample to 2.03 g/cm^3 in sintered sample, i.e. less than 5 % increase). On the other hand, pores grow considerably during sintering (peak for EPD sample is at 70 nm while for sintered sample 1.156 µm). On the other hand, when EPD sample is subsequently isostatically pressed, the average pore size does not change significantly (maximum moves from 70 nm to 62 nm) but the fraction of smallest pores disappear (no porosity below 50 nm) and on that account density increases. The densities measured with Hg porosimetry differ slightly from those measured with Archimedes method since the first method does not consider closed porosity.

The results (pore size and distribution and comparison of green and sintered sample) are also in agreement with literature; some authors report that during sintering without additives regions with a high level of densification appear, as well as regions with an increased number of large pores [75]. For better presentation the fracture surfaces of green and sintered deposit are shown in Figure 24.

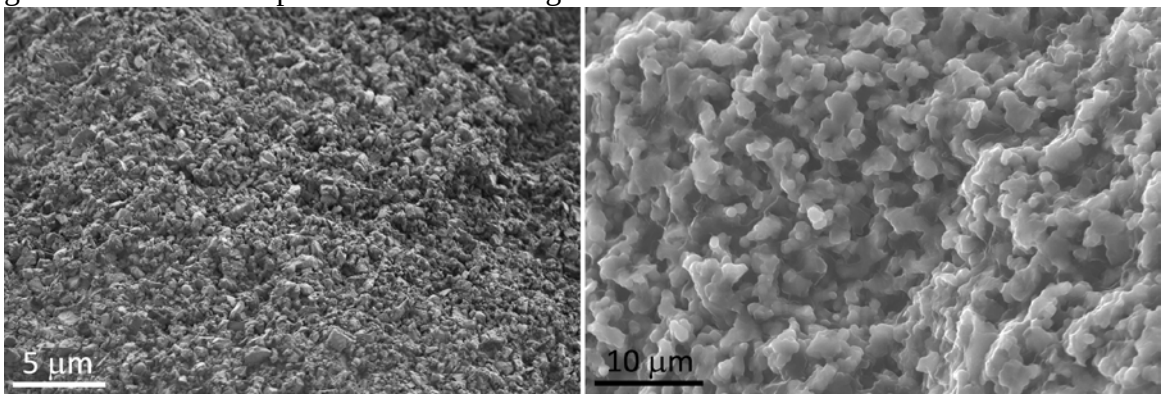

Figure 24: Microstructures of the fracture surface of green and sintered (in vacuum) SiC sample without additives

These microstructures are in agreement with pore opening distribution that was shown in Figure 23. The important aspect here is, however, the fact that between grains necks are

formed and that ensures solid skeleton that is responsible for the mechanical properties of the sintered samples.

4.2.2 Sintering with addition of boron carbide and carbon black

Since sintering of pure SiC is a demanding task that without applied pressure does not lead to completely dense material, also in our work sintering in vacuum was performed on SiC samples containing sintering additives, namely B_4C and carbon black. Microstructure of polished and fracture surface of the samples is shown in Figure 25 and Figure 26. Comparison between Figure 24 and Figure 25 reveals that when sintering additives are introduced this causes extensive grain growth (marked with arrows) in some areas while mostly grains still remain small. This is in contrast with sintering without additives where all grains are of approximately same size. Also the pores in the sample sintered with additives are considerably smaller and shrinkage is higher. Final density of the sample sintered at 2100 °C was ~75 % of TD. Another sample was sintered at 2200°C; its density was 90 % of TD and its microstructure is shown in Figure 26. In this case grains mostly fuse together and grow, pores still remain small. Small grains that were observed in the sample, sintered at lower temperature, disappear on account of large grains.

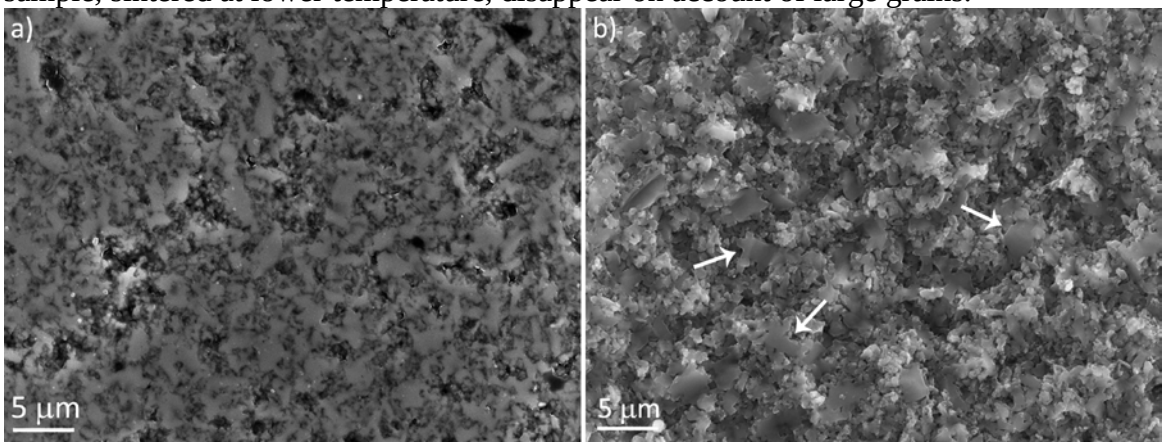

Figure 25: Polished (a) and fracture (b) surface of sample, sintered with addition of 3 wt.% carbon black and 0.5 wt.% B_4C sintered at 2100 °C. Arrows show exaggerated growth of some grains

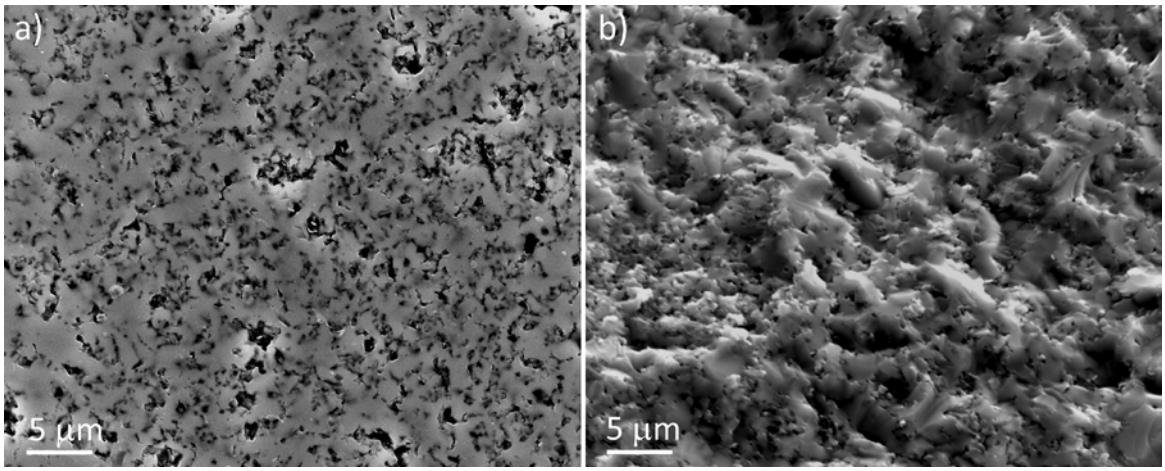

Figure 26: Polished (a) and fracture (b) surface of sample, sintered with addition of 3 wt.% carbon black and 0.5 wt.% B_4C sintered at 2200 °C

4.2.3 Sintering with addition of magnesium oxide

The third set of the samples, containing MgO, was sintered in open air. Pure SiC samples (without MgO) were made for comparison. Starting density of pure SiC deposited from ethanol suspension was only 1.61 g/cm^3 (i.e. 50.1 % of TD) and during sintering it increased to 1.87 g/cm^3 (58.3 % of TD) whereas SiC co-deposited with MgO had density of 1.92 g/cm^3 before and 2.33 g/cm^3 after sintering. Microstructures of samples sintered in open air are shown in Figure 27.

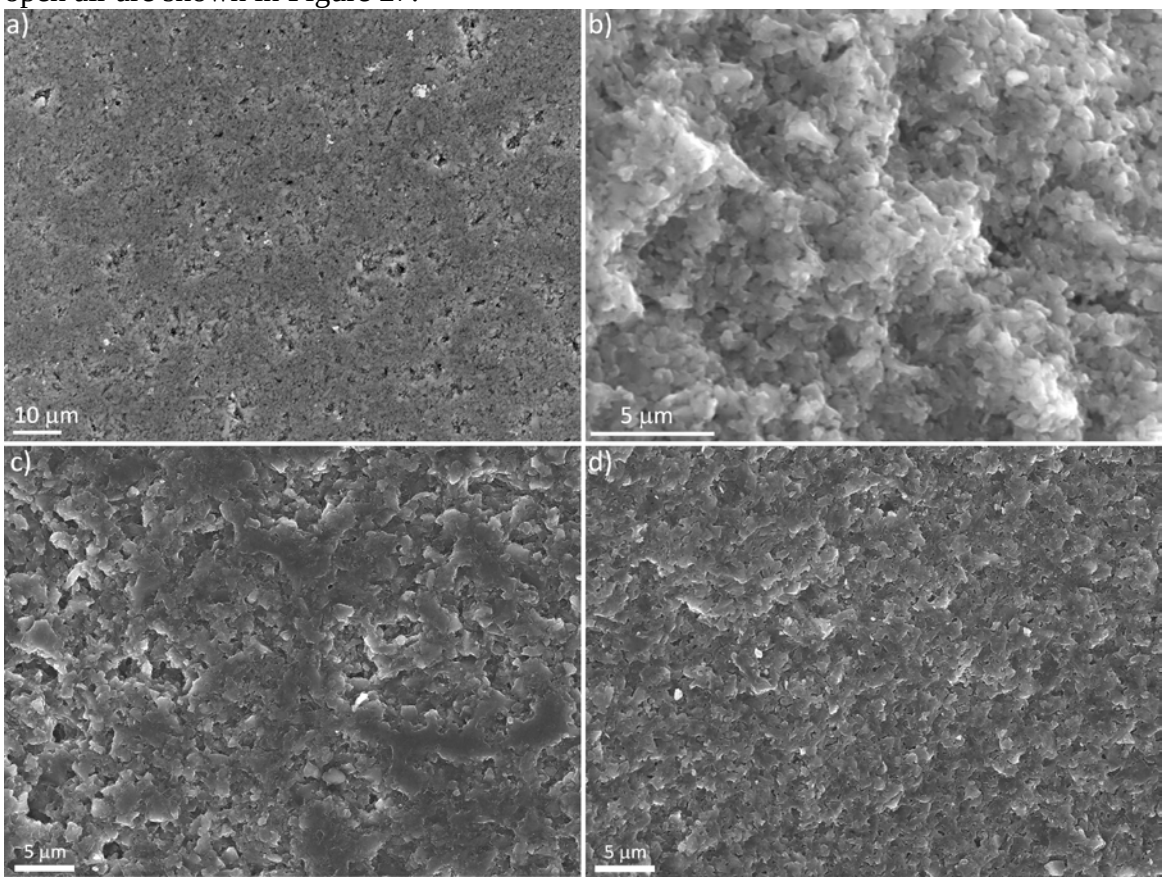

Figure 27: Polished (a, c) and fracture surfaces (b, d) of sintered samples of pure SiC (a, b) and SiC co-deposited with MgO (c, d); sample a) might contain some polymer that was used in metallographic preparation of the sample.

Microstructures of both, pure SiC and SiC with addition of MgO that were sintered in open air are shown in Figure 27. From fracture surfaces of both samples, Figure 27b and d we can conclude that there is no exaggerated grain growth and also pores remain small. Density of sintered deposit containing MgO is higher than of the one sintered in vacuum due to formation of SiO_2 that might affect sintering process. In order to more thoroughly observe the effect of MgO addition to SiC, followed by sintering in open air, also TEM study was done. TEM images and analyses are shown in Figure 28.

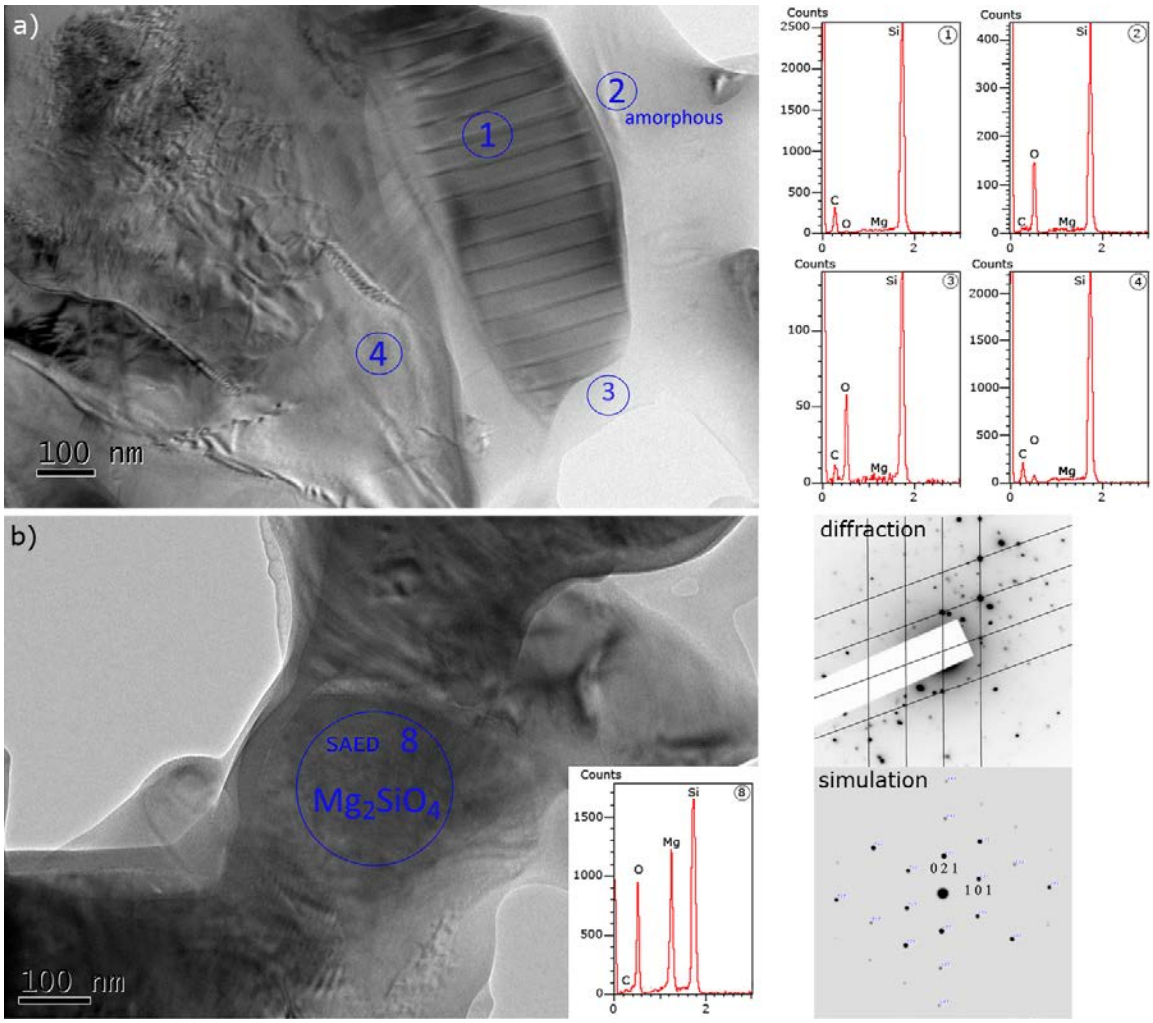

Figure 28: TEM image with the belonging EDS spectra and selected area electron diffraction pattern. Simulation corresponds to Mg_2SiO_4 (forsterite) crystalline phase

It has already been shown in the work of Novak et al. [91] that the surface of the SiC particles consists of thin layer of amorphous silicon oxycarbide, SiC_xO_y and SiO_2. When sample is exposed to oxygen at high temperatures SiO_2 layer is thickened on account of SiC oxidation. To prove that, sample containing 3 wt.% of MgO was also observed by means of transmission electron microscopy. In the Figure 28a, microstructure of the thinned sample is shown. Largest grain (marked with 1) is still ß-SiC while EDS on spots 2 and 3 shows the presence of large quantities of oxygen, suggesting that the amorphous phase consists mainly of silicon oxide. The spectrum 4 reveals less oxygen and also some carbon, suggesting the formation of SiC_xO_y. Sintering in open air results in formation of various Si-C-O phases while magnesium is present on all of the analysed points, however, the amount is not large. In the Figure 28b an isolated grain containing considerably larger amounts of Mg is shown. Diffraction pattern (SAED) reveals crystalline and not amorphous structure while simulation confirms matching with forsterite, Mg_2SiO_4 phase. Microstructure suggests that ß-SiC grains are embedded in amorphous oxygen-rich phase. MgO that reacts with SiO_2 results in the formation of Mg-Si-O crystalline phases.

4.2.4 XRD

XRD spectra in Figure 29 reveal the appearance of various crystal phases in our samples.

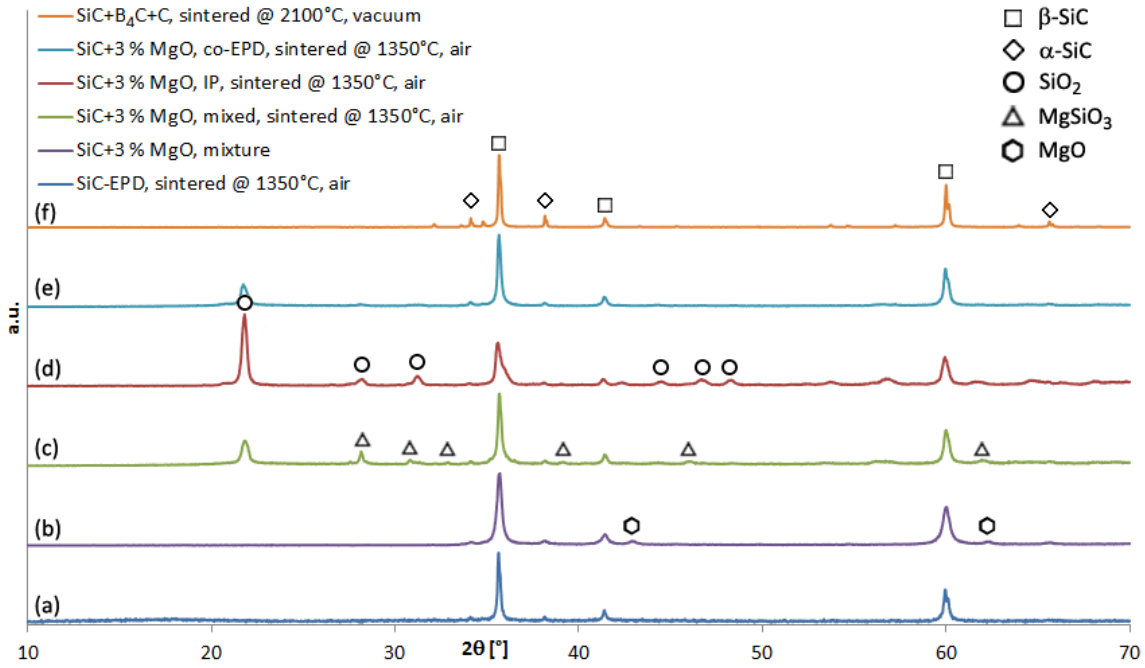

Figure 29: XRD of various SiC samples

The curve (f) belongs to the only sample sintered in vacuum and because of the presence of boron and carbon during high-temperature sintering the increase of α-SiC phase is observed. Other samples were sintered in air and consequently oxygen-containing phases appeared. In the XRD of SiC/MgO mixture before heat treatment (b) both phases are detected and indexed. Spectrum (c) reveals that the MgO either reacts or evaporates at elevated temperatures since it was not detected in the sample. Instead, crystalline SiO_2 (cristobalite) is formed. Also appearance of $MgSiO_3$ (enstatite) phase is detected, that is the result of the reaction between SiO_2 and MgO. It can be presumed that the addition of MgO is responsible for crystallization of SiO_2 since in pure-SiC deposit that was also sintered in open air at the same conditions there are no peaks for cristobalite detected. When the powders are only mixed together (c), the oxidation is less pronounced, presumably because the particles are not as close together as in the case of isostatically pressed sample (d). Also in the case of co-deposited SiC and MgO (e) the amount of SiO_2 is not as high, which is the result of the fact that the deposit does not have the same composition as the starting suspension. In all cases there is still some α-SiC present, which originates from the starting powder [106]. Combining the TEM study and the results of XRD we can conclude that presence of MgO in green sample results in appearance of $MgSiO_3$ phase and some isolated Mg_2SiO_4 grains detected in TEM.

4.3 Properties of sintered SiC-based ceramics

4.3.1 Flexural strength

In present work flexural strength of the samples was measured using ball-on-three-ball method on disc-shaped samples. The average results for 5-10 similar samples are shown in Figure 30.

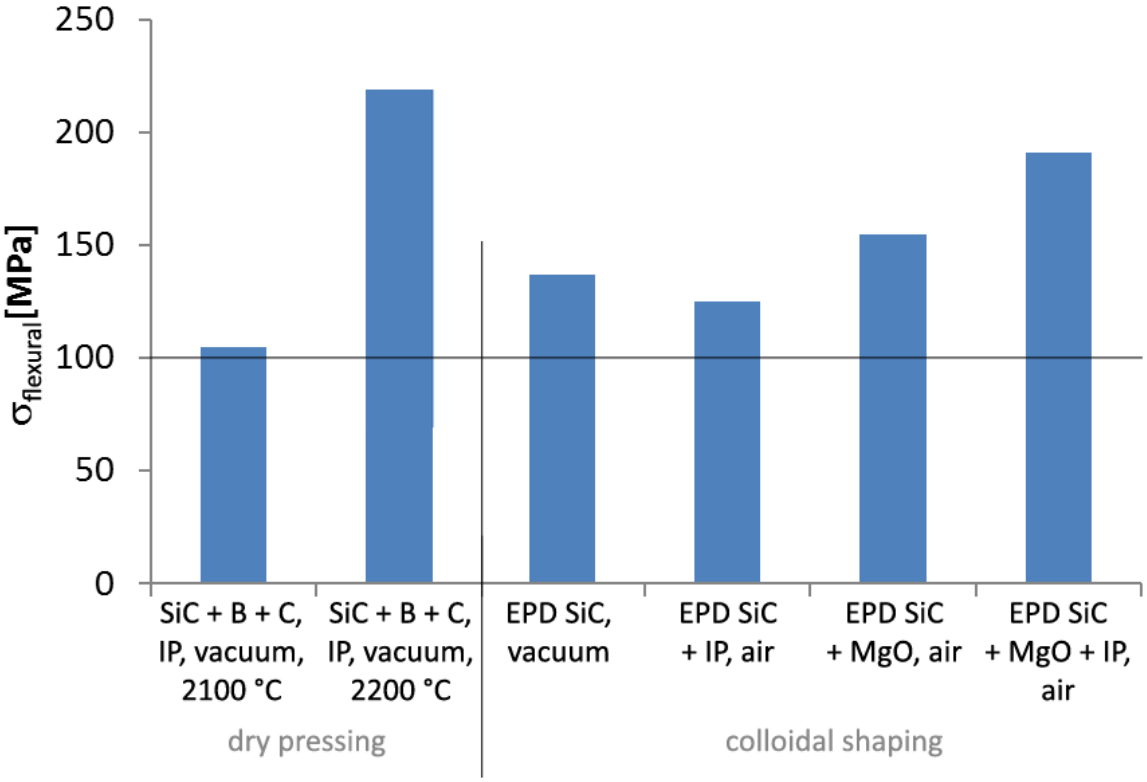

Figure 30: The results of flexural strength measurement, ball-on-three-ball method, EPD = electrophoretic deposition, IP = isostatic pressing

From the Figure 30 it is clearly seen that SiC sintered at 2200 °C in presence of boron and carbon, although being only dry pressed, has the best flexural strength among all samples. This can be ascribed to successful densification of the samples. When sample, containing boron and carbon was sintered at 2100 °C, its flexural strength is lowered from 220 MPa to 110 MPa. EPD SiC without additives was sintered in vacuum and in open air and values for flexural strength are comparable (135 MPa and 125 MPa, respectively). Addition of magnesium further improves flexural strength but only when samples were colloidally processed. In the case of dry pressing distribution of MgO was inhomogeneous and mechanical properties could not be measured. Samples that were co-deposited with MgO exhibited flexural strength of 155 MPa, while further isostatic pressing of the samples prior to sintering increased strength up to 180 MPa.

Since the porosity of the samples was not identical we have normalized all values for flexural strength to 100 % density (i.e. 3.21 g/cm^3). The results of normalization are given in Figure 31.

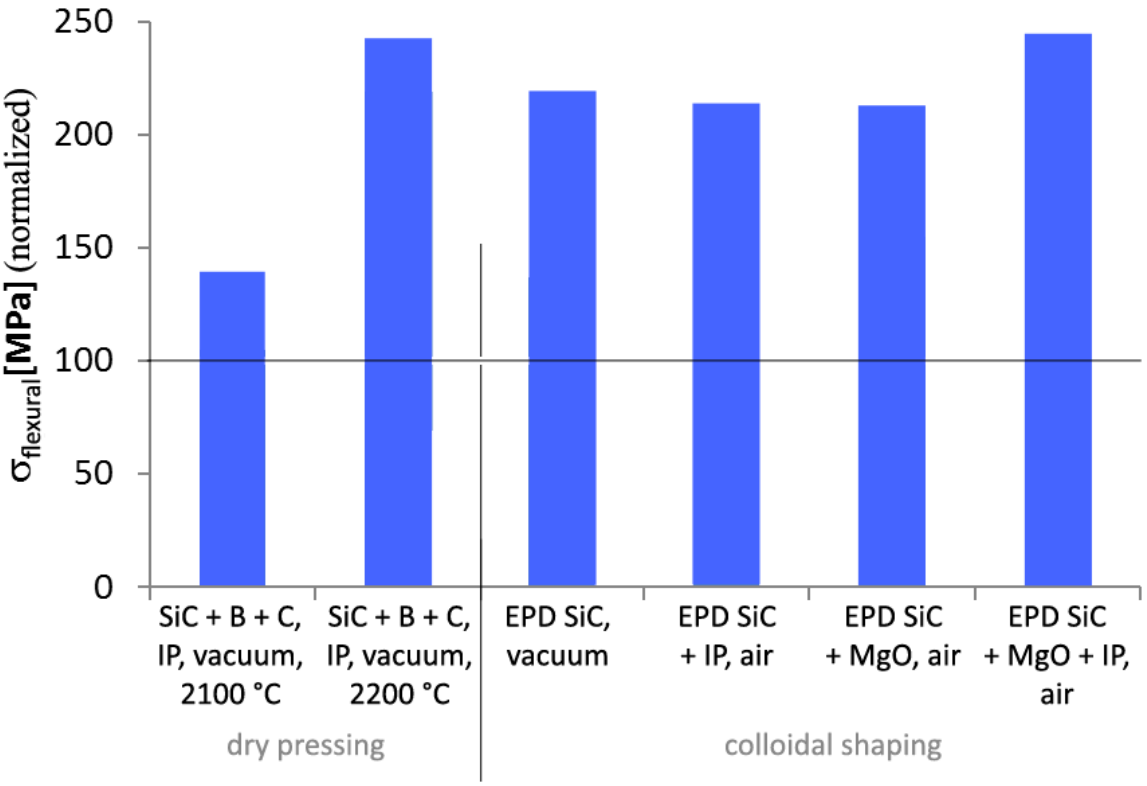

Figure 31: The results of normalised (to 100 % density) flexural strength for various samples

4.3.2 Elastic modulus

Elastic modulus was measured by two different techniques, by impulse excitation and by nanoindentation. Typical response for nanoindentation is shown in Figure 31.

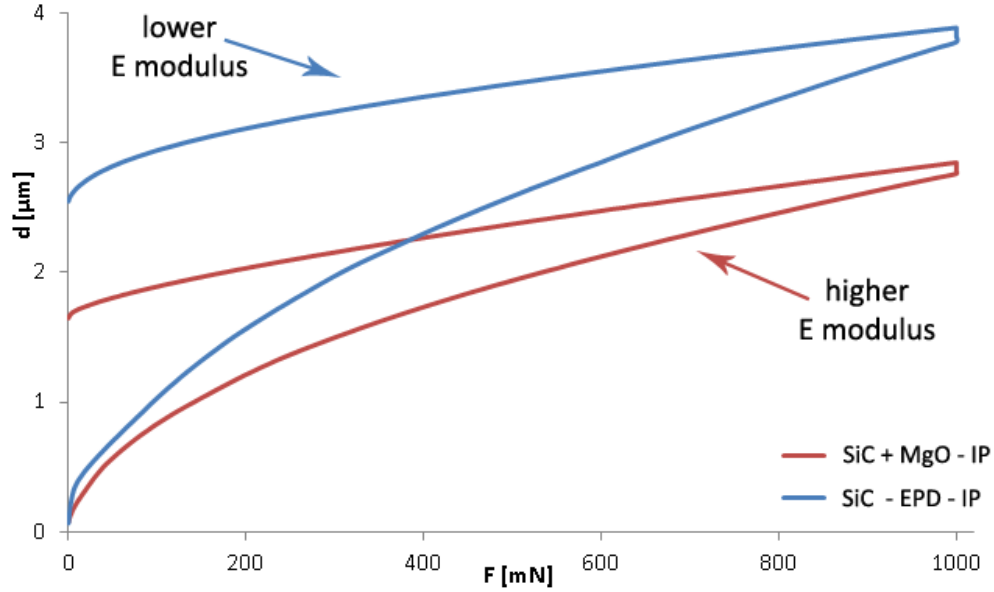

Figure 32: Typical graph for elastic modulus measurement on two samples by means of nanoindentation

In samples with lower elastic modulus the indentation is deeper while for higher elastic modulus the strain is smaller. Great advantage of this technique over acoustic

measurement is that it enables measurements on significantly smaller samples while for acoustic measurements much larger samples of regular geometry are required. Therefore, to prove its reliability, the elastic modulus was measured using both techniques on Y-TZP discs with various sintered densities, ranging from 47 to 99 %. Zirconia has been used as it was easier to manufacture specimens with precisely controlled porosity than in the case of pure SiC. The comparison is presented in Figure 32 showing that there is a good agreement between both techniques in the measured range which is also the range for the sintered samples produced and analysed in this work.

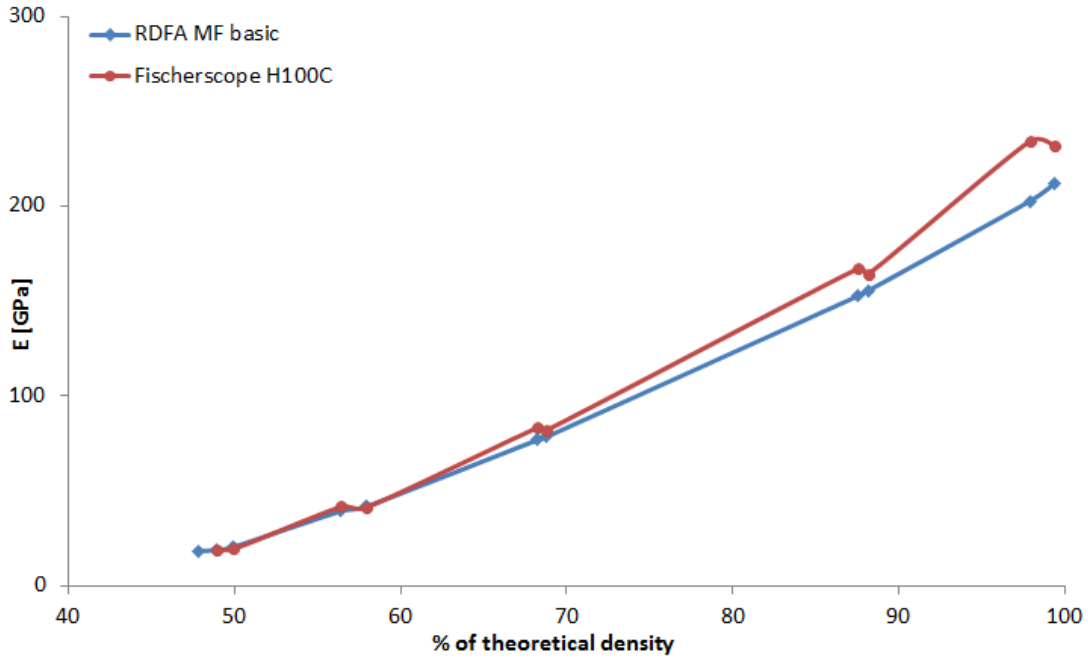

Figure 33: Elastic modulus of sintered Y-TZP ceramics of various densities measured with two different methods, RDFA MF basic = sound excitation technique, Fischerscope H100C = nanoindentation

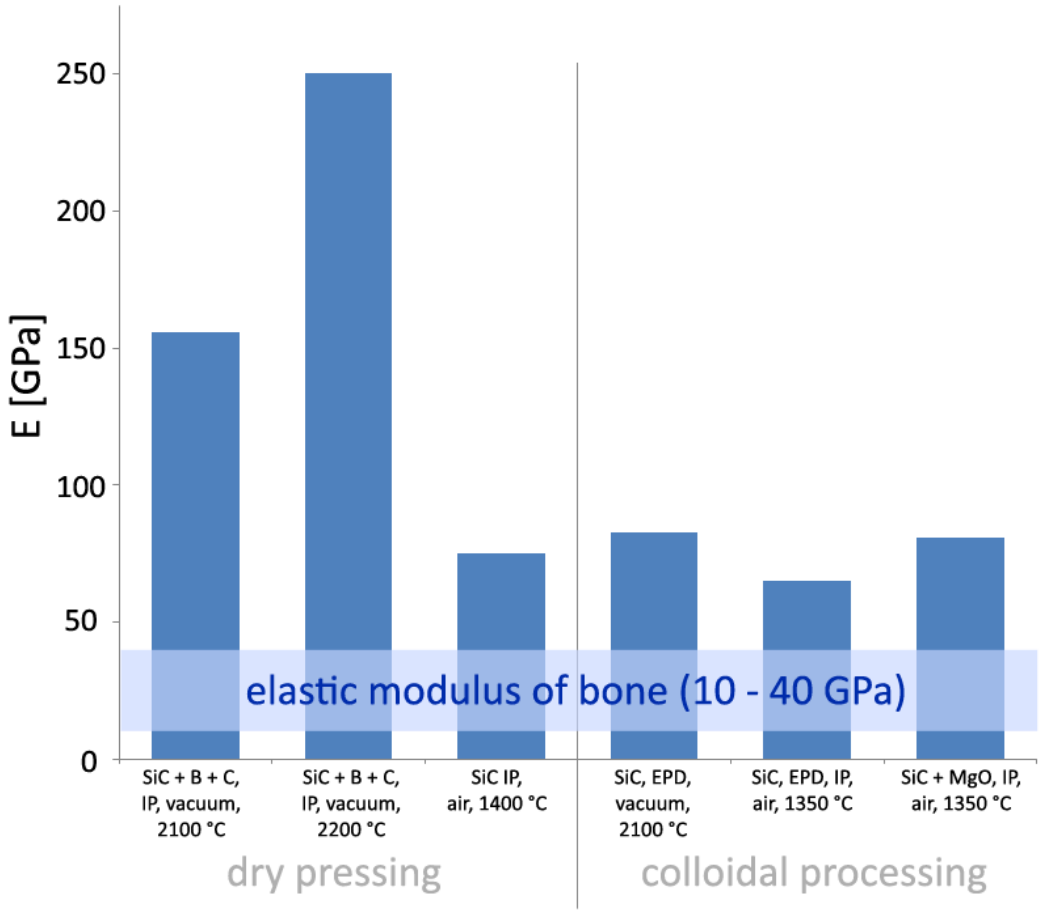

Figure 34: Results of elastic modulus measurement on various materials, EPD = electrophoretic deposition, IP = isostatic pressing

The results of the measurements of elastic moduli are shown in Figure 33. One can see that values range from 60 for air-sintered samples to over 250 GPa in the case of samples sintered with addition of boron and carbon; value for elastic modulus of bone (10-40 GPa) is shown with light blue bar. Still most values are too high for efficient bone replacement material due to possible stress shielding effect. Average values for elastic modulus of ten measurements were 65 and 80 GPa for air-sintered SiC and MgO-containing air-sintered SiC, respectively. Elastic modulus of solid-state sintered SiC without additives was also determined; due to large pores sound excitation technique had to be used and measured value was 83 GPa. Elastic modulus was increased when samples were sintered with boron and carbon; the values for 75 and 90 vol.% were 150 and 250 GPa, respectively.

4.3.3 Fracture toughness

The values of fracture toughness of our materials were estimated from Vickers indentation method and calculation according to Niihara [88] equation. This method lacks reliability on porous samples since elastic modulus is hard to determine with nanoindentation method so it was used only as a rough estimation. For the air-sintered samples K_{Ic} was determined for pure SiC and SiC with addition of MgO. Values for the materials were 2 and 2.9 MPa·m$^{1/2}$, respectively, whereas for sample sintered at 2200 °C with addition of boron and carbon fracture toughness reached 3.9 MPa·m$^{1/2}$. In the last case high value for fracture toughness is a result of much higher sintered density of the material (90 % of theoretical).

4.3.4 Wetting angle

Wetting angle of a material is important from the viewpoint of proteins and cells adhesion. It was found that surface wettability to some extent influenced the attachment of fibroblasts in medium with low serum content; it was better on hydrophilic surfaces [107]. This difference was almost unobservable with increasing serum concentration; however, still hydrophilic surfaces might have positive effect [2].

Surfaces were analysed in term of wetting angles; results are shown in Figure 34. Ti alloys and PVD-SiC coating on Ti served as comparisons.

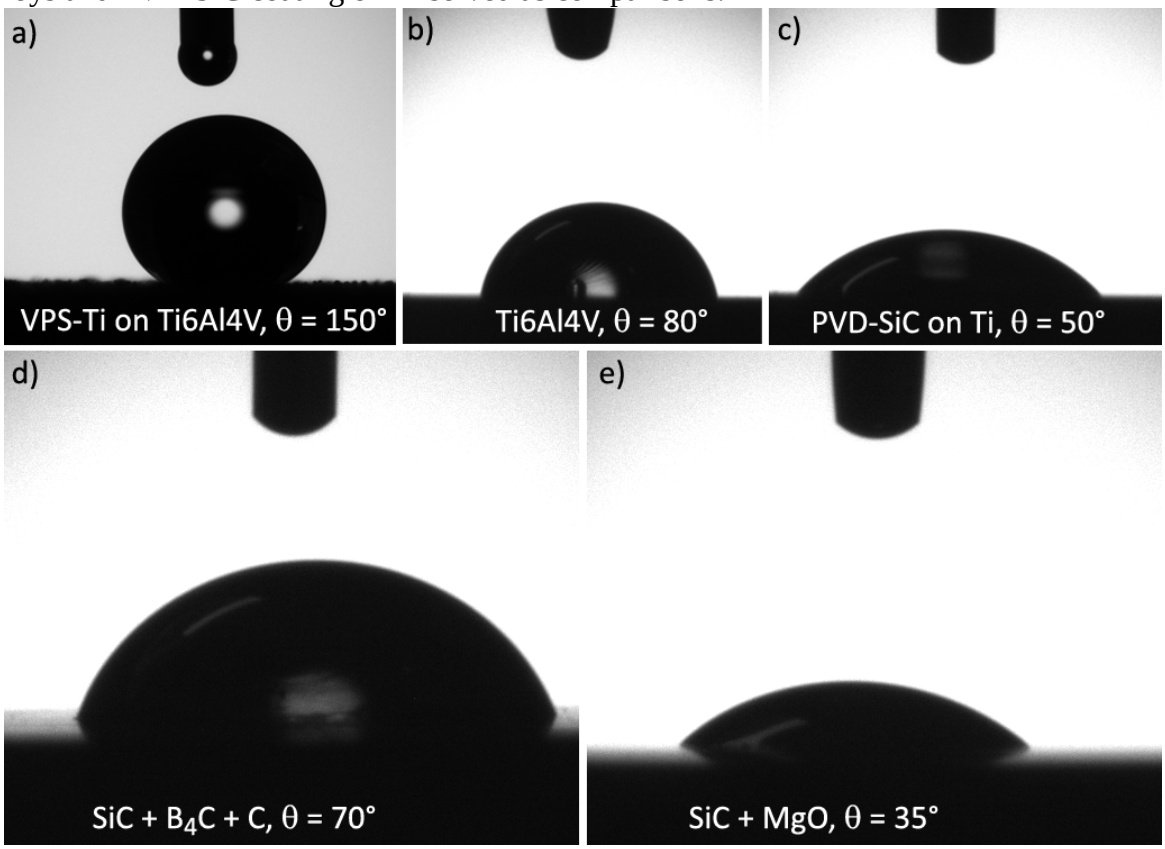

Figure 35: Wetting angles on various surfaces; a) VPS-Ti on Ti6Al4V, b) Ti6Al4V, c) PVD-SiC on Ti, d) SiC + B_4C + C, e) SiC + MgO. In these measurements effect of porosity on wetting was not explicitly studied

Titanium, especially when the surface is rough is strongly hydrophobic material; wetting angle reaches 150° (Figure 34a). This prevents substantial contact of surface with water and therefore adsorption of proteins is inhibited. Also contact angle on flat Ti6Al4V surface (Figure 34b) shows only slight hydrophilic behaviour (wetting angle ~80°). Poor wetting was improved by deposition of SiC layer (physical vapour deposition, PVD-SiC) on metal, its wetting angle was lowered to 50° (b). Those values were compared with values obtained for bulk SiC samples; on Figure 34c picture of droplet on SiC sintered with B_4C and carbon black is shown. Contact angle that was measured is 70°. On the other hand, SiC sintered with MgO in open air (d) shows good wettability (θ = 35°).

The difference in contact angles is even more pronounced on porous surfaces (Figure 34a); when material is hydrophobic, droplet stays on the surface whereas in the case of hydrophilic material water is imbibed into pores. Same can then be expected with serum and since the contact area, especially in porous materials, is big, the chance of protein adsorption is therefore higher.

4.3.5 Magnetic measurements

Magnetic response of SiC was measured and compared to magnetic response of Ti6Al4V alloy; results are presented in Figure 35.

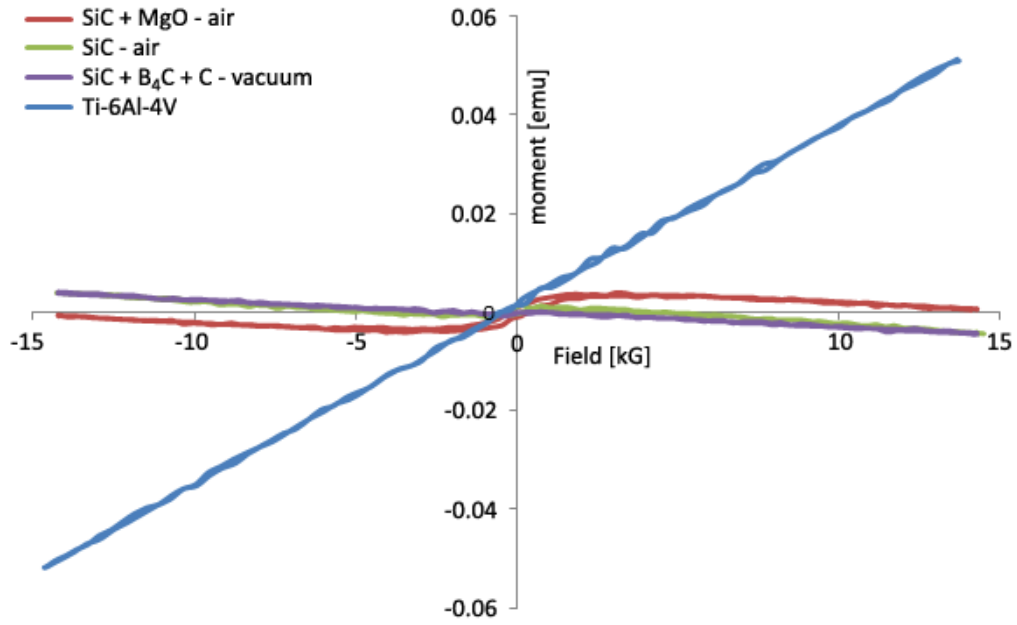

Figure 36: Magnetic measurements (vibrating sample magnetometer) of SiC samples, compared to commercially used Ti6Al4V alloy

While titanium alloy exhibits slight paramagnetic response, SiC samples are considered to be even diamagnetic. However, their response to applied magnetic field is negligible and does not represent any possible damage to the patient.

4.3.6 Inorganic bioactivity

Samples were tested for inorganic bioactivity using test in simulated body fluid (SBF). In our case, after three weeks of immersion of samples (SiC sintered with MgO and SiC containing boron and carbon) in SBF, no hydroxyapatite was observed. To improve the bioactivity, samples were coated with a layer of polymeric bioactive glass and heat treated to remove the organics from the sample. Already after 7 days of immersion in SBF some crystalline phase appeared on the surface, having resembling morphology as hydroxyapatite. The microstructure of the coating is shown in Figure 36.

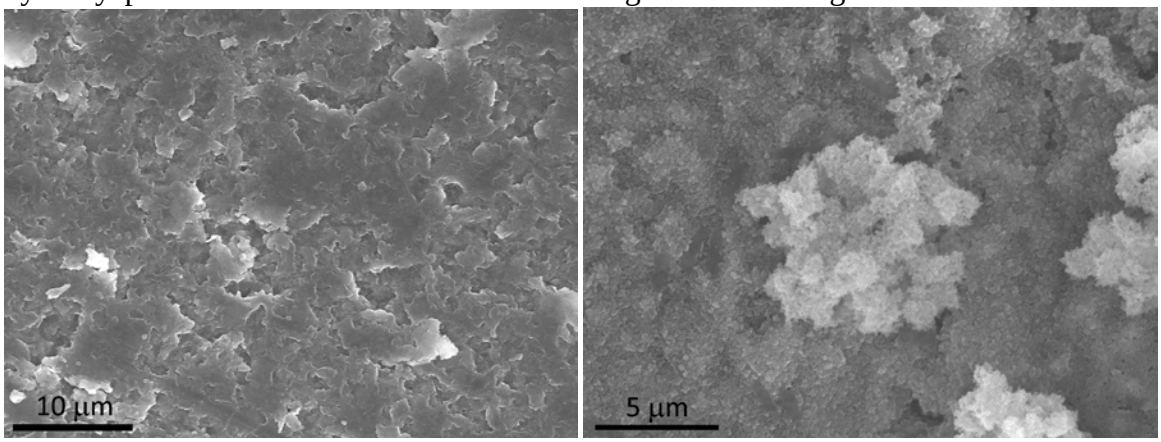

Figure 37: Results of SBF test on a) sample SiC sintered with MgO and on b) SiC sample sintered with B_4C and C and coated with thin layer of BAG

4.3.7 Dissolution of ions

To verify the amount of released ions from our samples, they were put in polyethylene bottles containing 10 mL of 0.9 % NaCl (physiological fluid) and left for 3-10 days at the temperature 36.5 °C to observe the dissolution of silicon, magnesium and vanadium ions. The results of experiments, i.e. measured concentrations are shown in Figure 37 and Figure 38, PVD-SiC (SiC prepared with physical vapour deposition on Ti substrate) served as a control.

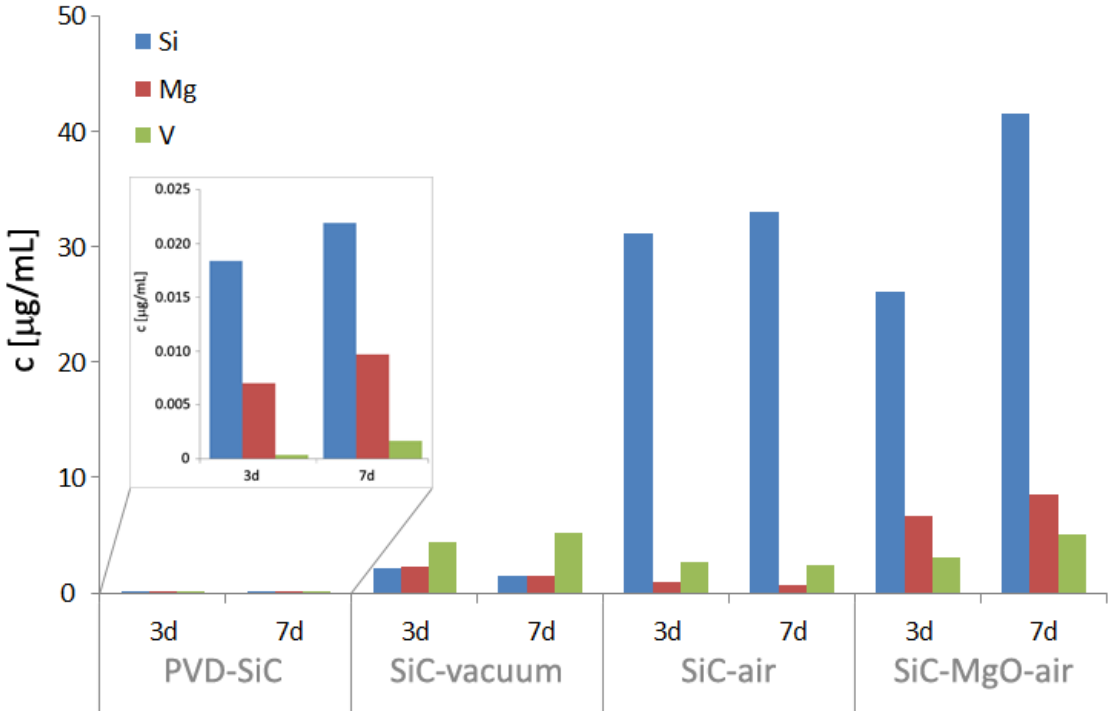

Figure 38: Dissolution of ions from various samples in physiological fluid after 3 and 7 days; enlarged insert shows results for PVD-SiC

As expected, higher concentration of released Si was observed in the case of the samples sintered in air than from the one sintered in vacuum, i.e. 30-40 µg/mL and ~2 µg/mL, respectively. Significantly lower concentrations were determined in the solution after immersion of PVD samples, which could be also ascribed to much lower surface area than in the case of the bulk porous SiC samples. In addition to Si, Mg was also detected in the solutions after immersion of all the samples; also in the case of PVD samples, for which we do not have an explanation. As expected, the concentration of Mg was also the highest in the case of SiC-MgO sample (~10 µg/mL). The presence of <2 µg/mL of Mg in SiC without additives could be explained by presence of Mg in the powder.

The biggest surprise was presence of vanadium in the SiC samples. Since the concentration of V is not negligible, and is due to reported toxicity unwanted, it represents the main issue regarding the objective of this work, i.e. avoiding presence of potentially toxic elements.

It is also observed in Figure 37 that concentrations after 7 days are slightly higher than after 3 days, which implies that the saturation has not been achieved in a few days and it is worth prolonging the immersion time in further studies.

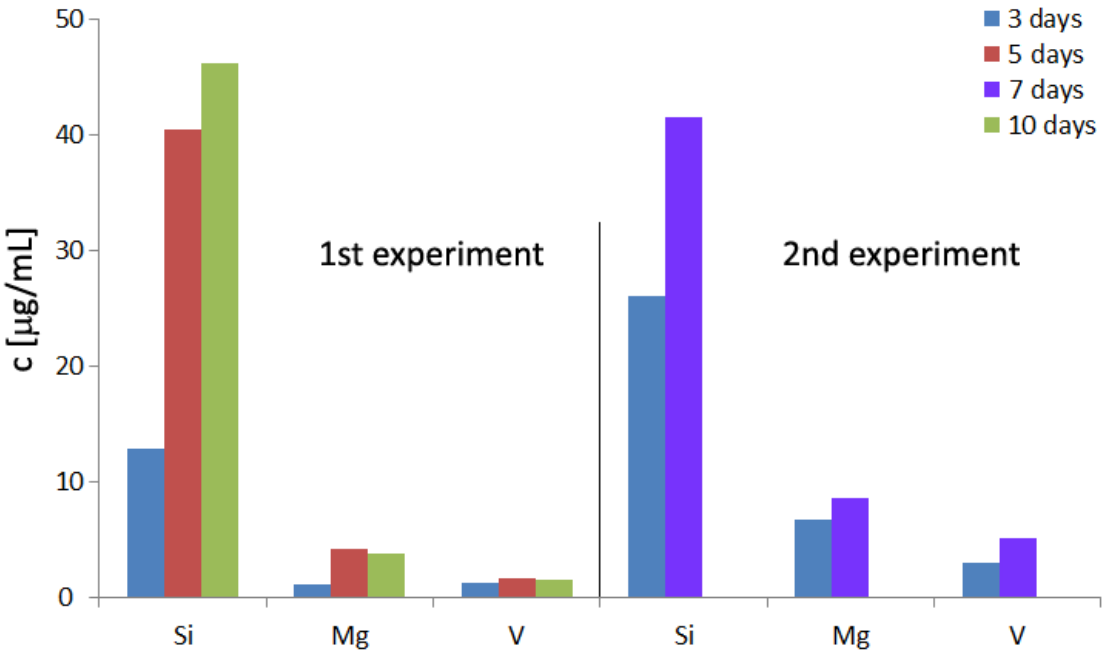

Figure 39: Dissolution of ions from sample SiC-MgO

To verify the reproducibility of the results, in Figure 38 results of two experiments are shown. Samples for both experiments were prepared in the same way, e.g. co-deposited from the SiC suspension containing 3 wt.% MgO and sintered at 1350 °C for one hour. One can see that the concentrations of ions in the solutions after immersion are comparable.

4.3.8 Cell response *in vitro*

Samples were grinded, washed and sterilized to perform cell attachment test and to show the preliminary cell response. After cell suspension was put on the surface and cell growth medium was added, cells were left to attach onto the samples and grow for 24 hours. In the very first set of experiments HepG2 cells (hepatic cell line) were used, one example of cell on the control surface is shown in Figure 39.

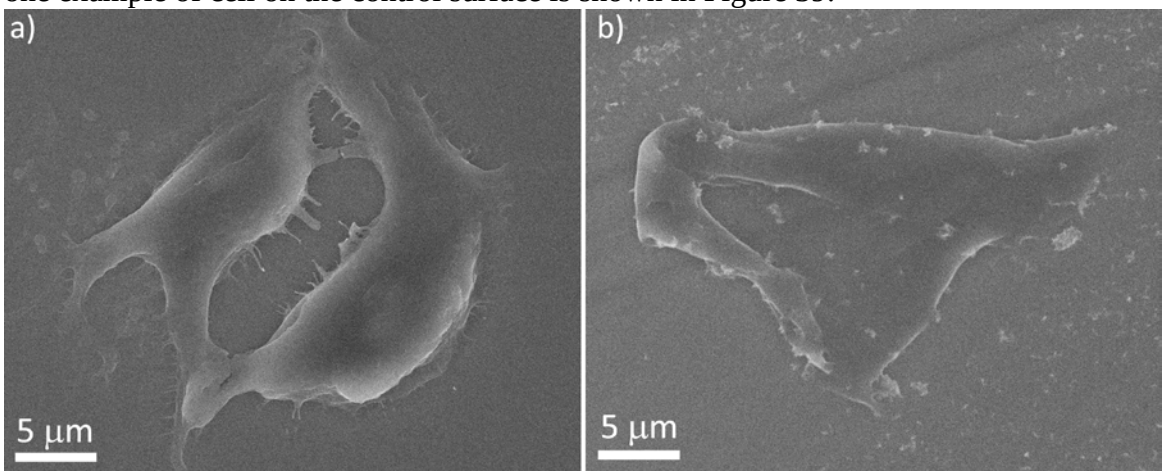

Figure 40: HepG2 cell on the surface of a) control and b) on PVD-SiC

For the following experiments cells were replaced by HeLa cell line (endothelial cells) which is, though relatively little, also used in materials science, especially to prove the potential cytotoxicity of analysed materials. In this case, cells were seeded, and after 24 hours detached from the surface and counted whereas second parallel of the samples was prepared for electron microscopy as described in "Experimental" section. The results of the assessment of cell viability are shown as a bar chart in Figure 40d.

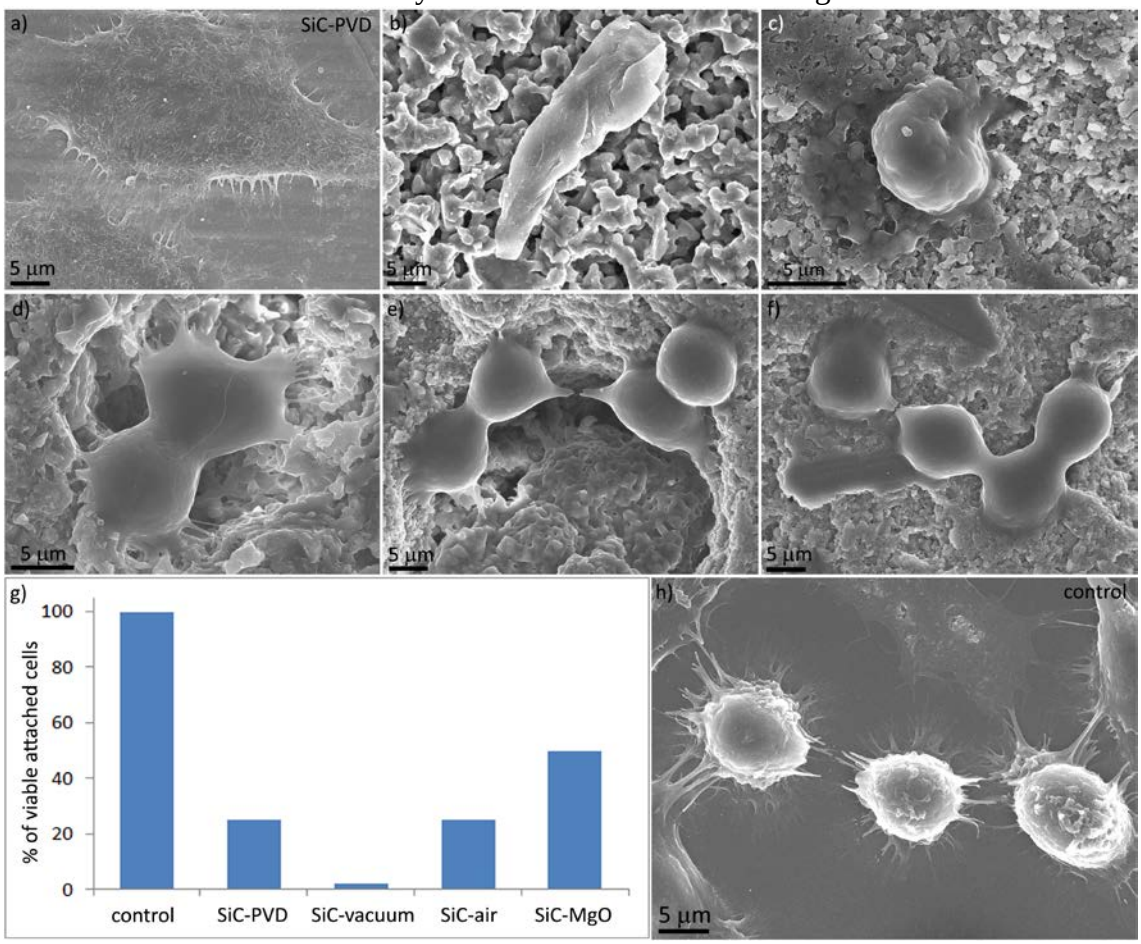

Figure 41: Cell response of HeLa epithelial cells on SiC-based materials prepared in different ways; a) PVD-SiC on titanium substrate served as SiC control, b) vacuum-sintered EPD SiC, c) air-sintered EPD SiC d-f) air-sintered SiC co-deposited with MgO, g) bar chart of attached cells on various surfaces, h) control (glass with polylysine)

One can see that in comparison to the control, the cell attachment was the best for air-sintered SiC that was co-deposited with MgO (Figure 40d, e and f); about 50 % of the cells attached. Less beneficial response was observed for the air-sintered SiC without additives (c) and PVD-SiC on Ti disc (a) where only approximately 25 % of the cells attached to the surface. Vacuum-sintered SiC (b) did not show beneficial properties towards cell attachment, since only 2 % of the cells were found on the surface. Possible reasons could be released vanadium, which is after three days in comparison to others higher in this sample (see Figure 37), or inappropriate surface charge for adhesion of proteins. In the Figure 40 cell morphology of HeLa cells on various surfaces is shown. On the SiC samples having much higher macro roughness and macroporosity than PVD-SiC where the cells are spread over the surface, morphology of the cells is more spherical (globular) and cells readily attach to the concave surfaces (e.g. inner surface of the pores, as observed in the case of SiC-MgO sample). On the basis of these preliminary results it can be concluded that among these materials SiC-MgO is the most promising candidate for the targeted biomaterial.

5 Discussion

In this study, electrophoretic deposition was employed for preparation of SiC green parts, mainly due to its proven versatility and ability to produce compacts with high green densities [108]. Comparison was made between dry pressing and colloidal shaping; it is shown (Figure 19) that green density in the case of colloidal processing is approximately 15-20 % higher (51 compared to 62.3 vol.% for uniaxial pressing and EPD, respectively) than when only dry pressing was employed.

Electrophoretic deposition (EPD) is s a colloidal technique that has been known for decades. In spite of the increasing interest in the shaping of advanced materials using EPD, this technique is not widely used in industry due to the limited understanding of the relationships linking the parameters of the EPD process to the properties of the products. It is based on the application of an electric field to a stable particulate suspension placed between two electrodes and is essentially a two-step process: In the first step, charged particles dispersed in a liquid are forced to move towards an electrode by applying an electric field to the suspension (electrophoresis); in the second step, the particles collect at one of the electrodes and form a relatively dense and homogeneous deposit [109]. The process yields only a powder compact, so EPD needs to be followed by a densification step, such as sintering, in order to obtain a fully dense material. In the production of free-standing objects, a metal or another conductive holder is used as an electrode. It is known that to achieve high densities of the deposits, several requirements with regard to the properties of the suspensions as well as the process parameters have to be fulfilled: insolubility of the material in the liquid used, high zeta potential and conductivity that should be neither too high or too low [94]. For this reason, a comprehensive investigation is needed for each particular system.

At first, electrokinetic properties of as-prepared suspensions were measured with the aim to establish the effect of solids content on zeta potential of the suspension. It was found that with increasing solids content the pH is lowering due to dissolution of SiO_2 on the surface of the particles. Consequently, the absolute value of zeta potential follows its natural sigmoidal curve and is at first increasing up to +35 mV, but after threshold powder concentration is reached (35 wt. % in aqueous and 25 wt.% in ethanol suspensions), zeta potential is lowered because the viscosity of the suspension rises substantially. Also the drop of the conductivity is observed at high concentrations of the powder, which can be also ascribed to high viscosity. However, since no stable concentrated suspension could be prepared solely by mixing water and SiC, zeta potential was increased by addition of base, e.g. TMAH and NaOH or by surface active agent, e.g. CTAB in water and PEI in ethanol.

TMAH is suggested to be a deflocculant [90] which contradicts our results since response of suspension to TMAH is the same as if NaOH was added. Besides, no shift of isoelectric point was observed, that further disproves this theory. In our case, TMAH was only used for pH modification and consequential increase in negative surface charge. The ideal amount of added TMAH was determined to be 0.1 % according to the mass of SiC since it combines high zeta potential (more than -60 mV) with reasonably low conductivity (below 0.5 mS/cm) and results in deposit that has 62 vol.% of solids. In literature it was reported that when using an optimally prepared suspension the produced

parts can have a fairly high green density [95]. SiC parts with a green density of up to 64 vol. % were produced from aqueous suspensions [76, 110].

The results of our study confirm that quality SiC deposits without sintering additives can be produced with relative ease either from aqueous as well as from ethanol suspensions with carefully selected composition. The problems of gas evolution due to the electrolysis of water were successfully overcome by using graphite instead of frequently used stainless steel electrode and/or by placing cellulose membrane in the front of the electrode. No obvious difference appeared between the suspensions and deposits with TMAH or NaOH, both being used as pH modifiers to increase the ZP values. Conversely, cationic surfactant, CTAB, does not work well; during cathodic deposition hydrogen bubbles are evolved and trapped in the deposit that is consequently brittle and with low solids content. On the other hand, cationic surfactant PEI that was used in ethanol suspensions enables cathodic deposition. Due to absence of water there is no problem regarding electrolysis and dense deposits were produced.

Electric field strength in the observed region (7.5 to 30 V/cm) was proven to have a minor effect on the quality of the deposit produced from aqueous suspensions; this result is also in agreement with the literature where it was stated that the homogeneity of the deposit is good at moderate applied fields that are in the region of 25 to 100 V/cm [111]. On the other hand, the applied field has a huge effect on the rate of the deposition; correlation is linear and is in agreement with Hamaker equation as well as with the results in the review article by Besra [109]. In contrast to electric field strength, concentration of the suspension affects deposition rate as well as the quality of the deposit, the latter being frequently overlooked in the literature. Although literature [112] reports that threshold concentration needed to obtain the deposit is relatively low (in the range of 0.5 vol.%), this is not in agreement with our results. It has to be stressed, however, that the results from the mentioned research apply to film formation and consequently mass of the deposit is really low (in the range of mg) while for production of bulk deposit solids content in the suspension is of crucial importance. In our work it was proven that better deposit with more homogeneous packing of the particles was obtained from more concentrated suspensions (i.e. 50 to 60 wt. % of solids) whereas more diluted suspensions resulted in deposit with low solids content (i.e. high amount of liquid medium in the deposit).

Green density appears of main importance for the later sintering process where especially in the case of solid state sintering without any additives the particles packing was found to play crucial role. We have determined a threshold value that has to exceed ~58 % of theoretical density to cause neck formation and growth of the grains and pores. Sufficiently high densities were reached only in the case of EPD-formed green parts, while in the case of dry pressed samples the green density was below the threshold limit and the resulting material after sintering at the same conditions appeared as not sintered at all (see Figure 21).

Addition of sintering additives, e.g. boron and carbon or MgO to the optimized SiC suspension significantly modified the electrokinetic properties and therefore additional studies were needed. In the first case (B_4C, C), naturally hydrophobic carbon particles were modified to hydrophilic by heating in concentrated HNO_3, after washing and re-dispersion. Further addition of TMAH that increased zeta potential enabled co-deposition of SiC, B_4C and C to form a homogeneous green part but unfortunately its density was too low (below 50 vol.%) although the stability of the suspension was good. Only taking into account surface charge of particles this would not be expected but since the conductivity of the suspension was too high (1.1 mS/cm) deposition was not efficient. MgO appeared to be more demanding, since it is slightly soluble in water. That caused high increase in suspensions conductivity and destabilization which made deposition

impossible. For this reason, instead of aqueous suspension, ethanol suspension was prepared. In this case, cathodic deposition appeared to be more beneficial; in terms of ethanol highly positive zeta potential (+30 mV) was obtained by addition of PEI that does not act exclusively as surface active agent but also as a binder and prevents extensive cracking during drying.

5.1 Sintering

Pressure-less sintering of SiC without sintering additive is a challenging task due to its covalent character that prevents diffusion of atoms and has not been well documented in literature. There is one report published in 1994 [113] that explores the origin of density gradients in sintered ß-SiC parts. Authors conclude that the density gradients are the consequence of evolution of CO that originates from the reaction between SiO_2 on the surface of the particles and either SiC or free carbon that is present in the system. Authors claim to have reached more than 98 % density when performing sintering at 2120 °C and holding time at 1500 °C for two hours. Holding temperature is said to be important for CO that is otherwise considered to be sintering retardant to leave the system. This study importantly points out the effect of carbon in the densification process. This sintering programme was in one experiment also repeated in our work but final density did not differ from that obtained by normal sintering programme, i.e. no increase in sintered density was observed and so the literature findings could not be confirmed.

Among the first discovered sintering additives for SiC was boron carbide [114], but breakthrough was achieved when combination of boron and carbon was proposed by Prochazka [115]. He found that at elevated temperature, SiC ceramics with boron and carbon additions, exhibit high strength and relatively high-creep resistance. These properties of boron- and carbon-doped SiC originate from the absence of grain boundary phases and existence of covalent bonds between SiC grains [32]. Later on this combination was thoroughly investigated by Stobierski and Gubernat who researched the effect of both, boron and carbon, separately [97, 98]. It was concluded that the optimal addition of carbon was 3 wt. %, whereas the addition of boron was determined to be 0.5 wt. %. Due to difficulties described before boron and carbon were introduced solely by mixing and dry pressing of the mixture. Even though in this set of experiments better density was obtained in the case of dry pressed samples over the electrophoretic deposition still the distribution of sintering additives was inhomogeneous. When temperature was set to 2100 °C final density of the sintered sample was ~75 % of theoretical while increasing temperature to 2200 °C resulted in densification to 90 % of TD.

Other potential additives for successful densification of SiC in vacuum at high temperatures were discussed by Negita [116]. Reactivities of sintering aids were examined in terms of free energies of the reactions between SiC and sintering aids, i.e. metals and metal oxides. It has been shown that at high temperatures in vacuum metal oxides such as Al_2O_3, BeO, Y_2O_3, CaO, ZrO_2, HfO_2 and rare-earth oxides could serve as potential additives but also in this research sintering temperature was above 2000 °C. In order to lower sintering temperature of SiC, liquid phase sintering was proposed. It is usually performed in argon at relatively high temperatures (1800-2000 °C) and in presence of oxide additives that form liquid phase. Most frequently used combinations are Al_2O_3-Y_2O_3, Al_2O_3-Y_2O_3-SiO_2, combination of aluminium carbide, boron carbide and carbon black, replacing Al_2O_3 with AlN, or simply ZrB_2. These additives are usually introduced in significantly high quantities, sometimes even up to 20 wt.% [87, 117-120]. Some other oxides are sometimes applied, such as earth-alkali metal oxides [121] (MgO, CaO) or rare-earth oxides such as ytterbium, samarium, and so on [122]. Although these combinations of additives combined with high temperatures result in dense SiC with good

mechanical properties, they all contain elements that are considered body-unfriendly and were therefore avoided in this study. Among elements proposed in the literature, only Ca and Mg have been reported to be body-friendly elements; others, such as Al and Be are reported to be toxic. We have decided to use MgO as a sintering additive, also because Mg is reported to be bone growth stimulating element [66, 123].

Considering Negita et al. [116], on the basis of the standard formation free energies, magnesium oxide should not act as an appropriate sintering additive at temperatures above 2000 °C in a vacuum. Even though theoretical calculations are not on behalf of MgO some researches using MgO were made by Foster and Thompson in 1999 [101] where they aimed to densify α-SiC in vacuum at high temperatures. However, due to inhomogeneous distribution of MgO throughout the sample the densification was not as successful as it could have been. Another article by Miyazaki and co-workers [124] dealing with the research of MgO influence on sintering SiC was published in 2001 and it discusses hot pressing of SiC with addition of 2-29 wt.% of MgO at 1900 °C. Authors concluded that there was only little reaction between SiC and MgO, small amount of Mg_2SiO_4 was formed and that indicated the presence of a liquid phase at higher temperatures. In all range of MgO additions fracture toughness ranged between 2.2 and 2.9 $MPa \cdot m^{1/2}$. Another attempt, this time at lower temperatures was made in 2007 by Tatli [99] who coated the SiC particles with MgO and sintered a green compact at 1550 °C. He claims to have reached more than 95 % of theoretical density when processing the coated and compacted powder in (presumably) argon atmosphere (atmosphere not being stated in the article). This idea was later on checked by Novak et al. [102, 125] who researched the system SiO_2-MgO-P_2O_5 and performed sintering in argon atmosphere or in open air. At temperatures around 1400 °C in the presence of oxygen and in combination with SiO_2 dense ceramics with a large amount of silica-rich amorphous secondary phase is formed.

In our work samples were sintered at 1350 °C in open air thus enabling oxidation. XRD analyses then confirmed formation of new crystalline phases, i.e. cristobalite (SiO_2) and Mg-Si-O phases, e.g. $MgSiO_3$ and Mg_2SiO_4, latter being confirmed with TEM. TEM analyses also confirmed that microstructure of the sample consists of SiC grains that are embedded in amorphous SiO_2-SiC_xO_y phase. Even though magnesium is concentrated in some isolated grains it is present in small quantities throughout the entire sample.

When producing green parts, due to reported problems with homogeneity when dry pressing was employed [101], in our work MgO was introduced directly to the suspension and co-deposited with SiC. MgO is soluble in water and solubility is claimed to be 0.086 g/L but when dissolved it forms magnesium hydroxide, $Mg(OH)_2$. Dissolution of MgO follows the reaction:

$$MgO + H_2O \rightarrow Mg(OH)_2 \rightarrow Mg^{2+} + 2OH^-$$

The reaction is basic and the pH of the saturated solution of MgO is 10.5. However, the ions that contribute to conductivity are now $Mg^{2+}$and OH^- that are the result of dissolution of $Mg(OH)_2$, solubility constant (K_{sp}) of which is reported to be $1.5 \cdot 10^{-11}$. When calculating the concentration of Mg^{2+} ions at the specified pH and considering only magnesium and hydroxide ions contribute to conductivity, the maximum resulting conductivity would be 18.2 mS/cm. This is on one hand much higher than the measured value (750 µS/cm) but on the other hand such conductivity (calculated as well as measured one) is far too high for successful EPD. Ethanol had to be used instead. Colloidal properties were tailored using PEI (results shown in Figure 16) and homogeneity of the deposition was demonstrated using EDS analyses of the green sample (see Figure 18). The amount of MgO in the final deposit is lower than in the starting suspension which is

presumably the consequence of bigger MgO particles compared to SiC. Homogeneity of SiC distribution, which is substantial problem in the case of dry pressing, was determined. Due to similar average Z of SiC and MgO it is not possible to distinguish between both powders on backscattered electron image. EDS analyses were performed on several parts of green sample and it was verified that distribution of sintering additive is homogeneous within 15 % deviation (see Figure 18). The ratio between MgO and SiC in deposit is lower than that in the starting suspension, indicating that the mobility of MgO is lower than of SiC. Possible explanation is that MgO particles are larger than SiC and therefore their mobility is hindered.

With the aim to prevent SiC from oxidation, sintering is preferentially performed under vacuum or in inert atmosphere. In air, SiC forms SiO_2 coating at 1200 °C which is able to protect SiC from further oxidation above 1600 °C. Reports on when extensive oxidation of SiC occurs are sometimes contradictory but detected temperature may depend on criteria of oxidation and on form of material (i.e. porous foam, layered ceramics, bulk ceramics, powder …). In general temperatures between 1400 and 1600 °C are determined [126-129]. Since in our case oxidation does not represent a problem and SiO_2 on the surface can also act beneficially towards biological response, samples were also sintered in open air at temperatures considerably lower than those required for conventional sintering. From the dilatometric curve (Figure 20) temperature of sintering was determined to be 1350 °C. When our samples were sintered at that temperature, increase in density was observed; from 1.61 to 1.87 g/cm^3 in the case of pure SiC and from 1.92 to 2.33 g/cm^3 for SiC containing MgO. It was shown that addition of MgO enhances densification, and that also resulted in improved mechanical properties compared to pure SiC.

5.2 Properties of SiC-based ceramics

5.2.1 Mechanical properties

Among the main properties required from the material to be used for bone implants are resistance toward fracture and elastic modulus that should be in ideal case similar to that of the natural bone in order to prevent stress shielding (i.e. stress transfer between an implant device and a bone is not homogeneous when elastic moduli of implanted material and bone are different. This results in bone resorption in vicinity of implants [2]). As expected, the elastic modulus for the SiC with total porosity of 30-40 % is significantly lower than that for the dense SiC (410 GPa).

Elastic moduli of air-sintered ceramics are 65 GPa for pure SiC and 80 GPa for SiC containing MgO. In comparison with natural cortical bone that has elastic modulus 10-40 GPa, both values are still higher, while they are much lower than for the titanium metal (115 GPa) and alloys (107 GPa for Ti6Al4V alloy). Besides, also elastic modulus for conventionally sintered SiC, i.e. with addition of boron carbide and carbon black is significantly higher and dependent upon temperature of sintering. Elastic modulus also depends on total porosity of samples treated in the same manner, as also reported in the literature [130, 131]; in samples containing boron carbide and carbon black E modulus is increased from 150 to 250 GPa when density is increased from 75 to 90 % of theoretical.

Flexural strength is also significantly affected by porosity of the SiC-ceramics: flexural strength of sintered ceramics with MgO reached 155 to 180 MPa in the case of electro co-deposited samples, latter being subsequently isostatically pressed while in the case of pure air-sintered SiC it was decreased to 125 MPa, also due to higher porosity of the sample. Flexural strength of samples with addition of boron and carbon was 110 and

220 MPa for samples sintered to 75 and 90 % density, respectively. Compared to titanium and its alloys these values are lower (tensile strength, that is usually to some extent lower than flexural strength, but of the same order of magnitude [132] is 960 MPa for Ti6Al4V alloy) while in comparison to tensile strength of human bone we can conclude that our material fulfils the requirements (tensile strength of bone being 90-140 MPa).

The main weakness of the as-prepared SiC ceramics is expressed in the fracture toughness, i.e. resistance to failure. It has to be taken into account that direct comparison between bone and monolithic SiC is not the most appropriate since bone is a composite material and has by default higher fracture toughness than materials that are not reinforced. From the literature data fracture toughness of the bone is high, dependent on the type of the bone as well as on direction of measurement it varies from 1 to 15 $MPa \cdot m^{1/2}$ [18]. On the other hand the values for both samples (air-sintered pure SiC and SiC with MgO) were 2.0 and 2.9 $MPa \cdot m^{1/2}$, respectively, which is much lower than for the titanium and its alloys (140 $MPa \cdot m^{1/2}$ and 75 $MPa \cdot m^{1/2}$, respectively) and also lower than for trabecular bone. It was stated in the literature that incorporating ceramic fibres can significantly improve the mechanical performance of the material [30]. Due to bonding between the fibres, changing in crack trajectories, and fibres stretching, fibrous porous materials are known to possess improved strength. It was reported by Guo [133] that fracture toughness of fibre toughened Si_3N_4 (pure material has K_{Ic} 6.1 $MPa \cdot m^{1/2}$) reached 17 and 24 $MPa \cdot m^{1/2}$ in the case of reinforcement with Si_3N_4 and SiC fibres, respectively.

It was shown in work by Zawrah [32] that the obtained mechanical properties of their samples (SiC sintered with Al_2O_3-Y_2O_5-CaO system) are favourable as compared with human cancellous bone and titanium for biomedical applications. This was also proven in our work on the SiC-MgO system. It is then possible to conclude that SiC biomaterial implants appear as quite interesting alternative to Ti implants, by showing more acceptable mechanical properties and lower specific weight. Moreover, taking into account the biomechanical requirements (density, elastic modulus, and strain to failure …) of a particular type of bone in the body that should be repaired; SiC ceramics can be tailored and selected according to the above properties.

5.2.2 Magnetic properties

Despite not highly relevant anymore, magnetic properties are still considered when it comes to artificial bone implants. This was of greater concern when implants were made mainly of stainless steel where response to strong outer magnetic field (when magnetic resonance imaging is performed) could not be excluded. Titanium is in general not magnetic material but due to safety issues presence of metal implant in the body usually prevents doctors from using magnetic resonance imaging. It was reported that, at least in the case of metallic cardiovascular pacemakers, there are currently no “MRI-safe” or “MRI-compatible” devices [23]. Besides, presence of metallic implants in MRI can cause substantial image artefacts and distortions on the very site of implantation [24].

For this reason SiC samples (SiC-C-B_4C, sintered in vacuum and air-sintered pure SiC and SiC-MgO) were tested with vibrating sample magnetometer (VSM), showing negligible response to applied magnetic field (see Figure 35). Therefore also from the viewpoint of potential use of MR imaging SiC is acceptable material.

5.2.3 Leaching of elements

It was reported in literature that corrosion resistance of SiC under normal biological conditions (neutral pH, body temperature) is excellent. The dissolution rate is well below 30 nm per year [134]. It was also stated that one of the properties that make this material particularly promising for biomedical applications is its chemical inertness that suggests the material resistance to corrosion in harsh environments such as body.

As stated before, the main aim of this study was to minimise any adverse effect of metal released from an implant into the body, and to replace the unwanted elements with elements with proposed beneficial effects towards bone regeneration. The analysis of concentration of elements released from our samples revealed that there is substantial concentration of silicon and magnesium ions, while no titanium or aluminium was detected. Surprisingly after 10 days of immersion of the samples in physiological solution at 36.5 °C, we detected also a high concentration of vanadium (~4 µg/mL). On the other hand, it was also reported that estimated intake for vanadium is 10 to 60 µg/day [62] and vanadium toxicity is still debatable issue [63] on which no firm conclusions can be made. Since the analyses were performed very carefully, using also blank solutions without samples in parallel, and as the same increased levels of vanadium have been recorded in all experiments except for the sample with SiC coating prepared by PVD technique, it is possible the supplied powder materials have been already contaminated as no other source of vanadium was found in chemicals or equipment used.

Even though the concentration of vanadium is quite alarming, since its nontoxicity is not unambiguously proven this problem can be overcome by careful choice of starting powders or by application of SiC coating that can have, due to different route of synthesis, much higher purity.

The comparison with currently used titanium alloys can be made; though the results are not shown here, it was measured that after 30 days of immersion of Ti6Al4V discs in physiological fluid about 0.3 ng/mL of vanadium but also 1 ng/mL of aluminium is released.

In order for SiC ceramics to be considered as a potential material for implants, great care has to be taken regarding the selection of pure starting materials. In this study, the role of the vanadium presence has to be considered in particular in cell-response test. In general, the concentrations of the elements released from the SiC samples are relatively high in comparison with the literature data on metal ions release [53]. This proceeds from much higher solubility of SiO_2 in comparison with metals. However, as described in literature [123, 135] release of silicon as well as magnesium are supposed to have beneficial effect on bone growth while the rate of dissolution is still so slow that the integrity of the part is not changed.

5.2.4 Wetting, bioactivity and cell response

Wetting of the implant surface with water or serum to which the material is exposed after implantation is important from the viewpoint of protein adhesion and subsequent cell attachment [107]. This is especially important in the case of highly porous samples; when material is hydrophobic, liquid does not penetrate into pores and so contact between proteins and surface is prevented. This is well presented in Figure 34a in the case of VPS-Ti; droplet stays on the very surface. By measuring wetting angle it was established that surface of SiC sintered with MgO has most hydrophilic character among all tested material (wetting angle 35°, see Figure 34) while sample sintered in vacuum with boron carbide and carbon has much higher wetting angle (70°), possibly due to less SiO_2. Good

wetting enables adhesion of proteins and consequential attachment of cells.

Bioactivity of the prepared samples SiC-MgO and SiC-C-B_4C was tested by the well known and widely used simulated body fluid test proposed by Kokubo [89], where the formation of hydroxyapatite on the examined sample immersed in SBF is observed. Cauliflower-shaped hydroxyapatite crystals consisting of thin plates are typically formed on “bioactive” materials like bioactive glass and hydroxyapatite within a relatively short time (days, sometimes even hours), while it is not formed on the surface of “bionert” material like metals including titanium and its alloys even after weeks of immersion [136]. The reliability of the test itself is a subject to more discussions, but in general it enables at least a rough estimation of the bioactivity of certain material in comparison with others. In the case of our SiC samples the hydroxyapatite layer was not formed even after 3 weeks that suggests negligible inorganic bioactivity. This also implies that the formation and dissolution of silica (and MgO) in simulated body fluid is very low which is also confirmed by the leaching test. On the other hand this implies a long-term stability of the material in body. The lack of inorganic bioactivity should not be taken as a major disadvantage and was simply overcome by coating with bioactive glass. The coating resulted in formation of hydroxyapatite within 7 days.

This test can be to some extent misleading since it does not cover the behaviour of the material in living organisms but solely the precipitation of inorganic, bone-like mineral phase, hydroxyapatite on the surface. In addition, not only surface chemistry but also topography and some other parameters affect possible precipitation. Due to all these arguments, the results cannot be taken as strongly conclusive.

Though not frequently used in testing of biomaterials, HeLa cells of epithelial origin were used in our study. There are few reports regarding HeLa cells as indicators of biomaterial’s behaviour [137-141], especially in terms of establishing cell toxicity. Seuss et al. [138] report in their study about the phenomenon of de-adhering of large fraction of cells with time. They have ascribed this to increasing pH that is the consequence of Mg alloy corrosion.

In our study, preliminary tests of cell response after 24 h of culturing show better response to air-sintered SiC containing MgO as sintering promoter. More than 50 % of the cells attached onto the surface while on the other materials at most 25 % cells were attached (see Figure 40). This might be ascribed either to favourable effect of magnesium and silicon or to good wettability and suitable surface charge.

It has to be stressed out that cells that attached to the surface were proven alive with trypan blue viability test. Still, in order to better evaluate response of the cells towards the material, prolonged exposure should be checked. From everything discussed above SiC should be further explored as potential biomaterial.

	Specific weight	Porosity [%]	E [GPa]	σ [MPa]	K_{Ic} [MPa·m$^{1/2}$]	Magnetic response	Wetting	Cell response	SBF bioactivity	Ions release
SiC	+++	++ (45 %)	+ (83 GPa)	+/−(135)	–	None	+/−	+/−	–	– (V)
SiC-BC	++	– (10 %)	– (150-250)	++ (220)	−/+ (3.9)	None	+/−	+/−	– (+ when BAG-coated)	– (V)
SiC-MgO	+++	++ (30 %)	+ (65-80)	+ (up to 180)	– (2.9)	None	++	++	–	+/−(Si, Mg, V)
Ti6Al4V	–	– (dense)	– (105-115)	+++ (960)	+++	Slight paramagnetic	–	++	–	–(Ti, Al, V)
bone	2.1 g/cm^3	30 – 50 %	10 – 40	90 – 140	1–15	None		+++++	+++++	+++++

Table 3: Qualitative estimation of the properties of SiC ceramics compared to Ti6Al4V and bone

6 Conclusions

In this PhD thesis feasibility study was made, regarding the potential of SiC to be used in biomedical applications. We have checked the hypothesis that SiC could in some applications replace currently used metallic materials since they have some disadvantages considering leaching of metal ions that can later cause adverse health effects. Beneficial effects of silicon on proliferation and differentiation of osteoblasts have been known for several decades and also SiC was mentioned as a potential biomaterial, however, to fulfil the demands for biomedical applications frequently used sintering additives (Al_2O_3-Y_2O_3) should be avoided due to suggested (neuro)toxicity of aluminium. Mechanical properties of final material should be in the range of human bone (i.e. elastic modulus between 10 and 40 GPa, compressive strength above 100 MPa, tensile strength 90-140 MPa and fracture toughness >5 $MPa \cdot m^{1/2}$) and therefore produced part should have adequate green density.

We have shown that green density highly affects solid-state sintering of SiC without additives and that threshold value of ~58 vol.% was determined, below which no extensive neck formation nor grain growth was observed. When green density was sufficient, firm porous network was formed. However, sintering in vacuum to high extent only resulted in grain and pore growth while no significant densification was observed.

Deposits with high green density were prepared from optimized suspension; i.e. high zeta potential (absolute value above 60 mV for aqueous and 30 mV for ethanol suspensions) and moderate conductivity. Existence of so called “conductivity window” has been shown; too low as well as too high conductivity has detrimental effect on electrophoretic deposition. For 60 wt.% aqueous SiC suspension this value should be 0.5 +/- 0.1 mS/cm while for 50 wt.% SiC suspension in ethanol in the range of 50 µS/cm.

Co-deposition in two systems (B_4C + C, MgO) was also performed in order to investigate the effect of introduction of sintering additives. Co-deposition of carbon black, boron carbide and SiC is possible if originally hydrophobic surface of carbon black is oxidized to achieve hydrophilicity but in our case, conductivity of aqueous suspension was too high to achieve suitable green densities. Therefore sintering with boron and carbon was performed solely by mixing all powders but after pressing and sintering a material with insufficient homogeneity was produced.

Co-deposition of SiC with MgO was also proven possible; water should be replaced with ethanol due to solubility of MgO in former. Surface of both powders was then modified with cationic surfactant (PEI) to prepare stable suspension with highly charged particles. Homogeneity of as-prepared deposit was observed; it was shown that distribution of Mg is fairly homogeneous across the sample; the homogeneity of distribution was given as relative standard deviation that was below 15 %. Sintering of deposit in open air in presence of MgO results in more pronounced oxidation, also new crystalline phases are formed (SiO_2, Mg-Si-O phases) and higher densification is achieved (density increased from 1.92 g/cm^3 to 2.33 g/cm^3).

Colloidal processing results in more homogeneous green body; this is also reflected in mechanical properties; flexural strength was above 100 MPa in all cases where colloidal processing was employed. Since compressive strength of bone is around 100 MPa and flexural strength of materials is lower than compressive this is reasonable value for our

material to have a potential to be used as an implant, however, strength of titanium and its alloys is still much higher. Elastic modulus that was measured by means of nanoindentation on samples sintered in air has values between 60 and 80 GPa; this is still higher than elastic modulus of bone that is reported 10-40 GPa but since elastic modulus of materials depends on porosity this property can be further tailored to better match properties of human bone, but that would also affect strength of the material. Higher porosity of the material on the other hand also results in better cell response, as stated in the literature [1, 142]. EPD SiC without additives that was sintered in vacuum had flexural strength 135 MPa and elastic modulus 83 GPa. On the other hand, elastic modulus of samples sintered with carbon black and boron carbide exceeds 150 GPa, in one case also 250 GPa. Fracture toughness that was estimated from Vickers indentation had values between 2 and 2.9 $MPa \cdot m^{1/2}$ for air-sintered samples while for sample sintered in vacuum with boron and carbon at 2200 °C fracture toughness increased to 3.9 $MPa \cdot m^{1/2}$. This is still rather low in terms of reliability but can be improved by addition of fibres.

SiC sample sintered with MgO has much more hydrophilic surface (θ=35°) than titanium, in particular porous metals that are strongly hydrophobic (θ=150°). Hydrophilicity is supposed to be beneficial for cell response as well as for adsorption of proteins when material comes into contact with serum or other biological fluids. Samples sintered in vacuum have values in between, θ=70°. Magnetic measurements show negligible response of SiC towards external magnetic field, even lower than that for Ti6Al4V. Also SiC is not subjected to radiofrequency heating so it can be considered a “MRI-safe” material. No inorganic bioactivity of our materials that was tested using simulated body fluid could be proved. However, when SiC was coated with thin layer of bioactive glass, crystal phase was formed having morphology that resembles hydroxyapatite. Dissolution experiments show leaching of silicon and magnesium ions, which are desired in terms of cell response, and vanadium ions, that could cause adverse reactions. Vanadium is presumably the result of impurities in the starting powder. Higher leaching of silicon was detected from air-sintered samples since SiO_2 is more soluble than SiC. Preliminary tests regarding adhesion and viability of HeLa cells on the surface of our samples show beneficial response especially on the surface of air-sintered SiC with addition of MgO. Cells more readily attached to concave surfaces, i.e. pores.

On the basis of all results it can be concluded that SiC, especially when sintered in air with addition of MgO has a potential to be used as a permanent orthopaedic material, for example as spinal implant. Response of cells is encouraging, mechanical properties (except fracture toughness) are sufficient while dissolution of potentially toxic ions can be avoided by careful choice of starting materials. From all of the presented results we can conclude that SiC is a potential, though not ideal, ceramics for bone implants.

Further investigation of this material should consider integrating fibres thus improving the reliability of the material and increasing (macro)porosity that would enable better bone ingrowth. However, special care should still be taken regarding mechanical properties, especially strength and fracture toughness. Cell response could be improved by integrating the proteins or other bone forming elements (e.g. strontium) to the surface of the material.

7 Acknowledgements

Although present dissertation is the result of my work, it has been affected by many mentionable people. Firstly, I would like to thank my PhD supervisor, asst. prof. dr. Saša Novak for her valuable advices, numerous brainstormings, fruitful discussions, patience and great ideas.

Secondly, I would like to thank prof. dr. Spomenka Kobe, my co-supervisor, for following my work, for advices and discussions on our monthly meetings.

I would like to thank my evaluation committee, asst. prof. dr. Goran Dražić, prof. dr. Metka Filipič and prof. dr. Michael Gasik for fast evaluation of my thesis and many valuable advices that improved this work.

Many people have also helped me with characterization of my material; special thanks go to dr. Jana Petkovič from National Institute of Biology for performing cell tests and helping me with interpretation of the results. Dare Eterovič (IJS, K6) is acknowledged for helping me with measurements of mechanical properties while Boris Arzenšek (Institute of Metals and Technology) helped me with Vicker's hardness indentations. I would also like to mention and thank dr. Srečo Škapin (IJS, K9) for XRD measurements and Anže Martinčič as well as prof. dr. Radmila Milačič (both IJS, O2) for ICP-MS measurements. Dr. Benjamin Podmiljšak is acknowledged for magnetic measurements.

I would also like to thanks all my co-workers, especially those from E-51 (Nataša Drnovšek, Ana Gantar, Darja Pečko, Martina Lorenzetti, Aljaž Ivekovič, Barbara Horvat) for fruitful discussions for ideas and for the support. Jaro Bele helped me with laboratory work and with his inventiveness he made a few things much easier.

Also I would like to thank my family and friends who supported me throughout all years of study. You are really valuable to me. Last but not least special thanks go to Andrej that, being in the same position, always finds encouraging words and is a great partner in dialogue. And … Heidi … thank you for your support, for being here for me, for standing my mood swings and for being the person that I can always rely on <3

8 References

1. Santin, M. (ed.) *Strategies in Regenerative Medicine: Integrating Biology with Materials Design* (Springer, New York, 2009).
2. Dee, K. C.; Puleo, D. A.; Bizios, R. *An introduction to tissue-biomaterial interactions* (Wiley-Liss, New Jersey, 2002).
3. Ni, G. X.; Lu, W. W.; Tang, B.; Ngan, A. H. W.; Chiu, K. Y.; Cheung, K. M. C.; Li, Z. Y.; Luk, K. D. K. Effect of weight-bearing on bone-bonding behavior of strontium-containing hydroxyapatite bone cement. *Journal of Biomedical Materials Research Part A* **83A**, 570–576 (2007).
4. Hing, K. A. Bone repair in the twenty-first century: biology, chemistry or engineering? *Philosophical Transactions of the Royal Society of London Series A: Mathematical Physical and Engineering Sciences* **362**, 2821–2850 (2004).
5. Williams, D. F. *The Williams Dictionary of Biomaterials* (Liverpool University Press, Liverpool, 1999).
6. Myllymaa, K. *Novel carbon coatings and surface texturing for improving biological response of orthopedic implant materials* (University of Eastern Finland, Kuopio, 2010).
7. Ratner, B. D.; Hoffman, A. S.; Schoen, F. J.; Lemons, J. E. (eds.) *Biomaterials Science: An Introduction to Materials in Medicine* (Elsevier Inc., London, 2004).
8. Cadosch, D.; Chan, E.; Gautschi, O. P.; Filgueira, L. Metal is not inert: Role of metal ions released by biocorrosion in aseptic loosening-Current concepts. *Journal of Biomedical Materials Research Part A* **91A**, 1252–1262 (2009).
9. Siddiqi, A.; Payne, A. G. T.; De Silva, R. K.; Duncan, W. J. Titanium allergy: could it affect dental implant integration? *Clinical Oral Implants Research* **22**, 673–680 (2011).
10. Best, S. M.; Porter, A. E.; Thian, E. S.; Huang, J. Bioceramics: Past, present and for the future. *Journal of the European Ceramic Society* **28**, 1319–1327 (2008).
11. Hench, L. L. The story of Bioglass (R). *Journal of Materials Science-Materials in Medicine* **17**, 967–978 (2006).
12. Juhasz, J. A.; Best, S. M.; Brooks, R.; Kawashita, M.; Miyata, N.; Kokubo, T.; Nakamura, T.; Bonfield, W. Mechanical properties of glass-ceramic A-W-polyethylene composites: effect of filler content and particle size. *Biomaterials* **25**, 949–955 (2004).
13. Campbell, A. The potential role of aluminium in Alzheimer's disease. *Nephrology Dialysis Transplantation* **17**, 17–20 (2002).
14. Exley, C. (ed.) *Aluminium and Alzheimer's disease: The science that describes the link* (Elsevier, Amsterdam, 2001).
15. Frisardi, V.; Solfrizzi, V.; Capurso, C.; Kehoe, P. G.; Imbimbo, B. P.; Santamato, A.; Dellegrazie, F.; Seripa, D.; Pilotto, A.; Capurso, A.; Panza, F. Aluminum in the Diet and Alzheimer's Disease: From Current Epidemiology to Possible Disease-

Modifying Treatment. *Journal of Alzheimers Disease* **20**, 17–30 (2010).

16. Exley, C.; Mamutse, G.; Korchozhkina, O.; Pye, E.; Strekopytov, S.; Polwart, A.; Howkins, C. Elevated urinary excretion of aluminium and iron in multiple sclerosis. *Multiple Sclerosis Journal* **12**, 533–540 (2006).
17. Dewidar, M.; Yoon, H.-C.; Lim, J. Mechanical properties of metals for biomedical applications using powder metallurgy process: A review. *Metals and Materials International* **12**, 193–206 (2006).
18. Koester, K. J.; Ager, J. W.; Ritchie, R. O. The true toughness of human cortical bone measured with realistically short cracks. *Nature Materials* **7**, 672–677 (2008).
19. Lisa A, P. Deformation, yielding, fracture and fatigue behavior of conventional and highly cross-linked ultra high molecular weight polyethylene. *Biomaterials* **26**, 905–915 (2005).
20. Teoh, S. H. Fatigue of biomaterials: a review. *International Journal of Fatigue* **22**, 825–837 (2000).
21. Liu, X.; Chu, P. K.; Ding, C. Surface modification of titanium, titanium alloys, and related materials for biomedical applications. *Materials Science and Engineering: R: Reports* **47**, 49–121 (2004).
22. Drnovšek, N.; Daneu, N.; Rečnik, A.; Mazaj, M.; Kovač, J.; Novak, S. Hydrothermal synthesis of a nanocrystalline anatase layer on Ti6A4V implants. *Surface and Coatings Technology* **203**, 1462–1468 (2009).
23. Baikoussis, N. G.; Apostolakis, E.; Papakonstantinou, N. A.; Sarantitis, I.; Dougenis, D. Safety of Magnetic Resonance Imaging in Patients With Implanted Cardiac Prostheses and Metallic Cardiovascular Electronic Devices. *Annals of Thoracic Surgery* **91**, 2006–2011 (2011).
24. Hargreaves, B. A.; Worters, P. W.; Pauly, K. B.; Pauly, J. M.; Koch, K. M.; Gold, G. E. Metal-Induced Artifacts in MRI. *American Journal of Roentgenology* **197**, 547–555 (2011).
25. EFSA Safety of aluminium from dietary intake. *The EFSA Journal* **754**, 1–34 (2008).
26. Piconi, C.; Maccauro, G. Zirconia as a ceramic biomaterial. *Biomaterials* **20**, 1–25 (1999).
27. Eichler, J.; Rodel, J.; Eisele, U.; Hoffman, M. Effect of grain size on mechanical properties of submicrometer 3Y-TZP: Fracture strength and hydrothermal degradation. *Journal of the American Ceramic Society* **90**, 2830–2836 (2007).
28. Guo, X. Property degradation of tetragonal zirconia induced by low-temperature defect reaction with water molecules. *Chemistry of Materials* **16**, 3988–3994 (2004).
29. Chevalier, J.; Gremillard, L. Ceramics for medical applications: A picture for the next 20 years. *Journal of the European Ceramic Society* **29**, 1245–1255 (2009).
30. Orlovskii, V. P.; Komlev, V. S.; Barinov, S. M. Hydroxyapatite and Hydroxyapatite-Based Ceramics. *Inorganic Materials* **38**, 973–984 (2002).
31. Cappi, B.; Neuss, S.; Salber, J.; Telle, R.; Knuchel, R.; Fischer, H. Cytocompatibility of high strength non-oxide ceramics. *Journal of Biomedical Materials Research Part A* **93A**, 67–76 (2010).
32. Zawrah, M. F.; El-Gazery, M. Mechanical properties of SiC ceramics by ultrasonic nondestructive technique and its bioactivity. *Materials Chemistry and Physics* **106**, 330–337 (2007).
33. Mazzocchi, M.; Bellosi, A. On the possibility of silicon nitride as a ceramic for

structural orthopaedic implants. Part I: processing, microstructure, mechanical properties, cytotoxicity. *Journal of Materials Science-Materials in Medicine* **19**, 2881–2887 (2008).

34. Mazzocchi, M.; Gardini, D.; Traverso, P. L.; Faga, M. G.; Bellosi, A. On the possibility of silicon nitride as a ceramic for structural orthopaedic implants. Part II: chemical stability and wear resistance in body environment. *Journal of Materials Science-Materials in Medicine* **19**, 2889–2901 (2008).
35. de Arellano-López, A. R.; Martínez-Fernández, J.; González, P.; Domínguez, C.; Fernández-Quero, V.; Singh, M. Biomorphic SiC: A New Engineering Ceramic Material. *International Journal of Applied Ceramic Technology* **1**, 56–67 (2004).
36. Naji, A.; Harmand, M. F. Cytocompatibility of two coating materials, amorphous alumina and silicon carbide, using human differentiated cell cultures. *Biomaterials* **12**, 690–694 (1991).
37. Carlisle, E. M. Silicon: A Possible Factor in Bone Calcification. *Science* **167**, 279–280 (1970).
38. Miguel, B. S.; Kriauciunas, R.; Tosatti, S.; Ehrbar, M.; Ghayor, C.; Textor, M.; Weber, F. E. Enhanced osteoblastic activity and bone regeneration using surface-modified porous bioactive glass scaffolds. *Journal of Biomedical Materials Research Part A* **94A**, 1023–1033 (2010).
39. Vitale-Brovarone, C.; Baino, F.; Verne, E. High strength bioactive glass-ceramic scaffolds for bone regeneration. *Journal of Materials Science-Materials in Medicine* **20**, 643–653 (2009).
40. Bal, B. S.; Rahaman, M. N.; Jayabalan, P.; Kuroki, K.; Cockrell, M. K.; Yao, J. Q.; Cook, J. L. *In Vivo* Outcomes of Tissue-Engineered Osteochondral Grafts. *Journal of Biomedical Materials Research Part B-Applied Biomaterials* **93B**, 164–174 (2010).
41. Goodman, S. B.; Barrena, E. G.; Takagi, M.; Konttinen, Y. T. Biocompatibility of total joint replacements: A review. *Journal of Biomedical Materials Research Part A* **90A**, 603–618 (2009).
42. Ramakrishna, S.; Mayer, J.; Wintermantel, E.; Leong, K. W. Biomedical applications of polymer-composite materials: A review. *Composites Science and Technology* **61**, 1189–1224 (2001).
43. Lyu, S.; Untereker, D. Degradability of polymers for implantable biomedical devices. *International journal of molecular sciences* **10**, 4033–65 (2009).
44. Fujishiro, Y.; Oonishi, H.; Hench, L. L. Quantitative comparison of *in vivo* bone generation with particulate Bioglass and hydroxyapatite as a bone graft substitute. in *10th International Symposium on Ceramics in Medicine*. (Elsevier Science Ltd., Paris, 1997).
45. Gerhardt, L.-C.; Boccaccini, A. R. Bioactive Glass and Glass-Ceramic Scaffolds for Bone Tissue Engineering. *Materials* **3**, 3867–3910 (2010).
46. Ni, G. X.; Lu, W. W.; Xu, B.; Chiu, K. Y.; Yang, C.; Li, Z. Y.; Lam, W. M.; Luk, K. D. K. Interfacial behaviour of strontium-containing hydroxyapatite cement with cancellous and cortical bone. *Biomaterials* **27**, 5127–5133 (2006).
47. Yuan, H.; Kurashina, K.; de Bruijn, J. D.; Li, Y.; de Groot, K.; Zhang, X. A preliminary study on osteoinduction of two kinds of calcium phosphate ceramics. *Biomaterials* **20**, 1799–1806 (1999).
48. Cadosch, D.; Chan, E.; Gautschi, O. P.; Meagher, J.; Zellweger, R.; Filgueira, L. Titanium IV ions induced human osteoclast differentiation and enhanced bone

resorption *in vitro*. *Journal of Biomedical Materials Research Part A* **91A**, 29–36 (2009).

49. Krewski, D.; Yokel, R. A.; Nieboer, E.; Borchelt, D.; Cohen, J.; Harry, J.; Kacew, S.; Lindsay, J.; Mahfouz, A. M.; Rondeau, V. Human health risk assessment for aluminium, aluminium oxide, and aluminium hydroxide. *Journal of Toxicology and Environmental Health-Part B-Critical Reviews* **10**, 1–269 (2007).
50. del Rio, J.; Beguiristain, J.; Duart, J. Metal levels in corrosion of spinal implants. *European Spine Journal* **16**, 1055–1061 (2007).
51. Passi, P.; Zadro, A.; Galassini, S.; Rossi, P.; Moschini, G. PIXE micro-beam mapping of metals in human peri-implant tissues. *Journal of Materials Science-Materials in Medicine* **13**, 1083–1089 (2002).
52. Kumar, V.; Gill, K. D. Aluminium neurotoxicity: neurobehavioural and oxidative aspects. *Archives of Toxicology* **83**, 965–978 (2009).
53. Okazaki, Y.; Gotoh, E. Comparison of metal release from various metallic biomaterials *in vitro*. *Biomaterials* **26**, 11–21 (2005).
54. Borrajo, J. P.; Gonzalez, P.; Serra, J.; Liste, S.; Chiussi, S.; Leon, B.; De Carlos, A.; Varela-Feria, F. M.; Martinez-Fernandez, J.; De Arellano-Lopez, A. R. Cytotoxicity study of biomorphic SiC ceramics coated with bioactive glass. *Boletin De La Sociedad Espanola De Ceramica Y Vidrio* **45**, 109–114 (2006).
55. Lelli, M.; Foltran, I.; Foresti, E.; Martinez-Fernandez, J.; Torres-Raya, C.; Varela-Feria, F. M.; Roveri, N. Biomorphic Silicon Carbide Coated with an Electrodeposition of Nanostructured Hydroxyapatite/Collagen as Biomimetic Bone Filler and Scaffold. *Advanced Engineering Materials* **12**, B348–B355 (2010).
56. Muller, K.; Valentine-Thon, E. Hypersensitivity to titanium: Clinical and laboratory evidence. *Neuroendocrinology Letters* **27**, 31–35 (2006).
57. Granchi, D.; Cenni, E.; Trisolino, G.; Giunti, A.; Baldini, N. Sensitivity to implant materials in patients undergoing total hip replacement. *Journal of Biomedical Materials Research Part B-Applied Biomaterials* **77B**, 257–264 (2006).
58. Gonzalez, P.; Serra, J.; Liste, S.; Chiussi, S.; Leon, B.; Perez-Amor, M.; Martinez-Fernandez, J.; de Arellano-Lopez, A. R.; Varela-Feria, F. M. New biomorphic SiC ceramics coated with bioactive glass for biomedical applications. *Biomaterials* **24**, 4827–4832 (2003).
59. Exley, C. Darwin, natural selection and the biological essentiality of aluminium and silicon. *Trends in Biochemical Sciences* **34**, 589–593 (2009).
60. Nayak, P. Aluminum: Impacts and disease. *Environmental Research* **89**, 101–115 (2002).
61. Haider, S. S.; Abdel-Gayoum, A. A.; El-Fakhri, M.; Ghwarsha, K. M. Effect of selenium on vanadium toxicity in different regions of rat brain. *Human & Experimental Toxicology* **17**, 23–28 (1998).
62. Barceloux, D. G. Vanadium. *Journal of Toxicology-Clinical Toxicology* **37**, 265–278 (1999).
63. Mukherjee, B.; Patra, B.; Mahapatra, S.; Banerjee, P.; Tiwari, A.; Chatterjee, M. Vanadium - an element of atypical biological significance. *Toxicology Letters* **150**, 135–143 (2004).
64. Exley, C.; Siesjo, P.; Eriksson, H. The immunobiology of aluminium adjuvants: How do they really work? *Trends in Immunology* **31**, 103–109 (2010).

65. Sul, Y. T.; Johansson, C.; Byon, E.; Albrektsson, T. The bone response of oxidized bioactive and non-bioactive titanium implants. *Biomaterials* **26**, 6720–6730 (2005).

66. Janning, C.; Willbold, E.; Vogt, C.; Nellesen, J.; Meyer-Lindenberg, A.; Windhagen, H.; Thorey, F.; Witte, F. Magnesium hydroxide temporarily enhancing osteoblast activity and decreasing the osteoclast number in peri-implant bone remodelling. *Acta Biomaterialia* **6**, 1861–1868 (2010).

67. Shadanbaz, S.; Dias, G. J. Calcium phosphate coatings on magnesium alloys for biomedical applications: A review. *Acta Biomaterialia* **8**, 20–30 (2012).

68. Liu, H. N. The effects of surface and biomolecules on magnesium degradation and mesenchymal stem cell adhesion. *Journal of Biomedical Materials Research Part A* **99A**, 249–260 (2011).

69. Hakki, S. S.; Bozkurt, B. S.; Hakki, E. E. Boron regulates mineralized tissue-associated proteins in osteoblasts (MC3T3-E1). *Journal of Trace Elements in Medicine and Biology* **24**, 243–250 (2010).

70. Benderdour, M.; Bui-Van, T.; Dicko, A.; Belleville, F. *In vivo* and *in vitro* effects of boron and boronated compounds. *Journal of Trace Elements in Medicine and Biology* **12**, 2–7 (1998).

71. Fail, P. A.; Chapin, R. E.; Price, C. J.; Heindel, J. J. General, reproductive, developmental, and endocrine toxicity of boronated compounds. *Reproductive Toxicology* **12**, 1–18 (1998).

72. Van Dyck, K.; Robberecht, H.; Van Cauwenbergh, R.; Van Vlaslaer, V.; Deelstra, H. Indication of silicon essentiality in humans - Serum concentrations in Belgian children and adults, including pregnant women. *Biological Trace Element Research* **77**, 25–32 (2000).

73. Jugdaohsingh, R.; Reffitt, D. M.; Oldham, C.; Day, J. P.; Fifield, L. K.; Thompson, R. P. H.; Powell, J. J. Oligomeric but not monomeric silica prevents aluminum absorption in humans. *American Journal of Clinical Nutrition* **71**, 944–949 (2000).

74. Van Landeghem, G. F.; De Broe, M. E.; D'Haese, P. C. Al and Si: their speciation, distribution, and toxicity. *Clinical Biochemistry* **31**, 385–397 (1998).

75. Ermer, E.; Wieslsaw, P.; Ludoslsaw, S. Influence of sintering activators on structure of silicon carbide. *Solid State Ionics* **141**, 523–528 (2001).

76. Iveković, A.; Dražić, G.; Novak, S. Densification of a SiC-matrix by electrophoretic deposition and polymer infiltration and pyrolysis process. *Journal of the European Ceramic Society* **31**, 833–840 (2011).

77. Allen, M.; Butter, R.; Chandra, L.; Lettington, A.; Rushton, N. Toxicity of particulate silicon carbide for macrophages, fibroblasts and osteoblast-like cells *in vitro*. *Bio-Medical Materials and Engineering* **5**, 151–159 (1995).

78. Wan, H.; Williams, R. L.; Doherty, P. J.; Williams, D. F. A study of cell behaviour on the surfaces of multifilament materials. *Journal of Materials Science-Materials in Medicine* **8**, 45–51 (1997).

79. Santavirta, S.; Takagi, M.; Nordsletten, L.; Anttila, A.; Lappalainen, R.; Konttinen, Y. T. Biocompatibility of silicon carbide in colony formation test *in vitro*: A promising new ceramic THR implant coating material. *Archives of Orthopaedic and Trauma Surgery* **118**, 89–91 (1998).

80. Torres-Raya, C.; Hernandez-Maldonado, D.; Ramirez-Rico, J.; Garcia-Ganan, C.; de Arellano-Lopez, A. R.; Martinez-Fernandez, J. Fabrication, chemical etching, and compressive strength of porous biomimetic SiC for medical implants. *Journal of*

Materials Research **23**, 3247–3254 (2008).

81. González, P.; Serra, J.; Liste, S.; Chiussi, S.; León, B.; Pérez-Amor, M.; Martínez-Fernández, J.; de Arellano-López, A. R.; Varela-Feria, F. M. New biomorphic SiC ceramics coated with bioactive glass for biomedical applications. *Biomaterials* **24**, 4827–4832 (2003).
82. Will, J.; Hoppe, A.; Müller, F. A.; Raya, C. T.; Fernández, J. M.; Greil, P. Bioactivation of biomorphous silicon carbide bone implants. *Acta Biomaterialia* **6**, 4488–4494 (2010).
83. Gonzalez, P.; Borrajo, J. P.; Serra, J.; Chiussi, S.; Leon, B.; Martinez-Fernandez, J.; Varela-Feria, F. M.; de Arellano-Lopez, A. R.; de Carlos, A.; Munoz, F. M.; Lopez, M.; Singh, M. A new generation of bio-derived ceramic materials for medical applications. *Journal of Biomedical Materials Research Part A* **88A**, 807–813 (2009).
84. Yakimova, R.; Petoral, R. M.; Yazdi, G. R.; Vahlberg, C.; Spetz, A. L.; Uvdal, K. Surface functionalization and biomedical applications based on SiC. *Journal of Physics D-Applied Physics* **40**, 6435–6442 (2007).
85. Aspenberg, P.; Anttila, A.; Konttinen, Y. T.; Lappalainen, R.; Goodman, S. B.; Nordsletten, L.; Santavirta, S. Benign response to particles of diamond and SiC: Bone chamber studies of new joint replacement coating materials in rabbits. *Biomaterials* **17**, 807–812 (1996).
86. Nordsletten, L.; Hogasen, A. K. M.; Konttinen, Y. T.; Santavirta, S.; Aspenberg, P.; Aasen, A. O. Human monocytes stimulation by particles of hydroxyapatite, silicon carbide and diamond: *In vitro* studies of new prosthesis coatings. *Biomaterials* **17**, 1521–1527 (1996).
87. Cupid, D. M.; Fabrichnaya, O.; Seifert, H. J. Thermodynamic aspects of liquid phase sintering of SiC using Al_2O_3 and Y_2O_3. *International Journal of Materials Research* **98**, 976–986 (2007).
88. Niihara, K.; Morena, R.; Hasselman, D. P. H. Evaluation of K_{1c} of brittle solids by the indentation method with low crack-to-indent ratios. *Journal of Materials Science Letters* **1**, 13–16 (1982).
89. Kokubo, T.; Takadama, H. How useful is SBF in predicting *in vivo* bone bioactivity? *Biomaterials* **27**, 2907–2915 (2006).
90. Li, W.; Chen, P.; Gu, M.; Jin, Y. Effect of TMAH on rheological behavior of SiC aqueous suspension. *Journal of the European Ceramic Society* **24**, 3679–3684 (2004).
91. Novak, S.; Kovač, J.; Dražić, G.; Ferreira, J. M. F.; Quaresma, S. Surface characterisation and modification of submicron and nanosized silicon carbide powders. *Journal of the European Ceramic Society* **27**, 3545–3550 (2007).
92. Huang, Q.; Gu, M.; Sun, K.; Jin, Y. Effect of pretreatment on rheological properties of silicon carbide aqueous suspension. *Ceramics International* **28**, 747–754 (2002).
93. Novak, S.; Rade, K.; Konig, K.; Boccaccini, A. R. Electrophoretic deposition in the production of SiC/SiC composites for fusion reactor applications. *Journal of the European Ceramic Society* **28**, 2801–2807 (2008).
94. Ferrari, B.; Moreno, R. The conductivity of aqueous Al_2O_3 slips for electrophoretic deposition. *Materials Letters* **28**, 353–355 (1996).
95. Ferrari, B.; Moreno, R. EPD kinetics: A review. *Journal of the European Ceramic Society* **30**, 1069–1078 (2010).

96. Moreno, R.; Ferrari, B. Effect of the slurry properties on the homogeneity of alumina deposits obtained by aqueous electrophoretic deposition. *Materials Research Bulletin* **35**, 887–897 (2000).
97. Stobierski, L.; Gubernat, A. Sintering of silicon carbide I. Effect of carbon. *Ceramics International* **29**, 287–292 (2003).
98. Stobierski, L.; Gubernat, A. Sintering of silicon carbide - II. Effect of boron. *Ceramics International* **29**, 355–361 (2003).
99. Tatli, Z.; Thompson, D. P. The use of MgO-coated SiC powders as low temperature densification materials. *Journal of the European Ceramic Society* **27**, 1313–1317 (2007).
100. Tikhomirov, A.; Sorokina, N.; Avdeev, V. Surface modification of carbon fibers with nitric acid solutions. *Inorganic Materials* **47**, 609–613 (2011).
101. Foster, D.; Thompson, D. P. The use of MgO as a densification aid for alpha-SiC. *Journal of the European Ceramic Society* **19**, 2823–2831 (1999).
102. Novak, S.; Drazic, G.; Konig, K.; Ivekovic, A. Preparation of $SiC_{(f)}$/SiC composites by the slip infiltration and transient eutectoid (SITE) process. *Journal of Nuclear Materials* **399**, 167–174 (2010).
103. Alexander, G. B.; Heston, W. M.; Iler, R. K. The Solubility of Amorphous Silica in Water. *The Journal of Physical Chemistry* **58**, 453–455 (1954).
104. Jurewicz, J. Einfluss der fluoridionen auf die anodische graphitoxydation bei der chloralkalielektrolyse. *Electrochimica Acta* **28**, 1501–1505 (1983).
105. Mukherjee, A.; Maiti, B.; Das Sharma, A.; Basu, R. N.; Maiti, H. S. Correlation between slurry rheology, green density and sintered density of tape cast yttria stabilised zirconia. *Ceramics International* **27**, 731–739 (2001).
106. Ovtar, S. *Kvantitativna določitev amorfne faze v vzorcih silicijevega karbida z rentgensko praškovno difrakcijo: diplomsko delo* (University of Ljubljana, Ljubljana, 2007).
107. Ellingsen, J. E.; Lyngstadaas, S. P. *Bio-implant interface: improving biomaterials and tissue reactions* (CRC Press, New York, 2003).
108. Tabellion, J.; Clasen, R. *Manufacturing of advanced ceramic components via electrophoretic deposition* (Trans Tech Publications Ltd, Zürich-Uetikon, 2002).
109. Besra, L.; Liu, M. A review on fundamentals and applications of electrophoretic deposition (EPD). *Progress in Materials Science* **52**, 1–61 (2007).
110. Novak, S.; Konig, K.; Iveković, A.; Boccaccini, A. R. Infiltration of a 3-D Fabric for the Production of SiC/SiC Composites by Means of Electrophoretic Deposition. *Key Engineering Materials* **412**, 237–242 (2009).
111. Basu, R. N.; Randall, C. A.; Mayo, M. J. Fabrication of Dense Zirconia Electrolyte Films for Tubular Solid Oxide Fuel Cells by Electrophoretic Deposition. *Journal of the American Ceramic Society* **84**, 33–40 (2001).
112. Radice, S.; Bradbury, C. R.; Michler, J.; Mischler, S. Critical particle concentration in electrophoretic deposition. *Journal of the European Ceramic Society* **30**, 1079–1088 (2010).
113. Ness, E. A.; Rafaniello, W. Origin of density gradients in sintered beta-silicon carbide parts. *Journal of the American Ceramic Society* **77**, 2879–2884 (1994).
114. Bind, J. M.; Biggers, J. V. Hot-pressing of silicon carbide with 1 % boron carbide addition. *Journal of the American Ceramic Society* **58**, 304–306 (1975).

115. Prochazka, S.; Scanlan, R. M. Effect of boron and carbon on sintering of SiC. *Journal of the American Ceramic Society* **58**, 72–72 (1975).

116. Negita, K. Effective sintering aids for silicon carbide ceramics: Reactivities of silicon carbide with various additives. *Journal of the American Ceramic Society* **69**, C308–C310 (1986).

117. Can, A.; Herrmann, M.; McLachlan, D. S.; Sigalas, I.; Adler, J. Densification of liquid phase sintered silicon carbide. *Journal of the European Ceramic Society* **26**, 1707–1713 (2006).

118. Ihle, J.; Herrmann, M.; Adler, J. Phase formation in porous liquid phase sintered silicon carbide: Part I: Interaction between Al_2O_3 and SiC. *Journal of the European Ceramic Society* **25**, 987–995 (2005).

119. Yoon, H. K.; Park, Y. H.; Park, J. S.; Kohyama, A. Kim, Y. J.; Bae, H. D. (eds.) *Effect of sintering additives on fabrication properties of liquid phase sintered SiC* (Trans Tech Publications Ltd, Zürich-Uetikon, 2005).

120. Gomez, E.; Echeberria, J.; Iturriza, I.; Castro, F. Liquid phase sintering of SiC with additions of Y_2O_3, Al_2O_3 and SiO_2. *Journal of the European Ceramic Society* **24**, 2895–2903 (2004).

121. Zawrah, M. F.; Shaw, L. Liquid-phase sintering of SiC in presence of CaO. *Ceramics International* **30**, 721–725 (2004).

122. Balog, M.; Sedlackova, K.; Zifcak, P.; Janega, J. Liquid phase sintering of SiC with rare-earth oxides. *Ceramics-Silikaty* **49**, 259–262 (2005).

123. Yang, J. X.; Cui, F. Z.; Lee, I. S. Surface Modifications of Magnesium Alloys for Biomedical Applications. *Annals of Biomedical Engineering* **39**, 1857–1871 (2011).

124. Miyazaki, H.; Hakomori, A.; Yasuda, K.; Matsuo, Y.; Yano, T.; Iseki, T. Densification and thermal, mechanical and electrical properties of SiC ceramics sintered with addition of MgO. *Journal of the Ceramic Society of Japan* **109**, 227–231 (2001).

125. Konig, K.; Novak, S.; Ivekovic, A.; Rade, K.; Meng, D. C.; Boccaccini, A. R.; Kobe, S. Fabrication of CNT-SiC/SiC composites by electrophoretic deposition. *Journal of the European Ceramic Society* **30**, 1131–1137 (2010).

126. Pavese, M.; Fino, P.; Ortona, A.; Badini, C. Potential of SiC multilayer ceramics for high temperature applications in oxidising environment. *Ceramics International* **34**, 197–203 (2008).

127. Krnel, K.; Sciti, D.; Bellosi, A. Influence of long term oxidation on the microstructure, mechanical and electrical properties of pressureless sintered AlN–SiC–$MoSi_2$ ceramic composites. *Journal of the European Ceramic Society* **23**, 3135–3146 (2003).

128. Presas, M.; Pastor, J. Y.; Llorca, J.; Martín, A.; Segurado, J.; González, C. Strength and toughness of cellular SiC at elevated temperature. *Engineering Failure Analysis* **16**, 2598–2603 (2009).

129. Badini, C.; Fino, P.; Ortona, A.; Amelio, C. High temperature oxidation of multilayered SiC processed by tape casting and sintering. *Journal of the European Ceramic Society* **22**, 2071–2079 (2002).

130. Hironaka, K.; Nozawa, T.; Hinoki, T.; Igawa, N.; Katoh, Y.; Snead, L. L.; Kohyama, A. High-temperature tensile strength of near-stoichiometric SiC/SiC composites. *Journal of Nuclear Materials* **307–311, Part 2**, 1093–1097 (2002).

131. Greil, P.; Lifka, T.; Kaindl, A. Biomorphic cellular silicon carbide ceramics from

wood: II. Mechanical properties. *Journal of the European Ceramic Society* **18**, 1975–1983 (1998).

132. Xiao, J. Z.; Li, J. B.; Zhang, C. On relationships between the mechanical properties of recycled aggregate concrete: An overview. *Materials and Structures* **39**, 655-664 (2006).
133. Guo, H.; Yoon, D. H.; Shin, D. W. Ohji, T.; Sekino, T.; Niihara, K. (eds.) *Fracture toughness of fibrous Si_3N_4 monolithic ceramics* (Trans Tech Publications Ltd, Zürich-Uetikon, 2006).
134. Gerhardt, R. (ed.) *Properties and Applications of Silicon Carbide* (InTech, Rijeka, 2011).
135. Thian, E. S.; Huang, J.; Best, S. M.; Barber, Z. H.; Bonfield, W. Silicon-substituted hydroxyapatite: The next generation of bioactive coatings. *Materials Science & Engineering C-Biomimetic and Supramolecular Systems* **27**, 251–256 (2007).
136. Drnovšek, N.; Rade, K.; Milačič, R.; Štrancar, J.; Novak, S. The properties of bioactive TiO_2 coatings on Ti6Al4V implants *submitted*, (2012).
137. Manukyan, K.; Amirkhanyan, N.; Aydinyan, S.; Danghyan, V.; Grigoryan, R.; Sarkisyan, N.; Gasparyan, G.; Aroutiounian, R.; Kharatyan, S. Novel NiZr-based porous biomaterials: Synthesis and *in vitro* testing. *Chemical Engineering Journal* **162**, 406–414 (2010).
138. Seuss, F.; Seuss, S.; Turhan, M. C.; Fabry, B.; Virtanen, S. Corrosion of Mg alloy AZ91D in the presence of living cells. *Journal of Biomedical Materials Research Part B-Applied Biomaterials* **99B**, 276–281 (2011).
139. Rota, A.; Schluter, C.; Salk, N. Surface modification of biomaterials by microstructuring. *Materialprufung* **47**, 203–206 (2005).
140. Kishida, A.; Matsuyama, T.; Kitajima, I.; Maruyama, I.; Akashi, M. Study of cell-material interaction by estimating NF-*k*B activation in HeLa S3 cells adhered onto hydrophilic substrates. *Biomaterials* **22**, 541–546 (2001).
141. Ko, H. F.; Sfeir, C.; Kumta, P. N. Novel synthesis strategies for natural polymer and composite biomaterials as potential scaffolds for tissue engineering. *Philosophical Transactions of the Royal Society a-Mathematical Physical and Engineering Sciences* **368**, 1981–1997 (2010).
142. Hannink, G.; Arts, J. J. C. Bioresorbability, porosity and mechanical strength of bone substitutes: What is optimal for bone regeneration? *Injury* **42, Supplement 2**, S22–S25 (2011).

Index of Figures

Index of Tables

Appendix

Original scientific article

1. Rade, K.; Novak, S.; Kobe, S. The shaping and densification of silicon carbide while avoiding alumina as a sintering additive. *Journal of Materials Science and Engineering* A **1**, 301–311 (2011).
2. Rade, K.; Novak, S.; Dražić, G.; Kobe, S. Co-deposition and densification of SiC with MgO for biomedical applications. *Journal of Materials Science* **47**, 3400–3406 (2012).
3. Novak, S.; Rade, K.; Koenig, K.; Boccaccini, A. R. Electrophoretic deposition in the production of SiC composites for fusion reactor applications. *Journal of the European Ceramic Society* **14**, 2801–2807 (2008).
4. Koenig, K.; Novak, S.; Iveković, A.; Rade, K.; Meng, D.; Boccaccini, A. R.; Kobe, S. Fabrication of CNT-SiC/SiC composites by electrophoretic deposition. *Journal of the European Ceramic Society* **5**, 1067–1210 (2009).
5. Petković, J.; Küzma, T.; Rade, K.; Novak, S.; Filipič, M. Pre-irradiation of anatase TiO_2 particles with UV enhances their cytotoxic and genotoxic potential in human hepatoma HepG2 cells. *Journal of Hazardous Materials* **196**, 145–152 (2011).

Published scientific conference contribution abstract

1. Drnovšek, N.; Daneu, N.; Novak, S.; Rade, K.; Kovač, J. Dvoplastna prevleka na zlitini Ti6A14V za biomedicinsko uporabo. V: *Materiali in tehnologije* **6**, 311–312 (2007).
2. Rade, K.; Kogej, Ksenija, Novak, S. Študij polimetakrilne kisline v prisotnosti različnih kationov v vodnem mediju. V: *Materiali in tehnologije* **6**, 315–316 (2007).
3. Drnovšek, N.; Daneu, N.; Rade, K.; Kovač, Janez. Dvoplastna prevleka na Ti6Al4V zlitini za biomedicinsko uporabo. V: *15th Conference on Materials and Technology*, 35 (8–10 October 2007, Portorož, Slovenia).
4. Rade, K.; Kogej, K.; Novak, S. Študij polimetakrilne kisline v prisotnosti različnih kationov v vodnem mediju. V: *15th Conference on Materials and Technology*, 59 (8–10 October 2007, Portorož, Slovenia).
5. Rade, K.; Daneu, N.; Novak, S. Structure and chemical composition of dentine and enamel studied by electron microscopy. V: *Summer school on Women-in-nano: career development and research trends* (Universitat Autònoma de Barcelona, Coma-ruga, Tarragona, Spain, June 2007).
6. Rade, K.; Novak, S.; Drnovšek, N.; Kobe, S. Hydroxyapatite/bioglass composites: Preparation and bioactivity characterization. V: *Hot nano topics*, 256 (23-30 May, Portorož, Slovenia).
7. Horvat, B.; Drnovšek, N.; Rade, K.; Novak, S.; Dražić, G. Preparation of nano-anatase TiO_2. V: *1st International conference on Materials and Technology*, 1 (13-15

October 2008, Portorož, Slovenia).

8. Rade, K.; Novak, S.; Kobe, S. Calcium phosphate based bone graft materials: Natural vs. synthetic. V: *WomenInNano winter school*, 101 (7-9 February 2008, Kranjska Gora, Slovenia).
9. Rade, K.; Novak, S.; Drnovšek, N.; Kobe, S. Kompoziti iz hidroksiapatita in biostekla: Priprava in karakterizacija bioaktivnosti. V: *Dan mladih raziskovalcev*, 1 (Institut "Jožef Stefan", Ljubljana, 2009).
10. Rade, K.; Novak, S.; Kobe, S. Effect of shaping technique on sintered densities of silicon carbide. V: *Shaping 4*, SC2–8 (4th International Conference on Shaping of Advanced Ceramics, 15-18 November, 2009, Madrid, Spain).
11. Rade, K.; Novak, S.; Kobe, S. Priprava silicijevega karbida v biomedicinske namene. V: *4. Dan Mladih Raziskovalcev KMBO*, 43 (11th February 2010, Institut "Jožef Stefan", Ljubljana, Slovenija).
12. Petković, J.; Küzma, T.; Rade, K.; Novak, S.; Filipič, M. Increased toxic potential of nano-sized and submicron-sized anatase TiO_2 particles after pre-irradiation with UV in human hepatoma HepG2 cells. V: *9th Congress of the Slovenian Biochemical Society*, 77 (12-15 October 2011, Maribor, Slovenia).
13. Drnovšek, N.; Novak, S.; Rade, K.; Murn, G.; Milačič, R.; Harmand, M.-F. Bioactive TiO_2 coatings on Ti6Al4V implants. V: *12th Conference of the European Ceramic Society*, (19-23 June 2011, Stockholm, Sweden).
14. Rade, K.; Novak, S.; Dražić, G.; Kobe, S. Electrophoretic co-deposition and densification of SiC with MgO for biomedical applications. V: *19th Conference on Materials and Technology*, 82 (22-23 November 2011, Portorož, Slovenia).
15. Drnovšek, N.; Novak, S.; Rade, K.; Murn, G.; Milačič, R.; Harmand, M.-F. Kostni vsadki na osnovi Ti6Al4V z izboljšano osteointegracijo. V: *5. Dan Mladih Raziskovalcev*, 54 (February 2011, Institut "Jožef Stefan", Ljubljana, Slovenia).
16. Rade, K.; Novak, S.; Kobe, S. Oblikovanje in sintranje SiC brez aluminija kot dodatka za sintranje. V: *5. Dan Mladih Raziskovalcev*, 54 (February 2011, Institut "Jožef Stefan", Ljubljana, Slovenia).